Spectrum resource assignment in cognitive radio sensor networks for smart grids

Sabrine Aroua

UNIVERSITÉ DE LA ROCHELLE

École Doctorale S2IM

Sciences et Ingénierie pour l'Information, Mathématiques
Laboratoire Informatique, Image et Interaction (L3i)
et

École Nationale des Sciences de l'Informatique
Laboratoire CRISTAL

Thèse de Doctorat

Discipline : Informatique et Applications

Présentée par :

Sabrine Aroua

Allocation des Ressources Spectrales dans les Réseaux de Capteurs à Radio Cognitive pour les Smart Grids

---

Soutenance le 11 Juillet 2018 devant le jury composé de :

Mme. Leila Merghem-Boulahia	Maître de conférences, Université de Troyes	Rapporteur
M. Mauro Fonseca	Professeur, UTFPR, Brésil	Rapporteur
M. Marcelo Dias de Amorim	Directeur de recherche, CNRS	Examinateur
Mme. Valeria Loscrì	Chargé de recherche, INRIA Lille	Examinateur
M. Yacine Ghamri-Doudane	Professeur, Université de La Rochelle	Directeur de thèse
Mme. Leila Azouz-Saidane	Professeur, ENSI Tunisie	Directeur de thèse
Mme. Inès El Korbi	Maître assistant, ENSI Tunisie	Co-encadrant de thèse

UNIVERSITÉ DE LA ROCHELLE

École Doctorale S2IM

Sciences et Ingénierie pour l'Information, Mathématiques

Laboratoire Informatique, Image et Interaction (L3i)

et

École Nationale des Sciences de l'Informatique

Laboratoire CRISTAL

THÈSE DE DOCTORAT

Discipline: Informatique et Applications

Présentée par :

Sabrine Aroua

Spectrum Resource Assignment in Cognitive Radio Sensor Networks for Smart Grids

Soutenance le 11 Juillet 2018 devant le jury composé de :

Mme. Leila MERGHEM-BOULAHIA	Maître de conférences, Université de Troyes	Rapporteur
M. Mauro FONSECA	Professeur, UTFPR, Brésil	Rapporteur
M. Marcelo DIAS DE AMORIM	Directeur de recherche, CNRS	Examinateur
Mme. Valeria LOSCRÌ	Chargé de recherche, INRIA Lille	Examinateur
M. Yacine GHAMRI-DOUDANE	Professeur, Université de La Rochelle	Directeur de thèse
Mme. Leila AZOUZ-SAIDANE	Professeur, ENSI Tunisie	Directeur de thèse
Mme. Inès EL KORBI	Maître assistant, ENSI Tunisie	Co-encadrant de thèse

Acknowledgments

Working as a PhD student was a challenging and enjoyable experience to me that could not be achieved without the support of a number of people to whom I want to give my thanks.

First, I would like to express my sincere gratitude to my co-advisor Dr. Inès El Korbi for her guidance and the efforts she spent correcting my papers and my dissertation. My discussions with her have been interesting and inspiring. My deepest thanks go also to my advisor Prof. Yacine Ghamri-Doudane for his advices, helps and my papers and dissertation's reviewing. I would like to thank Dr. Inès El Korbi and Prof. Yacine Ghamri-Doudane for the joint supervision of this work between the laboratory L3i (Laboratory Information, Image and Interaction) from the University of La Rochelle in France and the laboratory CRISTAL, pole RAMSIS from the National School of Computer Science (ENSI) in Tunisia. I also want to thank my advisor Leila Azouz-Saidane for placing her trust and confidence in me.

I would like to express my special appreciation and thanks to my reading committee, Mrs. Leila Merghem-Boulahia and Mr. Mauro Fonseca, for accepting to review this dissertation. Special thanks goes also to Mrs. Valeria Loscrì and Mr. Marcelo Dias de Amorim for generously offering their time and good will to serve as my dissertation committee.

Thank you to all the Ph.D. candidates, doctors, engineers and trainees affiliated to the two laboratories, L3i and CRISTAL, with whom I spent most of the time. Special thanks to Nouredine, Rim, Mohamed Ali, Dimitrios, Ricardo, Junaid, Soraya, Imen, Oumaima, Nadya and Hajer for the good moments spent together in both the L3i and CRISTAL offices.

Last but not least, words cannot express how grateful I am to my family; my parents and my brothers: Faker and Omar, for their tremendous help and support. They have spared no effort or time to help me achieve my goals. My heartfelt thanks goes to my friend Salma for her lovely support since the first time we met.

Abstract

With the advances in wireless communication technologies, cognitive radio sensor networks (CRSNs) stand as an efficient spectrum solution in the development of intelligent electrical power networks, the smart grids. The cognitive radio (CR) technology provides the sensors with the ability to use the temporally available licensed spectrum in order to escape the unlicensed spectrum resource scarcity problem. In this context, several challenging communication issues face the CRSN deployment for smart grids such as the coexistence of different electrical applications and the heterogeneous opportunities to access available licensed channels between smart grid sensors.

The work conducted in this thesis focuses on spectrum resource allocations for CRSNs in smart grids. After a comprehensive overview of both smart grid systems and CRSN characteristics that may impact data transmissions in smart grids, we concentrate our efforts on the development of new spectrum resource sharing paradigms for CRSNs in smart grids. The developed solutions focus on distributed and balanced spectrum sharing among smart grid sensors and on eventual CRSN deployment scenarios in smart grid areas. All along the thesis, channels are assigned without relying on a predefined common control channel (CCC) to exchange control messages before each spectrum access trial.

First, we focus on one-hop smart grid communication network topology. Sensors are placed one-hop away from a gateway/sink. We introduce two predictive channel assignment solutions for two one-hop smart grid systems: smart homes and neighborhood area networks (NANs). In smart homes, we develop the Cooperative Spectrum Resource Assignment (CSRA) approach. CSRA allows every node to access the spectrum while considering all its neighboring transmissions' need. Then, in NANs, sensors generate traffic with different priorities. Thus, we introduce the Distributed Unselfish Spectrum Assignment (DUSA) approach. In DUSA, every sensor accesses to the spectrum according to its monitored application's requirements. Both schemes, DUSA and CSRA, are based on partially observable Markov decision process formulations (POMDP). Simulation results show the CSRA and the DUSA's capabilities to fairly share spectrum resources and their abilities to improve the network spectrum utilization. In the second part of our work, we investigate the issues of the sensors' short transmission range in NANs. Thus, we introduce the concept of forwarding nodes to come over the sensors' shortage issues in NANs. Then, we develop the Dual-Spectrum Assignment for two-stage NAN topologies (D-SAN). D-SAN consists in two complementary channel allocation sub-policies. Each sub-policy is interested in the communication on one stage of the deployed network. D-SAN's performance evaluation reveals the ability of D-SAN to achieve a differentiated channel allocation in two-stage CRSNs for NANs. Thereafter, in the third part of this dissertation, we focus on multi-hop data transmission in smart grid NANs. In this context, we opt for a hierarchical CRSN topology. We propose the Predictive Hierarchical Spectrum Assignment (PHSA) paradigm. In PHSA, channels are assigned to the sensors based on local estimates of other nodes' priorities and

spectrum availability via a POMDP. Then, as an extension of PHSA, we introduce the Routing-based PHSA (R-PHSA) scheme. R-PHSA takes into consideration the routing aspects during the spectrum sharing. Simulation results of both PHSA and R-PHSA show their balanced spectrum sharing among deployed sensors and their capability to outperform existing clustering approaches without relying on a CCC. Finally, we concentrate our effort on event-based generated traffic in smart grid distribution substations. We propose the Distributed Event-driven data Aggregation and constrained multipath Reporting (DEAR) approach. DEAR allows sensors involved in the data aggregation and forwarding to select channels without interfering with neighboring nodes. DEAR is based on graph coloring paradigms. Performance evaluation reveals that DEAR ensures rapid data transmissions and efficient channel assignments in CRSNs.

The four contributions of this thesis achieve a distributed and fair opportunistic spectrum assignment in a way to consider different smart grid system characteristics.

Keywords: Smart grids, cognitive radio sensor networks (CRSNs), Partially Observable Markov Decision Process (POMDP), fairness, spectrum resource allocation, common control channel (CCC), event-driven.

Résumé

Avec le développement des technologies de communication sans fil, les réseaux de capteur à radio cognitive (CRSNs) représentent une solution efficace pour le déploiement des réseaux électriques intelligents, connus aussi sous le nom de smart grids. La technologie de radio cognitive permet aux nœuds capteurs d'utiliser les bandes de fréquences non utilisées par des utilisateurs avec licence afin de contourner les limitations des bandes de fréquences sans licence. Dans ce contexte, plusieurs problèmes de communication freinent le déploiement des CRSNs pour les smart grids tel que la coexistence de différentes applications électriques ainsi que l'hétérogénéité des disponibilités des bandes de fréquence avec licence entre les nœuds capteurs.

Les travaux de recherche menés dans cette thèse se focalisent essentiellement sur l'allocation des ressources spectrales pour les CRSNs déployés pour contrôler des smart grids. Après une étude approfondie des particularités des CRSNs, ainsi que des smart grids et des caractéristiques qui peuvent influer sur la transmission des données dans les smart grids, nous proposons des nouvelles techniques d'allocation de ressources spectrales qui prennent en considération des topologies de déploiement possibles des CRSNs dans les smart grids, tout en assurant d'une manière distribuée l'équité entre les nœuds capteurs déployés. Tout au long de notre travail, l'allocation des canaux est effectuée sans faire appel à un canal de contrôle en commun pour le partage des messages de contrôle avant chaque accès au spectre.

Dans la première partie de la thèse, nous nous intéressons à une topologie de déploiement à un saut des CRSNs pour les smart grids. Les capteurs sont placés à un saut d'un Gateway. Dans cette partie nous proposons deux techniques prédictives d'allocation de ressources radio avec licence pour les utilisateurs des smart grids déployés dans deux systèmes électriques différents: les maisons connectées (smart homes) et les réseaux de couvertures des voisinages (neighborhood area netwoks-NANs). Au niveau des smart homes, nous proposons une première méthode d'accès au spectre nommée Cooperative Spectrum Resource Assignment (CSRA). CSRA permet à chaque capteur déployé dans la maison d'accéder au spectre tout en considérant les besoins en transmission des données de ses voisins. Au niveau des NANs, nous développons une deuxième solution d'allocation des bandes des fréquences nommée Distributed Unselfish Spectrum Assignment (DUSA). Grâce à DUSA, chaque utilisateur dans le NAN accède aux ressources spectrales selon les besoins de l'application qu'il contrôle. Les deux solutions proposées sont basées sur des processus de Markov partiellement observés. Les résultats de simulation montrent que CSRA et DUSA ont la capacité de partager équitablement les ressources du spectre entre les utilisateurs des smart grids et d'améliorer l'utilisation du spectre dans réseau. Dans la deuxième partie de notre travail, nous nous intéressons au problème de courte portée des nœuds capteurs des smart grids. Pour pallier cet inconvénient, nous introduisons dans cette partie, l'utilisation de nœuds intermédiaires intelligents pour étendre la couverture des nœuds

surveillant les smart grids. Nous proposons alors une nouvelle technique d'allocation des bandes de fréquence, nommée Dual-Spectrum Assignment for two-stage NAN topologies (D-SAN). D-SAN permet un partage de ressources dans une topologie à deux étages pour des NANs. L'évaluation des performances de D-SAN révèle sa capacité à obtenir une allocation des canaux différenciée dans les CRSNs, déployé pour surveiller des NANs. La troisième partie de cette thèse est dédiée à la topologie hiérarchique des CRSNs pour les NANs. Dans ce contexte, nous introduisons deux nouveaux paradigmes de partage de ressources spectrales dans les NANs. Notre première solution est appelée Predictive Hierarchical Spectrum Assignment (PHSA). Elle permet aux nœuds capteurs d'accéder d'une manière opportuniste au spectre durant la communication intra et inter-cluster tout en respectant les besoins des clusters voisins de transmettre leurs données. Notre deuxième solution représente une extension de la première approche pour le partage opportuniste des bandes de fréquence; elle est nommée Routing-based PHSA (R-PHSA). R-PHSA considère les aspects du routage lors du processus de l'allocation des ressources. Les résultats de la simulation de PHSA et R-PHSA montrent leurs capacités de partager d'une manière équitable le spectre disponible entre les capteurs déployés et leur capacité à surpasser les approches hiérarchiques existantes sans faire usage d'un quelconque canal de contrôle en commun. Dans la dernière partie contribution de cette thèse, nous nous intéressons à l'allocation des bandes de fréquences pour les utilisateurs des smart grids pour gérer le trafic généré relatif à un évènement survenu dans le réseau. Dans ce contexte, nous introduisons une nouvelle approche d'agrégation de données et d'envoi de rapports générés localement au Gateway. La nouvelle solution développée est appelée Distributed Event-driven data Aggregation and constrained multipath Reporting (DEAR). Elle permet aux capteurs impliqués dans l'agrégation et la transmission de données de sélectionner leurs canaux sans interférer avec les nœuds voisins. DEAR est basé sur le paradigme de coloration de graphes. Son évaluation de performances révèle qu'il garantit des transmissions de données rapides et des affectations de canaux efficaces dans les CRSNs.

En résumé, les quatre parties contributions de cette thèse réalisent effectivement une allocation opportuniste des ressources spectrales d'une manière distribuée et équitable tout en considérant différentes caractéristiques du système sous-jacent aux réseaux électriques intelligents.

Mots clés: smart grids, réseaux de capteur à radio cognitive, processus de Markov partiellement observés, équité, allocation de ressources radio, canal de contrôle en commun, trafic relatif à un évènement survenu.

Contents

List of Figures

Acronyms

3G Third Generation of Mobile Networks.

4G Fourth generation of Mobile Networks.

Ack Acknowledgement.

ARCEP Autorité de Régulation des Communications Électroniques et des Postes.

CC Control Center.

CCC Common Control Channel.

CO_2 Carbon dioxide.

CR Cognitive Radio.

CRN Cognitive Radio Network.

CRSN Cognitive Radio Sensor Network.

CSMA/CA Carrier-Sense Multiple Access with Collision Avoidance.

CSRA Cooperative Spectrum Resource Assignment.

CTS Clear To Send.

D-SAN Dual-Spectrum Assignment for Neighborhood area networks.

DCA Distributed Control Algorithm.

DEAR Distributed Event-driven data Aggregation and constrained multipath Reporting.

DMS Distribution Management System.

DSA Dynamic Spectrum Access.

DUSA Distributed Unselfish Spectrum Assignment.

FCC Federal Communication Commission.

GCP Graph Coloring Problem.

GHG GreenHouse Gas.

GPS Global Positioning System.

HAN Home Area Network.

HAN-G Home Area Network-Gateway.

ICT Information and Communication Technology.

ISM Industrial, Scientific and Medical.

MAC Medium Access Control.

MHz Megahertz.

MW Megawatts.

NAN Neighborhood Area Network.

NAN-G Neighborhood Area Network-Gateway.

PDR Packet Delivery Ratio.

PHSA Predictive Hierarchical Spectrum Assignment.

PLC Power Line Communication.

POMDP Partially Observable Markov Decision Process.

PU Primary User.

QoS Quality Of Service.

R-PHSA Routing-based Predictive Hierarchical Spectrum Assignment.

RER Renewable Energy Resources.

RTS Request To Send.

SG Smart Grid.

SNR Signal-to-Noise Ratio.

SU Secondary User.

TOU Time-Of-Use.

TV Television.

U.S. United States.

UHF Ultra High Frequency.

UK United Kingdom.

VHF Very High Frequency.

WAN Wide Area Network.

WSN Wireless Sensor Network.

Chapter 1

Introduction

Contents

Smart Grids (SGs) are the modern electrical power grid concept in which information and communication technologies (ICTs) are used to ensure the integrity of the electrical power infrastructure [1–3]. One of the widely recognized communication technologies for the SGs is the cognitive radio sensor networks (CRSNs) [2]. Within this context, this thesis addresses the exploitation of unused licensed frequency bands in CRSNs for non-critical SG traffic transmission.

1.1 Why Smart Grids?

The SGs emerge as a response to multiple problems that face the traditional electrical networks. Some examples of these are:

- Dangerous blackouts [4]: A blackout represents a power shortage that leads to a total crash of the power grid. It is the result of an imbalance between power generation and power consumption. In traditional power grids, there have been more and more massive blackouts. On August 14, 2003, an historical large scale power blackout took place in the United States (U.S.) and Canada. It remained for up to 4 days and affected around 50 million people and 61,800 megawatts (MW) of electric load [5]. Hence, the power grid needs to become more safe and reliable.

- Inefficient power transmission and distribution [6]: The demand for electricity has increased dramatically. As a result, the power grid has become more and more susceptible to congestion. In the U.S., since 2002, congestion costs have come in at $7-10\%$ of annual total billings [7]. Hence, the power grid needs to be more efficient.
- Greenhouse gas (GHG) emissions [8]: The environmental impacts of the electricity generation and distribution are significant. In the United Kingdom (UK), the power sector accounts for 27% of UK total GHG emissions [9]. Hence, the power grid needs to be more economic.
- Shortage in the fossil fuel energy [10]: Fossil fuels, including coal, oil and natural gas, are currently the world's primary energy source [11]. However, as cited in [12], coal reserves are available up to 2112, and will be the only fossil fuel remaining after 2042. Thence, the power grid needs to be more diversified.

The key goal of SG communication networks is then to enhance the safety, reliability, efficiency and economy of more diversified power systems. To achieve this, a set of ICT tools are built on the top of smart sensors/devices deployed everywhere in the grid. These smart sensors/devices help to fulfill multiple SG applications such as building automation, distributed energy generation and outage management [13–15]. The deployed SG sensors can use different communication technologies to communicate [2,16]. One of the candidate SG communication technologies is the cognitive radio technology [1,2].

1.2 What is Cognitive Radio Technology?

All wireless communication signals travel over the air via radio frequencies, called spectrum. Basically, two kinds of spectrum resources exist:

- **Unlicensed spectrum**: Wireless users send data without having licenses from telecommunication regulatory bodies such as the Federal Communication Commission (FCC) in the U.S. and the authority for regulation of the electronic communications and postal sectors (ARCEP) in France [17].
- **Licensed spectrum**: It represents the portion of the spectrum that is assigned to license holders based on long-term basis for large geographical regions [18].

An increasing number of wireless technologies such as WiFi, ZigBee and Cordless phones are today operating in the free access portion of spectrum [19]. Thus, unlicensed frequency bands are getting more and more crowded [20]. From another side, spectrum utilization measurements show that the fixed licensed spectrum assignment policy results in poor spectrum utilization [21,22]. Therefore, to solve the gap between the over-scarce unlicensed spectrum and the under-utilized licensed spectrum, the cognitive radio (CR) technology has been geared to improve the overall spectrum utilization [23]. Being equipped with CR capabilities, unlicensed devices can benefit from intermittent periods of unoccupied licensed frequency bands. Thus, in cognitive radio networks (CRNs), two kinds of wireless users coexist: primary users (PUs) and unlicensed/secondary users (SUs). The PUs are the prioritized spectrum users. They are not aware of the SUs' existence. The SUs have to operate without disturbing the PUs' transmission.

1.3 Motivations and Contributions

The extensive deployment of ICTs to monitor all sets of electrical devices in the power grids results in a large amount of data that should be transmitted from the monitored devices to a central control center (CC) for processing [24]. The collected data may contain information that has to be processed in real time such as outage detection and power demand. However, it may also include information that will be stored for future processing. For example information about underlying causes of critical occurred events, the quantity of consumed/produced energy as well as those related to distributed management and control may not be rapidly sent to a CC [25, 26]. This second kind of data can be exploited to improve and to optimize the electrical network functioning. Thence, using CR technology in SGs to transmit this type of data would be an intelligent low-cost solution that increases the SG efficiency. The CR technology will allow unlicensed SG sensors to prevent congested free access spectrum and to get benefit from temporarily available licensed frequency bands.

In this thesis, we are interested in distributed channel allocations in CRSNs for SG monitoring purposes. However, different electrical applications are monitored in the SGs. They have not all the same impact on the SG power distribution. This results in a prioritized deployment of SG sensors. Thus, our work will focus on fair channel assignment paradigms for SG sensors. A fair spectrum access will be achieved when every SG sensor gets benefits from available frequency bands as its monitored application needs in terms of communication requirements. From another side, in CRNs, one dedicated common control channel (CCC) is widely assumed to exist by the research community. It is used to exchange control messages between SUs. However, this may not always be possible given the licensed network dynamics [27]. Accordingly, all along this dissertation, channels will be opportunistically accessed to transmit data from wireless SG sensors to a SG CC without using a CCC.

In accordance with the CRSN topologies for SGs in addition to the generated SG traffics, we organize our work into four contributions. They mainly focus on the communication aspects in the SG communication access networks where the CRSNs are widely recognized. A smart grid communication access network is composed of home area networks (HANs) and neighborhood area networks (NANs).

Our first contribution is interested in one-hop SG communication network topologies that we need to handle in some smart grid settings such as in smart homes/houses and NANs. The SG sensors are placed one-hop away from a gateway/sink. In this contribution, we introduce more specifically two probabilistic channel assignment mechanisms for the two SG areas mentioned above, namely smart homes and NANs. In smart homes, the sensors periodically collect information from their monitored domestic applications. Thus, we develop a new channel allocation scheme named Cooperative Spectrum Resource Assignment (CSRA) for CRSNs that is targeted to be deployed in smart homes [28]. In CSRA, every node estimates the need of its interfering nodes to transmit data. Then, it predicts the channels that will be used by every deployed node. Spectrum resources are allocated through a Partially Observable Markov Decision Process formulation (POMDP). In NANs, the monitored SG applications have different communication requirements. For example, a sensor that monitors a military office is more important than a sensor monitoring a simple home located in the same neighborhood. Thus, we propose a Distributed Unselfish Spectrum Assignment approach (DUSA) for the CRSNs deployed in NANs [29]. DUSA allows every sensor to access to the spectrum according to the requirements of its monitored application. Performance evaluation of both CSRA and DUSA reveals their capacity to fairly share the spectrum resources and to improve the spectrum utilization compared to CCC-based resource allocation schemes while both solutions don't use CCCs.

The second contribution of this thesis tackles the SG sensors' short transmission range. Thus, we propose the deployment of forwarding nodes to extend the SG sensors' coverage. Then, we introduce the Dual-Spectrum Assignment for NANs (D-SAN). D-SAN focuses on the channel assignment in the proposed two-stage NAN topology. It is composed of two channel allocation schemes. The first scheme is used by NAN monitoring sensors to send their generated data to forwarding nodes. Channels for the first stage communication are allocated based on the impact of every monitored application on the electricity distribution. Then, the second scheme is executed by forwarding nodes to allocate channels for their communication with a sink/gateway. The channel allocations of both approaches are based on POMDPs. Simulation results demonstrate that D-SAN is able to efficiently achieve a differentiated channel allocation in such a two-stage SG CRSN deployment scenario. This is valid, however, only if the area to be covered is not too large. Now, if this one is large, the data transmission to the gateway can take place in a multi-hop manner through the deployed SG sensors (this is, of course, subject to network density). In this case, the use of specific forwarding nodes can be avoided.

Our third contribution is then interested in hierarchical multi-hop data transmissions in CRSNs for SGs. Here, we focus on spectrum sharing in cluster-based CRSNs. Thus, we design a novel Predictive Hierarchical Spectrum Assignment (PHSA) scheme in CRSNs [30]. First, PHSA organizes sensors into clusters. Then, licensed channels are distributively affected to SUs for intra-cluster and inter-cluster communication through a POMDP. In the second part of this contribution, we introduce the Routing-based PHSA (R-PHSA).

R-PHSA is an extension of PHSA that takes into consideration the routing aspects during the channel assignment process. Simulation results of both PHSA and R-PHSA show their balanced spectrum sharing among deployed sensors and their capability to outperform existing clustering approaches without being dependent on a CCC. Now, in the first, second and third contributions, we concentrate our efforts on periodic smart grid data reporting to the control center. However, a second kind of smart grid traffic is present in the network. It is the event-based traffic.

Thus, our fourth and last contribution is rather interested in channel allocation for event-based generated SG traffic. Here, we introduce a new channel allocation scheme for CRSNs, called Distributed Event-driven data Aggregation and constrained multipath Reporting (DEAR) [31]. DEAR is used by sensors deployed for early events' detection in distribution SG substations. To perform an efficient data processing, DEAR uses the clustering during the data aggregation phase. Then, it performs the data reporting through a constrained multi-hop Beam routing. In both phases, the channel allocation is achieved based on the graph coloring paradigm. DEAR's performance evaluation shows its capability to efficiently assign channels during the data aggregation and the data reporting phases.

The contributions presented above are further investigated in details throughout this dissertation as it is described in the next section.

1.4 Organization of the Thesis

This dissertation shows, throughout seven chapters, how channels would be assigned to SG cognitive radio sensors without using a CCC to exchange control messages before every access to the spectrum. Channel allocation processes will be studied while considering the different deployment scenarios of CRSNs for SG monitoring. The organization of this thesis is as follows:

In Chapter 2, we present the motivations behind the transitions from traditional electrical grids to SGs. We also list the SG characteristics and challenges that may face SG communication networks. Then, we detail the motivations behind using the CRSNs for SG systems. Thereafter, we present an overview of the cognitive radio technology. Finally, we position our work in relation to the existent literature.

Chapter 3 details our first contribution. Specifically, we describe the network settings in smart homes and in NANs. Then, we detail the metrics that are used by both smart home and NAN sensors to estimate the need of every node to transmit data. Thereafter, we introduce the proposed channel allocation approaches, CSRA and DUSA. Extensive simulations of both CSRA and DUSA are then performed and discussed showing their fair channel allocation and their capacity to improve the spectrum usage compared to existing solutions while avoiding using a CCC.

Through Chapter 4, we introduce our second contribution. Here, we propose the use of forwarding nodes to extend NAN monitoring sensors' coverage. Thus, we present a new CRSN topology for NAN monitoring. Then, based on this network organization, we develop D-SAN, a new channel allocation scheme for two-stage CRSNs for NANs. Simulation results prove that the proposed scheme achieves a balanced channel allocation among prioritized NAN sensors.

In Chapter 5, we present our third contribution. In this chapter, we opt for hierarchical CRSN deployment for NANs. We develop a new clustering algorithm that is not dependent on a CCC. Then, we present the PHSA scheme to allocate channels in hierarchical CRSNs for SGs. Thereafter, we develop R-PHSA, as an extension of PHSA to improve the routing aspects in PHSA. Performance evaluation results are then discussed to reveal that both schemes achieve a differentiated spectrum sharing among deployed SG sensors that responds to the heterogeneous generated traffic requirements.

In Chapter 6, we detail the fourth and last contribution. Thus, we introduce the network model that allows the distributed channel allocation once an event is detected. Then, we introduce our DEAR approach. In other terms, we detail the channel allocation during the data aggregation and reporting phases. Finally, simulation results are discussed to show the DEAR 's rapid data transmission and efficient channel assignment.

To conclude, we briefly sum up our contributions and we explore future research directions as well, in the final chapter.

Chapter 2

Cognitive Radio Sensor Networks for Smart Grids: Motivations, Challenges and Opportunities

Contents

Smart grids (SGs) are the new trend of the electric power grid development. To bring the SGs into existence, advanced communication/networking technologies are integrated into the electrical power grids [32]. Cognitive radio sensor networks (CRSNs) have been widely considered as an edge cutting technology to make the electrical grid smarter. In this chapter, we first introduce the existing research efforts on motivations, challenges and opportunities of SGs communication networks. Next, we focus on the CRSN capabilities, functioning and deployment for SGs. Thereafter, we position our problems in relation to the identified issues in the two introduced technologies, i.e., the SGs and the CRSNs.

2.1 Smart Grid Communication Networks

The SG concept represents a new challenging direction in communication research. This challenge lies in the complex system of electrical power grids. In this section, we explain in detail the need to a transition from traditional power grids to SGs. Then, we introduce the existing SG communication network architecture, the generated SG traffic characteristics and the commonly encountered problems that impede successful SG communication networks. Finally, we present the needs of SGs to CRSNs.

2.1.1 From Traditional Electrical Networks to Smart Grids

Large parts of electrical power grids are more than a century old [33]. During all this period, there has been no change in the basic structure of the electrical power grid [16, 34]. However, different other industry sectors have dramatically changed due to the integration of information and communication technologies (ICTs) into our daily life. Thus, the electrical networks are today creaking and struggling to satisfy the modern consumers' supply. As a result, the appearance of SGs and the coverage of electrical infrastructure by communication networks became a necessity to make the electrical grid suitable for our modern life. In the following, we present the key motivations of empowering the electrical power grid by incorporating communication network capabilities into it building up the first layer of the SG concept [35].

2.1.1.1 Motivations

- **Improved quality of service**: A principle objective for ICTs in SGs is to enhance the quality and the reliability of the services provided to final consumers. SG communication networks allow to reduce outage times when failures take place in power systems [36]. Furthermore, different communication technologies are able to detect and locate a potential equipment failure before an outage occurs. For example, transformers with communicating sensors can provide temperature and loading data to the SG distribution management system (DMS). Thereafter, the DMS can, in turn, identify a potential failure point and then predict an outage [37]. From another side, thanks to the new costumer notification methods that may include different information such as billing status and "day before" announcements of critical peak event days, the final consumers are now able to understand, manage and optimize their energy usages [38].
- **Lower fossil fuels consumption/carbon dioxide emissions**: The continuous electrical infrastructure control reduces the consumers' peak demand charges. Thus, electrical networks will not suffer from blackouts. As a consequence, carbon dioxide (CO_2) and greenhouse gas emissions caused by blackouts and electrical grid congestion during peak hours will be minimized. Furthermore, inefficient fossil fuel burning will be reduced [39].
- **Facilitated renewable energy integration**: According to United States Department of energy report [40], the electricity demands have increased by 2.5% during the last 20 years. Thus, given the proven fossil fuel reserves fluctuation, renewable energy resources such as wind, solar and hydro power represent efficient solutions to face the increasing serious energy shortage. However, many renewable energy sources are intermittent in nature. Thus, communication technologies in SGs play a crucial role to integrate these energy resources into our daily consumption of electricity. In fact,

they provide the SG DMS detailed information on the quantity of energy generated by renewable energy sources distributively installed in the grid. Thereafter, the SG DMS improves their decisions and re-configures the network topology to distribute the electricity in a more efficient manner [41].

2.1.1.2 Smart Electrical Network Characteristics

The emergence of the SG technology has introduced various changes in the electrical power grid structure and in its concept of functioning. In the following, we summarize the main differences between a traditional and a modern power grid [42].

- **Distributed electricity generation**: Electrical networks were primarily built for centralized power generation and electricity is delivered from one end to the other. In modern electrical grids, the electricity is generated in a distributed manner. Renewable power generators are installed distributively, in locations where environmental conditions promote an efficient power generation. Furthermore, in SGs, the power flow is bidirectional. Every final user can produce his own power energy and distribute/buy it to/from his neighborhood [43].
- **Consumer participation**: In a traditional power grid, the users are unaware of their consumption. They are not involved in the energy distribution. However, today, the SG communication infrastructures are able to provide a bidirectional data flow between the consumers and the SG control center. Thus, a SG power consumer becomes active and always involved in organizing and managing his energy consumption [35].
- **Sensors**: In traditional power grids, a limited number of smart communicating devices, i.e. sensors, are deployed and they are deployed only in certain control systems and transmission lines. However, in SGs, the sensors are tremendously deployed. They cover entirely the power infrastructure [44].
- **Integrating renewable energy resources (RERs)**: The main advantage of SGs is the ability to better integrate RERs into the power network and supervise power production and consumption thanks to SG communication networks.

  Table 2.1, summarizes the comparison between SGs and traditional power grids.

2.1.2 Smart Grid Communication Network Architecture

In SGs, ICTs are integrated into the power infrastructure starting from the main/central power generators to the user-end premises. Therefore, the SG communication network architecture that is commonly accepted in the literature is designed in accordance with

Table 2.1: Traditional power grids vs smart grids.

Characteristics	Traditional grids	Smart grids
Electricity generation	Centralized	Distributed
Grid topology	Radial	Network
Sensors deploymet	Few sensors	Lot of sensors
Information/power flow	Unidirectional	Bidirectional
Consumer participation	Passive	Active
Integrating RERs	Seldom	Often
Outage recovery	Manually restoration	Self-reconfiguration
Control type	Passive control	Active control
Environmental pollution	High	Low

the electrical network architecture [1, 2, 32, 34, 42, 45]. As illustrated in Figure 2.1, a general architecture for SG communication networks is composed of three segments: Home Area Networks (HANs), Neighborhood Area Networks (NANs) and Wide Area Networks (WANs). In the following, we present these three representative SG segments.

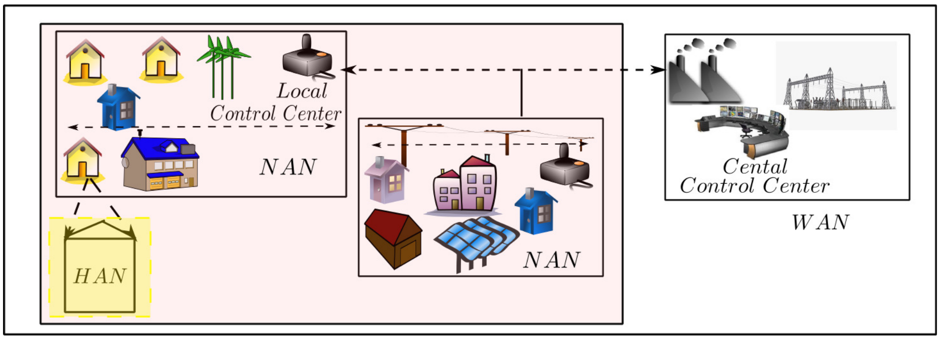

Figure 2.1: Smart grid communication network architecture.

2.1.2.1 Home Area Network (HAN)/User-End Premise

Sensors are in charge of controlling a variety of smart devices within a home. They send the collected/sensed information to a HAN-gateway (HAN-G). The HAN-G is the central node. It communicates with the external environment. Furthermore, in SGs, every home is equipped with a smart meter that can be integrated with the HAN-G. It provides instant information to consumers such as their power bills, time-of-use (TOU) prices and TOU rates [46]. A HAN covers up to 200 m^2 and HAN sensors communicate with a data rate that may reach 100 kb/s.

2.1.2.2 Neighborhood Area Network (NAN)/Power Distribution Segment

NAN endpoints are basically the smart meters and HAN-Gs. They send their collected homes' information such as energy consumption and production recording to local control centers (CCs). The smart meters play a crucial role in SGs. In fact, the information sent to local CCs is used for many purposes, to follow the users' power consumption records, to efficiently distribute electricity, to integrate renewable energy resources into our daily power usage and so on. NAN endpoints integrate multiple other wireless devices such as power quality monitoring devices deployed in distribution feeders and transformers, smart cameras, etc. Thus, data including different kinds of information such as distribution automation, power outage management and power quality monitoring is transmitted to local CCs to be thereafter sent to the central SG CC [47]. NANs usually span several square kilometers, and each smart meter needs from 10 to 100kb/s to transmit data [48].

2.1.2.3 Wide Area Network (WAN)/Power Transmission Segment

WAN serves as backbone for communication between NAN local CCs, SG substations, and the central CC [2]. It covers electrical segments where large amounts of bulk power are generated by bulk generation and then delivered to the distribution segments [49]. WANs may cover very large areas and generally the WAN data transmissions require from 10 to 100 Mb/s.

Figure 2.2 provides in relation to the SG segments an overview of the different SG applications. Furthermore, Table 2.2 gives the main technologies that suit these applications' requirements [2, 16].

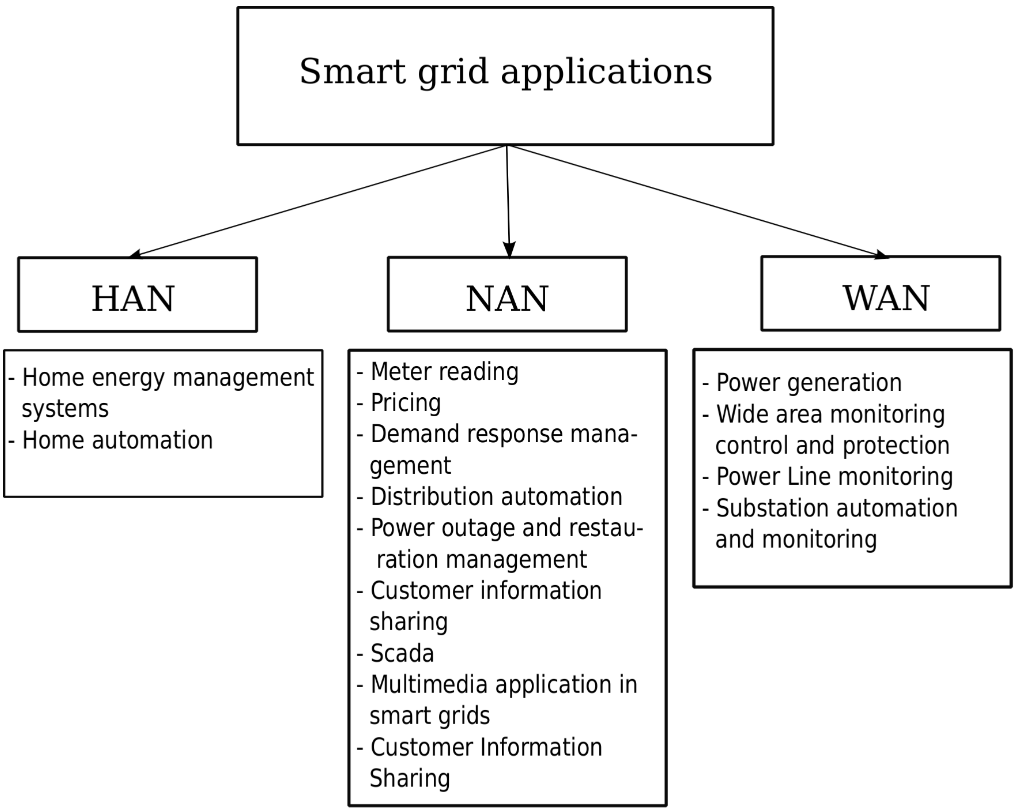

Figure 2.2: Smart grid applications.

Table 2.2: Smart grid communication technologies.

Technology	Licensed/ Unlicensed spectrum operation	Data rate	Applications	SG segment	Limitations
WSN	Unlicensed	250 Kbps	Smart lighting, Energy monitoring, Home automation, Automatic meter reading	HAN, NAN	Low data rate, short range
GSM	Licensed	Up to 14.4 Kbps	SCADA, Automatic meter reading	HAN, NAN	Range depends on the availability of cellular service, Expensive call costs
WiMAX	Both	Up to 75 Mbps	Real time pricing, Outage detection and restoration	HAN, NAN	Network speed degrades with increasing distances, costly radio frequency hardware, High frequencies do not penetrate through obstacles
Optical Network	Licensed	Up to 500 Mbps	Physical network infrastructure control	NAN, WAN	High-cost, Interoperability
Digital Microwave Technology	Licensed	Up to 3Gbps	Alarm between distributed energy resources and distributed substation feeder	NAN, WAN	Susceptible to precipitation, Multipath interferences
Power Line Communication (PLC)	-	2-3 Mbps	Automatic meter reading, Low voltage distribution	HAN, NAN	Harsh and noisy medium, Low bandwidth

2.1.3 Challenges in Smart Grids

Given the large geographical area of the electrical power network and its direct impact in our daily life and in almost all industrial sectors, the choice of the appropriate SG communication technologies should be performed in a way to raise all the following challenges [48,50]:

- **Challenging environment**: The SG power infrastructure is largely affected by natural catastrophes and difficult weather conditions that may result in blackouts and outages extremely expensive for the electric utilities [34]. Under harsh climate, SG communication networks should continuously and reliably transmit data to the SG CC. Thus, SG communication networks should support a secure end-to-end transport layer.
- **Quality of Service (QoS)/Variety complexity**: As in [51], the SG traffic is basically classified into alarm and periodic data. Moreover, given the various SG applications that may coexist in the same area, every kind of traffic may be divided into multiple sets of data with different priorities, traffic characteristics and impacts

on the electricity distribution [48]. Thus, SG communication networks should ensure that the QoS requirements of all kinds of traffic are meet.

- **Highly varying traffic/Velocity complexity**: The quantity of generated SG traffic varies very frequently during a day according to many factors [52]. For example, solar energy is only available for a certain period of time during a day. Thus, the quantity of data generated by sensors and smart meters controlling renewable energy resources depends on the availability of these resources. Thence, SG communication networks should adapt to a large fluctuation of the SG traffic while keeping the QoS requirements [50].

- **Large amount of data/Volume complexity**: In SGs, smart meters are widely deployed. Moreover, different other SG data sources are deployed in SGs such as:

  - Energy market pricing and bidding,
  - Management, control and maintenance of equipments in the three SG segment,
  - Operating utilities.

  Therefore, we can conclude with the huge amount of the large variety of traffic with different characteristics that should be transmitted on the SG communication networks. As stated in [25], by 2009, the amount of data in electric utilities' system has already reached the level of TeraBytes (TBs) per day. Accordingly, a massive amount of such data, continuously generated, places pressure on the SG communication infrastructure due to the limited bandwidth and spectrum resources [25, 50].

- **Veracity complexity**: The reliability and the correctness of SG data play a profound role for decision making in electrical networks [53]. In fact, given the large amount of SG traffic and the abnormality in data, SG utilities should be prudent when making decision since collected data may be uncertain and imprecise.

- **Interoperability**: The SG communication network represents a system of heterogeneous systems where the SG data travels among them. In every area, a variety of communication technologies and standards may coexist to respond to specific QoS requirements of different types of SG applications. Therefore, interoperability becomes a large challenge to make a SG works [50].

- **Security**: The tight dependence between the communication and the power infrastructures has introduced new threats into the cyber-physical system. In fact, adversaries can make use of the vulnerabilities in cyber-security to disrupt the operations of SG by paralyzing or manipulating the communication networks [54].

2.1.4 Cognitive Radio Sensor Network as a Key Technology for Smart Grids

Given the above presentation, the 4-V factors (**V**elocity, **V**olume, **V**ariety and **V**eracity complexities) describing the SG data characteristics completely illustrate its big data aspect [24–26, 55].

In this context, several works were interested in the SG massive data problems and multiple techniques were proposed to ensure efficient analysis and storage of the SG data [26, 56, 57]. In the same direction, the SG big data aspect should also be considered at the communication level. For instance, the communication technology for SG data transmission have to be carefully chosen since a reliable SG data transmission directly impacts all the other SG functions.

2.1.4.1 Wireless Sensor Networks for Smart Grids

As shown in Table 2.2, multiple communication technologies have been proposed to control the SGs. In fact, given the SG massive data property and the large geographic extent, restricting the SG communication network to a simple high data rate technology such as optical network and WiMAX would be very expensive. The deployment of such expensive technologies can be limited to critical SG data that has to be transmitted and processed in real time. As a result, in the literature, economical communication technologies, such as power line communication (PLC) and wireless sensor networks (WSNs), represent the widely recognized communication technologies for the SGs [58–62].

PLC represents a natural candidate since it does not necessitate additional communication infrastructure [60]. It uses the existing wiring power infrastructure to transmit data traffic. However, electromagnetic interference is a major challenge that negatively impacts the power line data transmission. Furthermore, its signal quality is widely affected by the power network topology that may be damaged after a natural disaster.

On the other hand, WSNs have particularly attracted the attention of research and industrial communities especially for short distance connection in SGs [60]. The collaborative and low-cost nature of WSNs bring multiple benefits over traditional electric monitoring systems, including accurate sensing capabilities, improved fault tolerance, extraction of localized events. Under realistic environmental conditions, works in [61, 63, 64] showed that WSNs are able to support different SG applications such as: meter reading, real time pricing, building and industrial automation, line fault and outage detection, as well as wind/solar farm Monitoring. Furthermore, the wireless communication capabilities of WSNs make this technology as a candidate solution for SGs for the following reasons [34]:

- It facilitates the integration of intelligent mobile devices such as smart control devices and electrical vehicles. In fact, these systems have an important impact on improving the human power consumption behavior, giving a clear record of its consumed energy and smoothing the power flow of SG [65].

- It allows the control of renewable energy resources in isolated areas such as mountains and islands [66].
- Natural catastrophes and severe weather have less negative impacts on wireless communication compared to the high-cost technologies such as fiber optical networks [34].

In this regard, WSNs enable low-cost and low-power communications for diverse sets of smart grid applications.

2.1.4.2 Cognitive Radio Sensor Networks for Smart Grids

In the same context, multiple short range wireless technologies have been developed for WSNs, i.e., IEEE 802.15.4 [67], Zigbee [68] and WirelessHART [69]. Generally, these technologies use the unlicensed ISM (industrial, scientific and medical) bands that are also shared with different other wireless standards. Table 2.3 illustrates the usage of ISM bands used by the IEEE 802.15.4 standard and their corresponding applications. On the one side, in recent years, the global wireless data usage has grown by nearly 70% annually [70]. Thus, given the free spectrum access in the ISM bands, the number of wireless users operating in unlicensed channels is in continuous growth leading to an over-crowded unlicensed spectrum resources.

Table 2.3: The IEEE 802.15.4 defined frequency bands.

Frequency low	**Frequency high**	**Number of frequency bands**	**Availability**	**Applications**
868.0 MHz	868.6 MHz	1	Europe	UNB / Sigfox Z-Wave / Sigma Designs Weightless-N / Nwave
902.0 MHz	928.0 MHz	10	America, Greenland and eastern Pacific Islands	UNB / Sigfox LoRa Z-Wave / Sigma Designs Weightless-N / Nwave
2.4 GHz	2.48 GHz	16	Worldwide	Bluetooth 802.15.1 WiFi 802.11b/g ZigBee 802.15.4

On the other side, available literature shows that spectrum utilization, on a block of licensed radio frequency band, varies from 15% to 85% at different geographic locations at a given time [71]. Thus, the over-crowded unlicensed spectrum and the under-utilized licensed spectrum resources encourage researchers to allow SG sensors, primarily operating on unlicensed spectrum, to get benefits from temporally available licensed frequency bands through the cognitive radio technology [72]. Therefore, CRSNs represent an intelligent and low-cost solution to deal with crowded unlicensed spectrum and to improve the SG data transmission throughput.

In SG cognitive radio networks (CRNs), the SG sensors are considered as secondary network users (SUs). Their access to the spectrum is conditioned by the licensed channels' vacuity of primary users (PUs). In the opposite, in traditional WSNs, sensors are primary spectrum users since there is no privileged PUs and all users have the same right to access to the unlicensed spectrum. However, field tests in ISM frequency bands showed that wireless links in SG environment have high packet error rates and variable link capacities because of obstructions, electromagnetic noise, multipath effects and fading [61]. Accordingly, despite the prioritization of unlicensed users during their transmissions in traditional WSNs, if a sensor encounters noises during its transmission in an ISM frequency band, it will be then difficult to prevent the use of this noisy channel and to switch to another one. In fact, the number of ISM bands is limited and they are shared with multiple other technologies. Thus, when SG sensors utilize both unlicensed and licensed spectrum, if a node encounters a high noise or PU signals at a particular spectrum band, then, it switches to another available frequency band that allows a better signal propagation and coverage such as the available TV channels [73, 74] or it adapts its communication parameters and keeps the same used spectrum resources without disturbing the primary signal. Indeed, the TV channels placed in the VHF and UHF spectrum provide a better coverage than unlicensed channels. They travel further and penetrate buildings easily [75].

To sum up, CRSN deployment for SG systems can be exploited to deal with the unlicensed spectrum scarcity and to address the harsh propagation conditions of SGs. In the following, we introduce in detail the cognitive radio technology and an overview of exiting works that recognize the use of this technology for the SG monitoring.

2.2 Cognitive Radio Sensor Networks

The cognitive radio (CR) is a critical enabling technology for future communication and networking. It enables unlicensed users to exploit the channels' vacuity as far as primary users claim access to resources [76]. In the U.S., the FCC has opened up unused licensed TV bands called TV white space for unlicensed opportunistic use. TV white space is designated to a specific portion of VHF/UHF bands, i.e., 54-698 MHz in the U.S. and 470-790 MHz in Europe [77]. In this section, we first introduce, the sensors capabilities when being equipped with the CR technology. Then, we present the medium access control (MAC) and the control message exchange strategies used in CRNs to allow the opportunistic access to licensed spectrum.

2.2.1 Cognitive Radio Functionalities

In CRNs, cognitive sensors/devices, .i.e., SUs, can dynamically adapt their operating parameters such as transmission power, frequency and modulation type to their used spectrum and surrounding radio environments. However, before adapting these parameters, the SUs have to get necessary information from the radio environment. To this end, the SUs are equipped with the following CR functionalities.

2.2.1.1 Spectrum Sensing

Spectrum sensing is one of the basic function of CRNs. It allows SUs to detect licensed signals and then to identify the vacant channels. Available spectrum resources are called spectrum holes. Different spectrum sensing techniques are available in CRNs. Table 2.4 lists the most important techniques in this context.

Table 2.4: Spectrum sensing techniques.

Techniques	**Test statics**	**Advantages**	**Disavantages**
Energy detection	Energy of the received signal samples	- Easy to implement - Does not require prior knowledge about primary signals	- Very unreliable due to noise uncertainty - Cannot differentiate a primary source from other signal sources
Feature detection	Cyclic spectrum density function of the received signal, or by matching general feature of the received signal to the already known primary signal characteristics	- More robust against noise uncertainty and better detection in low signal-to-noise ratio (SNR) regime than energy detection - Can distinguish among different types of transmissions and primary systems	- Specific features must be associated with primary signals - Particular features may need to be introduced
Matched filtering and coherent detection	Projected received signal in the direction of the already known primary signal or a certain waveform pattern	- More robust to noise uncertainty and better detection in low SNR regimes than feature detection - Requires less signal samples to achieve good detection	- Requires precise prior information about certain waveform patterns of primary signals - High complexity

Given the possibility of false PUs' detection, different strategies have been proposed in the literature to decide about the availability of the sensed resources [78]:

- **Distributed/Local sensing**: Every SU is able to independently determine the presence or absence of licensed signals in a certain spectrum.

  - **Advantages**: low computational and implementation complexities.
  - **Disadvantages**: sensitive to model uncertainty, fading and shadowing. Thence, feature and matched filter detection are the most recognized sensing techniques for the distributed sensing.

- **Cooperative sensing**: the spectrum sensing results from multiple SUs are used to detect licensed signals.
  - **Advantages**: Accurate licensed signal detection. Moreover, it reduces the required sensing time.
  - **Disadvantages**: The implementation complexity is high. Accordingly, the energy detection technique is generally recognized as the well suited for a cooperative spectrum sensing.

2.2.1.2 Dynamic Spectrum Access

Dynamic spectrum access (DSA) is a new strategy to share spectrum. It allows SUs to access to spectrum holes in licensed portions of spectrum. As introduced in [79, 80], three spectrum sharing paradigms exist:

- **Underlay transmissions**: SUs are allowed to share an occupied licensed channel while generated interference stays below a given threshold. This spectrum sharing strategy results in poor performance compared to the amount of generated interference it can cause to PUs.
- **Overlay transmissions**: SUs exploit the knowledge of PUs' messages to either cancel or mitigate interference at both primary and secondary users' side.
- **Interweave transmissions**: A SU transmits only in spectrum holes, i.e., in available frequency bands. Periodically, it senses its used channel. If it detects a licensed signal, then it immediately vacates the channel to avoid harmful interference.

2.2.2 Control Information Exchange in Cognitive Radio Networks

In CRNs, before starting data transmission, control messages are exchanged among the SUs. They may contain signaling information, i.e., request to send (RTS)/clear to send (CTS), spectrum sensing results, routing information, etc. Basically, three techniques exist to allow the control message exchange [23, 81]:

- **Out-of-band control channel**: SUs share one dedicated common control channel (CCC), assumed to be always free of licensed signals. This technique does not require synchronization among SUs. Furthermore, to prevent that a node misses control messages sent by other nodes, every SU is assumed to be equipped with a dedicated transceiver that is continuously tuned to this CCC (Figure 2.3).

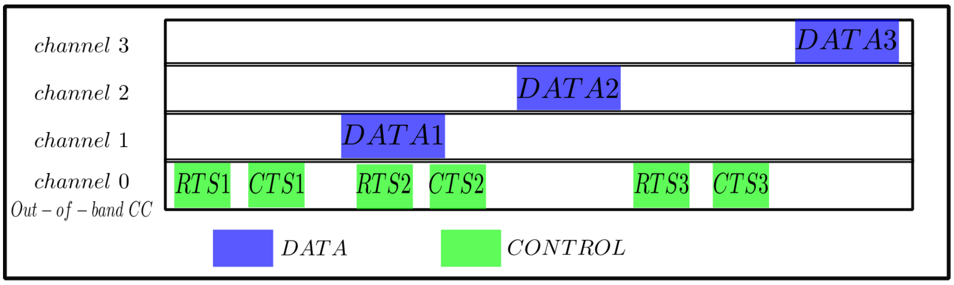

Figure 2.3: Out-of-band control channel.

- **In-band control channel**: In the opposite of the out-of-band control channel solution, here the dedicated CCC is one of the channels used to opportunistically transmit data. Time is divided into two parts: a control phase and a data phase. As shown in Figure 2.4, during the control phase, all sensors switch their transceivers to an available channel (the CCC) to overhear control messages and to be aware of the network status. Thus, during this period, SUs don't gain access to the channels sensed free of PUs. Therefore, free data frequency bands are wasted and system efficiency is reduced.

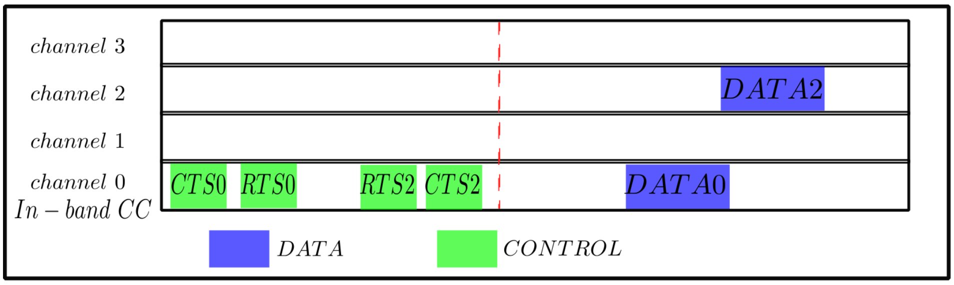

Figure 2.4: In-band control channel.

- **Channel hopping sequence**: Based on a list of licensed channels, every node fetches a vacant channel by continuously switching from one channel to another (Figure 2.5). In addition to the high energy consumption, the channel hopping scheme also engenders delayed data transmission. In fact, in [82–84], the authors designed the order of channels to visit in order to minimize the required time to achieve a successful RTS/CTS message exchange between a receiver and an emitter on available channels.

The first two techniques, i.e., out-of-band and in-band control channel, represent the most common techniques in literature. Especially, the out-of-bands control channel technique is widely used since a CCC is assumed to be always free of PUs [85–87]. However, in real environments, these techniques cannot be easily deployed and may have many inconveniences such as:

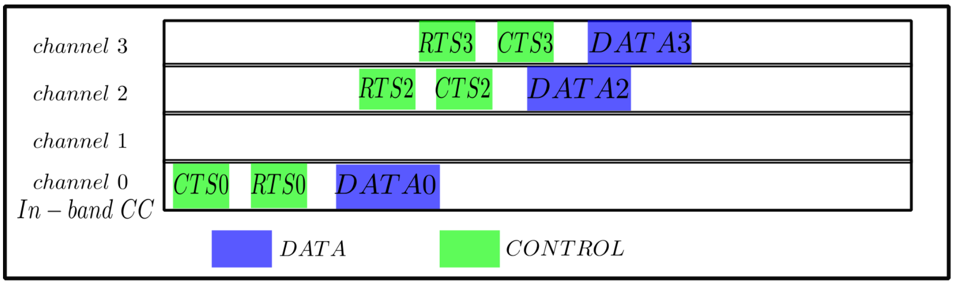

Figure 2.5: Channel hopping sequence.

- Finding one CCC always free of PUs is not practical: Given the dynamic PUs activities, we cannot prohibit the access of PUs to a given channel since it is used as a CCC. Thus, if the CCC is sensed occupied by licensed signals, then SUs will postpone their data transmissions.
- A CCC may represent a bottleneck: If a large number of contenders transmit data at the same time, then the increasing number of control messages saturates the CCC which leads to failed channel allocation and potentially poor performances [72].
- A CCC threatens the system's security: A dedicated CCC is widely used by attackers. They can jam the dedicated CCC and then the communication would not be possible. Moreover, they can use it to attack the privacy of users [88, 89].

2.3 Problem Position in Relation to the Studied Literature

All along this thesis, we recognize the deployment of CRSNs in SG power access networks. Our work focused on the power distribution segment, since in the proximity of inhabitants' zones, several telecommunication operators provide paying services to citizens, such as 3G and 4G on licensed bands that may be, depending on the user traffic, vacant of any signal [2]. We consider the CRSNs as an intelligent solution to deal with the large amount of SG data and with the limited unlicensed spectrum resources. Different works in literature focus on the deployment of CRSNs for the two SG communication networks covering the power access network: the smart homes and the NANs [50, 90–95]. These works, especially, investigate the architectural deployment of CRSNs in both smart homes and NANs. In fact, given the centralized electrical power control and monitoring, they always consider the presence of one central gateway in every monitored area. The gateway collects information from the existing sensors. Furthermore, two CRSN topologies are basically considered to deploy the SG sensors: one-hop and multi-hop topologies. [90, 91] and [50] have used the one-hop topology to deploy CRNs for SG systems. The SG sensors are in direct communication with their associated gateway. Despite its simplicity, the one-hop topology is not always practical given the sensors' short transmission range. Accordingly, in [92–94] and [95] the multi-hop data transmission has been used to achieve the communication between the gateway and the SG sensors.

Now, the overview that we presented in this chapter about the SG communication network characteristics, architecture, and challenges, in addition to the CRN functionalities and strategies used to exchange control messages, drives us to concentrate our efforts on the communication aspects in CRSNs for SGs. The objective of our thesis is to provide spectrum sharing solutions for SG CRSNs, while avoiding a CCC use to exchange control messages before every access to the spectrum. Every deployed SG sensor becomes able to predict the channels' vacuity of its neighbors. This estimation allows distributed channel allocation processes that avoid control messages exchange among the sensors before every access to the spectrum. Furthermore, all along this dissertation, we are interested in the SG data transmission from SG monitoring to a central gateway. Data is fairly transmitted to a gateway, while taking into consideration different deployment topologies of CRSNs in SGs.

Our first contribution focuses on spectrum resource allocations in one-hop CRSNs for smart homes and NANs. A balanced opportunistic access to the spectrum is achieved in every system. It considers the heterogeneity in the channels' availability in addition to the heterogeneous sensors' need to access to the spectrum. The second and the third contributions investigate fair channel assignments in multi-hop CRSNs for SGs. Based on CRSN deployment scenarios for SGs, SG data is sent to a gateway in a multi-hop manner. In the second contribution, we introduce a two-stage CRSN topology for NANs. We use forwarding nodes to extends monitoring NAN sensors' coverage. In the third contribution, the multi-hop data transmission to the sink is achieved through deployed monitoring sensors based on a hierarchical CRSN topology. Finally, in the forth contribution, we concentrate our effort on the event-based generated SG traffic since in the previous contributions we are interested in periodic SG data transmissions. A fair data transmission is achieved when all sensors that detect the same information gain access to the spectrum and correctly transmit their data in a multi-hop manner to a central gateway without using a CCC.

2.4 Conclusion

Intelligent electrical networks are attracting the research and industrial communities given their challenging and unique characteristics. Besides, cognitive radio technology represents an intelligent and low-cost solution to improve unlicensed SG users data transmission. In this chapter, we reviewed SG communication network characteristics, architecture, challenges and needs for cognitive radio technology. Then, we reviewed the cognitive radio technology. Finally, we explained our contributions related to SGs and CRSNs. Accordingly, in this dissertation, we concentrate our efforts on CRSN deployment for SG power access networks. We focus on the spectrum resource assignment for smart grid users while avoiding the CCC use to exchange control messages before every access to the spectrum. All along this dissertation, we develop new channel assignment solutions that don't use a CCC. They exploit potential CRSN deployment topologies for SGs, as well as the different existing types of electrical traffic. In the next chapter, we investigate channel assignment paradigms in one-hop CRSN topology for HANs and NANs to periodically transmit data to a gateway. The forth and the fifth chapters focus on periodic data transmissions to a NAN gateway through two different multi-hop CRSN topologies for NANs. Then, Chapter 6 tackles the distributed channel allocation once an event-based traffic is generated in SGs without using a CCC. The different contributions will be detailed in the next chapters.

Chapter 3

Fair Channel Assignment for CRSN-based One-Hop Smart Grids

Contents

One-hop CRSNs are widely considered for SG control, especially for monitoring smart homes and neighborhood area networks (NANs). In this chapter, we are interested in distributed and fair channel assignment for one-hop CRSNs deployed to monitor these two SG systems. Here, we focus on periodic transmissions on SGs such as traffic related to smart metering, building automation and distributed energy management. We propose two different spectrum sharing schemes adapted to each studied SG systems:

- **CSRA**: The Cooperative Spectrum Resource Allocation in CRSNs for smart homes.
- **DUSA**: The Distributed Unselfish Spectrum Assignment in CRSNs for smart grid NANs.

CSRA allows sensors monitoring smart homes to estimate their neighboring nodes' needs to send their data and then to predict their selected channels. Hence, all SG sensors have the same priority to access the radio channels. DUSA is adapted to SG NANs where the SG sensors have different priorities and impacts on the controlled electrical infrastructure. In both schemes, we use Partially Observable Markov Decision Processes (POMDPs) to allow SG nodes to fairly and distributively allocate channels, without using a CCC.

The remainder of this chapter is organized as follows. In Section 3.1, we present the motivations behind adopting the two channel assignment schemes CSRA and DUSA in one-hop CRSNs deployed to monitor smart homes and NANs, respectively. In Section 3.2, we illustrate a literature review of existing works on distributed channel assignment in flat CRSNs. Thereafter, in Section 3.3, we present our system model. The fairness metrics that we use to estimate the need of every SG node to access to the spectrum are introduced in Section 3.4. The proposed channel assignment schemes, CSRA and DUSA, are introduced in Sections 3.5 and 3.6, respectively. Then, in Section 3.7, we evaluate the performance of the two proposed schemes through simulations. Discussions conducted based on obtained results are illustrated in Section 3.8. Finally, in Section 3.9, we conclude the chapter.

3.1 Context and Motivations

Power distribution segments play an important role in SGs since consumers' buildings and renewable energy resources are placed in this segment. Accordingly, in the electrical power distribution networks, there are two kinds of communication networks that have to be considered: the indoor and the outdoor communication networks.

- The indoor systems are the HANs, i.e., the communication networks deployed to control consumers' areas. Figure 3.1 depicts a general one-hop indoor communication network. One central node called the HAN's gateway (HAN-G), periodically, collects data from the sensors monitoring domestic electrical appliances. The collected data contains information related to the amount of energy consumed and produced by every monitored domestic appliance. Thus, all sensors placed in the same consumer's home, have to fairly share available spectrum resources to allow the HAN-G to get clear measurements of the power consumption and production inside the home.
- The outdoor communication networks are the NANs. In a NAN, the HAN-Gs are considered similar to simple sensors. They, periodically, transmit their collected data to a local control center, i.e., the NAN's gateway (NAN-G). As depicted in Figure 3.2, a NAN-G also receives data from all sensors monitoring the various NAN's electrical elements such as sensors responsible of street lights, solar power plants, administrative buildings, residential homes, etc. The NAN-G uses the data collected from

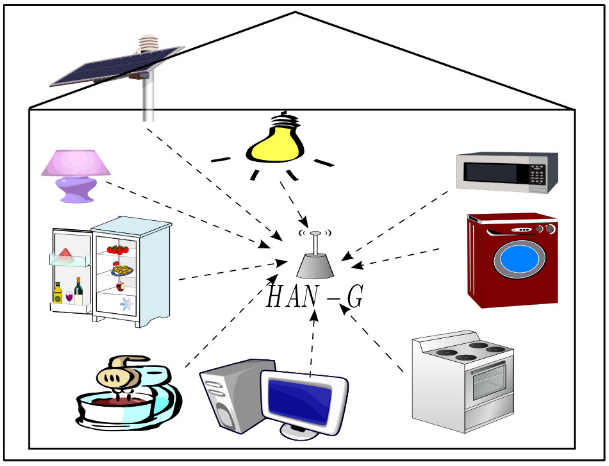

Figure 3.1: Smart home communication network topology.

these different elements to manage the SG electrical power. However, given the diversity of NAN's elements and the corresponding usage and applications, the data collected by NAN-Gs are very heterogeneous and wouldn't have the same impact on the SG power distribution. For example, data generated by a HAN-G monitoring a consumer's home where multiple renewable energy resources are installed is considered more important for the electricity distribution than data generated by a HAN-G monitoring a consumer's home where no renewable energy resources are deployed. The heterogeneity of the traffic at the NAN level has to be considered during the spectrum sharing process. Indeed, NAN sensors have different weights to transmit their generated data. Sensors that generate important data have to gain more access to the spectrum than sensors with non-important generated data. Accordingly, as the generated data is important, then as the traffic source nodes are considered prioritized and have to obtain more opportunities to transmit their data compared to non-prioritized nodes.

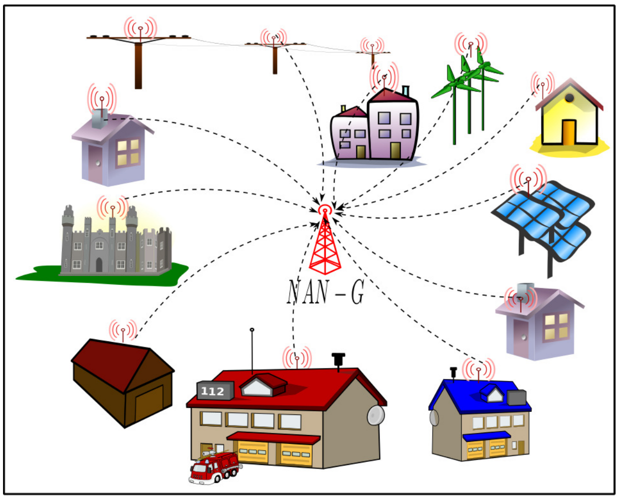

Figure 3.2: NAN communication network topology.

In a HAN, respectively a NAN, the HAN-G, respectively the NAN-G, has to get reliable and clear visions of its monitored element. Therefore, the one-hop CRSN topology has been widely recognized for smart home and NAN monitoring. The direct communication between the monitoring sensors and their associated gateway allows a real-time communication. Moreover, given the small scale of both smart home and NAN areas, the one-hop CRSNs are considered as an encouraging communication solution.

With all this in mind, in this chapter, we intend to tackle fair spectrum sharing among sensor nodes monitoring one-hop HAN and NAN SG applications using the CR technology. In the literature, several works were interested in spectrum assignment scenarios in one-hop CRSNs. However, they all account for CCC to share the channels' availability between SUs. As stated and motivated in the previous chapter, in this dissertation, our objective if to allow SG sensors to derive licensed channels' availability without relaying on a CCC in a way to achieve one fair spectrum sharing in one-hop SGs.

Therefore, we introduce in this chapter two predictive channel assignment schemes in CRSNs for one-hop SGs:

- **CSRA**: The Cooperative Spectrum Resource Allocation scheme is used to fairly allocate licensed spectrum resources in smart homes where home appliances generate traffic with the same data rate. But, the sensors have different views of the primary users activity depending on their locations in the home areas.
- **DUSA**: The Distributed Unselfish Spectrum Assignment scheme is dedicated to the channel assignment in one-hop NANs' areas. In this context, the traffic coming from the buildings/monitored elements will be different depending on the application the sensor network is about to control. The channel allocation here also considers the different applications priorities and how these priorities are conducted to achieve fairness between the involved nodes.

In both solutions, as we avoid CCC, the channels' availability information will be distributively derived using POMDPs. CSRA and DUSA are evaluated through the OMNeT++ network simulator. Simulation results reveal that both CSRA and DUSA achieve a fair sharing of spectrum resources and improve the network spectrum utilization compared to the CCC-based resource allocation schemes.

3.2 Related Work

CRSNs have been widely used to monitor SG systems, especially smart homes and NANs. Given the centralized SG power monitoring, the star topology represents the dominant solution to deploy the networks [50,90,96]. However, few works focus on channel assignment in SG areas. A large number of existing studies focus on CRSN architectural direction.

Generally, they assume the presence of one central node that is responsible of the spectrum sharing among the monitoring sensors [50, 96]. In [50], one spectrum broker is assumed to exist in a SG to sense and share available frequency channels among different NAN gateways that exist in a SG. In [96], one central node, called cognitive base station (CBS), is present in every monitored system to sense available spectrum and share it among deployed sensors to allow every node to access to the spectrum according to its priority. The gateway node can play the role of this central unit. However, being dependent on a central unit to periodically sense and assign channels to SUs will necessitate a continuous communication between the central unit and the deployed sensors. As we target the CCC avoidance all along this thesis, the channel assignment processes wouldn't be centralized. Furthermore, this solution is not recognized given the CCC inconveniences added to the "single point of failure" eventual problems.

On the other hand, if we consider prioritized SG systems, several works were achieved in this research area. In [97,98], authors proposed a Distributed Control Algorithm (DCA). To model the prioritized SG area, the traffic flows are differentiated into different priority classes according to their QoS requirements. Every class maintains three-dimensional service queues attributing delay, bandwidth and reliability to data. The problem is formulated as a Lyapunov drift optimization to enhance the weighted service of the traffic flows originating from different classes. Every sensor uses the proposed DCA to satisfy its own QoS and to select the channel with the lowest noise level that responds to the QoS required by the stored data packets. In these two complementary works, the SG sensors operate distributively and selfishly, without considering the needs of neighboring nodes. One CCC is always assumed to exist for a continuous control message exchange. In [90], a cognitive radio channel allocation scheme for prioritized SG traffic has been examined. The scheduling approach differentiates the SG traffic into three categories: control commands, multimedia sensing data, and meter readings. Periodically, before every access to the spectrum, the SUs exchange control information with the base station. Thereafter, this later makes spectrum allocation decisions subject to available resources and according to the SUs' priorities.

In all the previously presented works, a CCC is always assumed to organize the sensors' transmission on licensed channels. Therefore, to avoid the limitations introduced by the use of a CCC, we propose in this chapter fully distributed channel allocation schemes, namely CSRA and DUSA, for smart homes and NANs monitoring, respectively.

3.3 One-hop CRSN Models for Smart Homes and NANs

In this chapter, one-hop CRSNs are deployed in both smart homes and NANs. In this section, we first, introduce the basic assumptions and notations we consider to model the installed networks, the medium access scheme that smart home and NAN users use to transmit SG traffic, and finally the licensed signal model we consider in our work.

3.3.1 Notations and Basic Assumptions

We model a CRSN deployed to monitor indifferently a smart home or a NAN by the list $\mathcal{S} = \{n_1, \ldots, n_N\}$ of N SG sensors. Every node $n_i \in \mathcal{S}$ is equipped with a single radio interface able to switch the list $\mathcal{H} = \{c_1, \ldots, c_K\}$ of K licensed channels. The SG users ($n_i \in \mathcal{S}$) represent the secondary network users (SUs). They access to a given frequency band $c_k \in \mathcal{H}$ if it is sensed not occupied by licensed signals. As depicted in Figures 3.1 and 3.2, the smart home sensors, respectively the NAN sensors, send their data to the HAN-G, respectively to the NAN-G, through one-hop data transmission. The HAN-Gs and the NAN-Gs, are equipped with K radio interfaces to allow the reception of simultaneous data packets sent by nodes $n_i \in \mathcal{S}$ on idle licensed channels ($c_k \in \mathcal{H}$).

Despite their similarities, HAN and NAN systems may present some particularities that are proper to each system. Thence, if we consider smart homes, the sensors in these systems are subject to the following assumptions:

1. All the deployed sensing devices have the same neighboring list of nodes. We denote by $\mathcal{N}_i$ the node n_i's neighboring set. Accordingly, $\forall n_i \in \mathcal{S},\ \mathcal{N}_i = \mathcal{S}$.
2. The sensors have the same priority to transmit data [99].
3. The data packet arrival rate is the same for all the deployed sensors.

On the other side, in SG NANs, we assume that:

1. If n_j is one neighbor of n_i then this does not imply that $\mathcal{N}_i$ is equal to $\mathcal{N}_j$ ($n_j \in \mathcal{N}_i \nRightarrow \mathcal{N}_j = \mathcal{N}_i$). In fact, given the large scale of SG NANs compared to the home areas, every NAN sensor may have its own list of neighboring nodes $\mathcal{N}_i$.
2. Given the heterogeneous monitored NAN applications, each node n_i generates data packets according to a Poisson process with its own average arrival rate α_i [100].
3. Each node n_i has a finite buffer of size B to store its generated data packets.

Now, in both systems, we assume that the sensors monitoring the same electrical area are synchronized in time. In fact, SG communication networks require an accurate reference time. The network synchronization allows the monitored area to autonomously operate and to get the ability to be energetically isolated from the main power grid. Therefore, every SG segment becomes able to operate in an islanding mode.

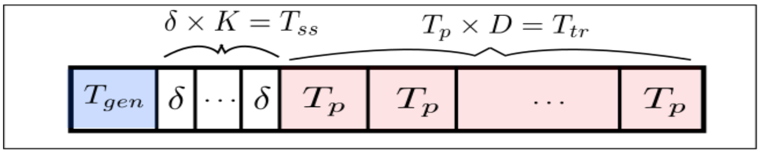

Figure 3.3: The frame structure.

3.3.2 Smart Grid Users' Medium Access Scheme

Since we opt for synchronized transmissions, all sensor nodes in both NAN and HAN systems will opt for the same frame format as depicted in Figure 3.3. Thus, the time will be divided into frames of fixed duration T. We denote by the frame t the frame starting at time t. Each frame is composed of three sub-periods: data generation T_{gen}, sensing T_{ss} and transmission T_{tr} sub-periods. The frame structure is initiated by a data generation sub-period having a duration T_{gen}. Once data is generated, every SU senses the K channels. Every channel is sensed during δ ms ($K \times \delta = T_{ss}$). Once the channels' status are obtained, a node n_i can start its data transmission. The data transmission sub-period lasts for T_{tr} and is divided into D micro-slots. We denote by T_p the duration of one micro-slot. During the first micro-slot, n_i uses the CSMA/CA algorithm to exchange, with the gateway, a RTS/CTS messages on its selected channel c_k [98]. During the micro-slot number d ($d \in [2, D]$), n_i can only send one data packet followed by the reception of an acknowledgement (Ack) sent by the gateway. If a SU does not receive an Ack for a given data packet, it stops the transmission in the current frame and postpones it to the following frame.

3.3.3 Licensed Traffic Modeling

One of the basic thesis' goals is to avoid the use of a CCC before every spectrum access trial while achieving a balanced spectrum sharing among SG users. Thus, each sensor will distributively execute an algorithm to estimate the channels that can be selected by its neighbors during every frame. The channel selection process is widely dependent on the activities on the licensed channels. Thus, the smart grid users need to accurately characterize the PU's behavior. To this end, we assume for a given node n_j ($j \in [1, N]$) that PU services arrive in each channel c_k ($k \in [1, K]$) according to a Poison process with an average arrival rate λ_k^j. The occupancy of each channel can be then modeled by a two-state Markov chain (Busy, Idle) [101].

The Busy state models the state of the channel occupied by primary signals. The Idle state represents the state of the channel able to be used by SUs, i.e., free of PUs. As shown in Figure 3.4, β_k^j and μ_k^j represent the probabilities of channel c_k switching from the Idle state to the Busy state and from the Busy state to the Idle state, respectively, as sensed by n_j.

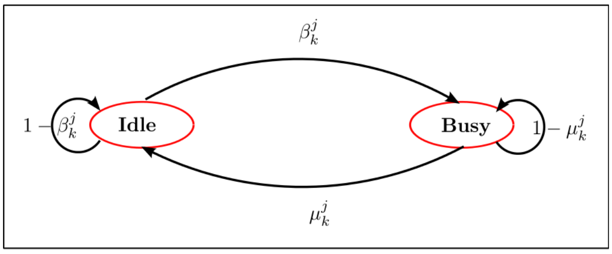

Figure 3.4: The wireless channel model.

$\omega_k^j(t)$, as given in Equation (3.1), denotes the probability that n_j senses c_k in the Idle state during the frame t. $\omega_k^j(t)$ is the probability that n_j senses c_k in the Busy state at the frame $t-1$ and switches to the Idle state at the frame t as well as the probability that n_j senses c_k in the Idle state at the frame $t-1$ and stays free of the primary signal at the frame t. The steady probability of the channel c_k Idle state ω_k^j is given by Equation (3.2).

$$\omega_k^j(t) = (1-\omega_k^j(t-1))\beta_k^j + \omega_k^j(t-1)(1-\mu_k^j) \tag{3.1}$$

$$\omega_k^j = \lim_{t\to+\infty} \omega_k^j(t) = \frac{\beta_k^j}{\mu_k^j + \beta_k^j} \tag{3.2}$$

Once n_j senses c_k Idle during T_{ss}, the probability Pna_k^j that no PU arrives during one micro-slot of the T_{tr} sub-period is expressed as introduced in Equation (3.3):

$$Pna_k^j = e^{-\lambda_k^j T_p} \tag{3.3}$$

Based on the above system description, we proceed in the next section to the presentation of the metrics that will be adopted as the fairness indicators between sensor nodes in HANs and NANs depending on the node/traffic priorities.

3.4 One-hop Smart Grid Metrics for Fair Spectrum Sharing

Every sensor node $n_i \in \mathcal{S}$ has to consider its neighboring nodes' priorities during its access attempts in a way to achieve a fair spectrum access. However, since our work does not rely on central control channels to continuously exchange control messages, every node should use a measurement of every neighboring node's need to transmit data. This measurement will be estimated locally in every node. It represents a fairness metric that will be used to achieve a balanced spectrum usage among deployed sensors. In fact, once the fairness metric is obtained, every node uses Partially Observable Markov Decision Processes (POMDP) to predict a fair channel distribution among neighboring nodes. Thus, it obtains its appropriate channel. We use POMDPs given the probabilistic measurements of both the fairness metrics and the channels' availability. Now, given the differences between the HAN and the NAN systems, we propose that sensors deployed in each area use their appropriate fairness metric to characterize neighboring nodes' priorities to access to available spectrum resources.

3.4.1 Smart Home Users' Fairness Metrics

In a smart home, sensors have the same packet arrival rate. However, the channels' vacuity may change, during the time, from one node to another. Thus, smart home sensors have to get almost the same benefits from the access to the spectrum while considering that channels' availability depends on both time and location. A good estimator of the spectrum access fraction achieved by each sensor node would be the amount of data successfully sent by each node to the HAN-G. This would be literally traduced by the aggregate accumulative average data packets successfully sent $s_i(t)$ by every deployed node $n_i \in \mathcal{S}$. Therefore, the fairness of the channel allocation scheme can be traduced as the ability to always maintain almost the same estimated values $s_i(t)$ for all the nodes $n_i \in \mathcal{S}$. For instance, the probability for a given node to access to the medium in the current frame essentially depends on how it accessed the medium in the past frames. Indeed, if two nodes n_1 and n_2, respectively, succeeded to transmit L_1 and L_2 packets up to the frame $(t-1)$, such as $L_1 \ll L_2$, then during the frame t, n_2 should have a higher opportunity to access to the medium than n_1. However, as sensors don't share information about each others' transmission, each node n_i will locally estimate the number of packets successfully transmitted by each neighbor n_j on a given channel c_k $(k \in [1, K])$.

With all this in mind, we model the behavior of a sensor node n_i during the different phases of a frame t by the discrete time Markov chain depicted in Figure 3.5.

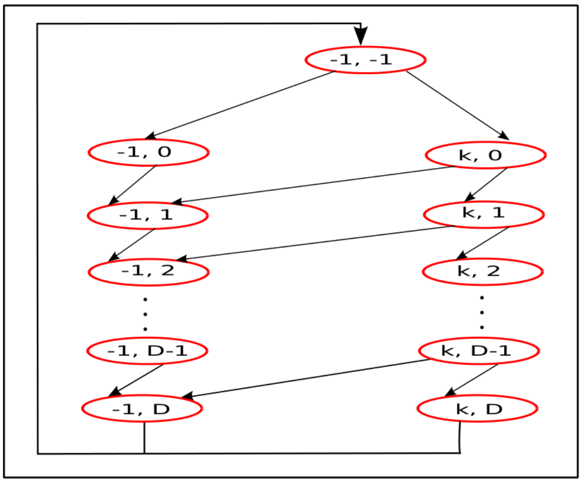

Figure 3.5: Markov chain for smart home sensor's behavior.

Let (c, d) be the two-dimensional n_i's state during a frame t. The first dimension c indicates if the considered node n_i is using the channel c_k or not ($c \in \{-1, k/\ k \in [1, K]\}$). The second dimension d represents the micro-slot counter/the frame sub-period ($d \in [-1, D]$). In the following, we introduce the different possible n_i's states:

- $(-1, -1)$: n_i generates data during the generation sub-period T_{gen} of the frame t.
- $(k, 1)$: n_i has successfully sent the RTS/CTS on c_k.
- $(-1, 0)$: n_i has postponed its data transmission because c_k is busy during T_{ss}.
- $(-1, d)$: n_i is not transmitting data ($c = -1$) at the end of the micro-slot number d ($d \in [1, D]$). This may be due to a PU appearance on c_k during the previous micro-slots or because c_k is sensed busy during T_{ss}.
- (k, d): n_i has successfully sent the data packet number $d - 1$ where $d \in [2, D]$ on c_k (the first micro-slot is used to exchange the RTS/CTS).

The transition probabilities between the different states are then expressed as:

- $P[-1, d/k, d-1] = 1 - Pna^i_k(1 - Ploss_k)$: The probability of leaving the channel c_k due to a PU appearance on c_k or due to the packet loss probability $Ploss_k$ during the micro-slot number d ($d \in [1, D]$). $Ploss_k$ can be caused by the obstacles and the electromagnetic noise of the electrical devices [61].
- $P[k, d/k, d-1] = Pna^i_k(1 - Ploss_k)$: The successful transmission probability of the data packet number $d - 1$ ($d \in [2, D]$).
- $P[-1, d/-1, d-1] = 1$: The probability of a micro-slot counter increment ($d \in [1, D]$).

From the above described Markov chain, every node n_j becomes able to estimate $av_{j,k}$, i.e., the average data packets successfully sent by its neighbor n_i during a fame t, on its selected channel $c_k \in \mathcal{H}$ as introduced in Equation (3.4). Then, it calculates the n_j's accumulative aggregate average data packets successfully transmitted by n_i until the end of the frame t. Thereafter, it concludes the n_i's need to access to the spectrum during the frame $t + 1$ compared to the other deployed sensors.

$$av_{j,k} = [(D-1)\prod_{d=1}^{D} P[k, d/k, d-1] + \sum_{d=1}^{D-2} d \times P[-1, d+2/k, d+1] \prod_{d'=1}^{d+1} P[k, d'/k, d'-1]]\omega^i_k \tag{3.4}$$

3.4.2 NAN Users' Fairness Metrics

Now, in NANs, in addition to the different sets of available frequency bands among the deployed sensors, the sensors have also heterogeneous priorities to access to the spectrum. Since we consider the packet arrival rate α_i as the n_i's weight to transmit its generated data, we propose to use the buffer occupancy as a simple, nevertheless accurate, indicator of the sensor node's priority. For instance, as the node n_i's buffer size increases, its priority to access to the spectrum becomes very urgent hence avoiding the n_i's saturation. Therefore, we introduce in this section the three-dimensional Markov chain presented in Figure 3.6. It calculates the probabilities that a given sensor node has b packets stored in its buffer during a frame ($b \in [0, B]$).

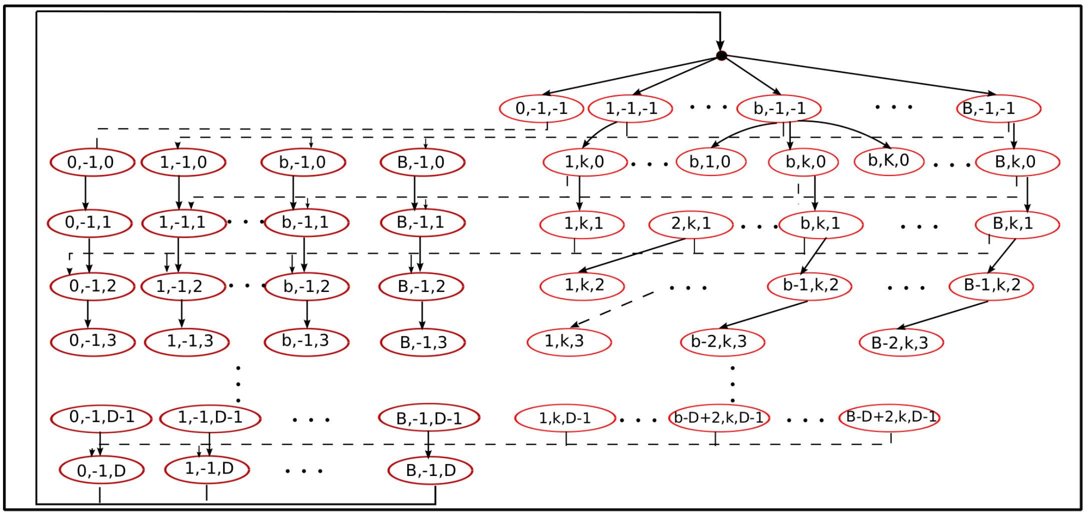

Figure 3.6: Markov chain for NAN sensor's buffer occupancy estimation.

We denote by (b, c, d) the three-dimensional n_i's state during a frame t. The first dimension b ($b \in [0, B]$) models the n_i's buffer occupancy. The second dimension c, where $c \in [-1, 1, 2, \ldots, K]$, represents the channel used for data transmission. Because the number of data packets stored changes according to the frame sub-period, the third dimension d ($d \in [-1, D]$) represents the micro-slot counter.

In the following, we introduce the different states (b, c, d) of this Markov chain in addition to the transition probabilities between them for a given node n_i ($i \in [1, N]$). We denote by $\pi(b, c, d)(t)$ the probability that a given node be in the state (b, c, d) during the frame t.

The Markov chain can be divided into 5 blocks as follows:

1. $(b, -1, -1)$: the n_i's buffer occupancy at the end of the data generation sub-period T_{gen} ($b \in [0, B]$).
2. $(b, c, 0)$: the buffer occupancy at the end of the data sensing sub-period T_{ss} ($c \in \{-1, 1, \ldots, K\}$).

- $P[b,k,0/b,-1,-1] = \Omega_k^i$: the probability that n_i selects c_k for data transmission ($b \in [1,B]$ and $k \in [1,K]$). Ω_k^i is introduced in Equation (3.5).

$$\Omega_k^i = \frac{\prod_{q=1}^{K}(1-\omega_q^i)\omega_k^i}{1-\omega_k^i}[1+\sum_{\substack{l=1\\l\neq k}}^{K}\omega_k^i \sum_{\substack{1\leq i_1\leq i_2\leq\ldots\leq i_l\leq K\\(i_1,i_2\ldots,i_l)\neq l-uplet(k,\ldots,k)}} [\frac{\prod_{p\in\{i_1,i_2,\ldots,i_l\}}\frac{\omega_p^i}{1-\omega_p^i}}{\omega_k^i+\sum_{p\in\{i_1,i_2,\ldots,i_l\}}\omega_p^i}]] \tag{3.5}$$

- $P[0,-1,0/0,-1,-1] = 1$: the probability that n_i does not transmit because of its empty buffer ($b = 0$).
- $P[b,-1,0/b,-1,-1] = \Omega_{-1}^i$: the probability that n_i does not select a channel during T_{tr} because all the sensed channels are busy ($k = -1$). Ω_{-1}^i is introduced in (3.6) ($b \in [1,B]$).

$$\Omega_{-1}^i = 1 - \sum_{k=1}^{K}\omega_k^i \tag{3.6}$$

3. (b,k,d): the buffer occupancy during T_{tr} when n_i transmits data in c_k ($k \in [1,K]$).

   - $P[b,k,1/b,k,0] = Pna_k^i(1-\tilde{Ps}_k^i)(1-Ploss_k)$: the probability of a successful RTS/CTS exchange in c_k where $b \in [1,B]$. This is achieved if c_k is free of primary and secondary signals. $\tilde{Ps}_k^i$, presented in Equation (3.7), is an approximation of the probability that at least one neighbor sends a RTS in c_k. $P\tilde{emp}_j$ is the estimated probability that an interfering node n_j has an empty buffer.

$$\tilde{Ps}_k^i = 1 - \prod_{n_j\in N_i}((1-P\tilde{emp}_j).(1-\Omega_k^j)) \tag{3.7}$$

   - $P[b,k,d/b+1,k,d-1] = Pna_k^i(1-Ploss_k)$: the probability of the successful transmission of the $d-1$ data packet during the micro-slot number d in the channel c_k where $d \in [2,D-1]$ and $b \in [1,B-d+1]$ (the first micro-slot, i.e., $d = 1$, is used to exchange the RTS/CTS messages).

4. $(b,-1,d)$: the n_i's buffer occupancy in the sleeping state during the T_{tr} transmission sub-period.

   - $P[b,-1,1/b,k,0] = 1-P(b,k,1/b,k,0)$: the probability of a RTS/CTS exchange failure in channel c_k ($b \in [1,B]$ and $k \in [1,K]$).
   - $P[b,-1,d/b,k,d-1] = 1-Pna_k^i(1-Ploss_k)$: the transmission failure probability of the data packet number $d-1$. It is caused by a primary signal appearance in c_k or the packet loss ($b \in [1,B-d+2]$, $k \in [1,K]$ and $d \in [2,D]$).

- $P[0,-1,d/1,k,d-1] = Pna^i_k(1-Ploss_k)$: the successful transmission probability of the last data packet in the buffer ($k \in [1, K]$ and $d \in [2, D-1]$).
- $P[b,-1,d+1/b,-1,d] = 1$: the micro-slot counter-increment of a a non-transmitting node ($b \in [0, B]$ and $d \in [0, D-1]$).

5. $(b,-1,D)$ where $b \in [0, B]$: the occupancy of the sensor's buffer at the end of the frame.

- $P[b,-1,D/b+1,c_k,D-1] = Pna^i_k(1-Ploss_k)$: the successful transmission probability of the $D-1$ data packet ($b \in [0, B-D+1]$).
- $P[B,-1,-1/b,-1,D] = Pgen^i(X \geq B-b)$: the packet blocking probability, i.e., n_i generates at least $(B-b)$ packets ($b \in [0, B-1]$).
- $P[B,-1,-1/B,-1,D] = 1$: the packet blocking probability of a congested buffer.
- $P[b+l,-1,-1/b,-1,D] = Pgen^i(X = l)$: the probability that n_i generates l data packets ($b \in [0, B-1]$ and $l \in [0, B-b-1]$).

Given the data packet arrivals according to the Poisson process during T_{gen}, the probabilities $Pgen^i(X \geq l)$, i.e., that n_i generates at least l data packets, and $Pgen^i(X = l)$, i.e., that n_i generates l data packets, are, respectively, introduced in Equations (3.8) and (3.9).

$$Pgen^i(X = l) = e^{-\alpha_i T_{gen}} \frac{(\alpha_i T_{gen})^l}{l!}, \ l \geq 0 \tag{3.8}$$

$$Pgen^i(X \geq l) = 1 - \sum_{h=0}^{l-1} e^{-\alpha_i Tgen} \frac{(\alpha_i Tgen)^h}{h!}, \ l \geq 0 \tag{3.9}$$

By using this three-dimensional Markov chain, a NAN sensor n_i ($i \in [1, N]$) becomes able to calculate the probabilities that a neighboring node n_j ($n_j \in \mathcal{N}_i$) has b stored data packets in its buffer queue ($b \in [0, B]$), in order to estimate the n_j's priority to access to the spectrum. In fact, as the probability $\pi(b,-1,-1)$ that n_j has a high number b of stored data packets increases, then as its priority/need to transmit increases accordingly.

We have introduced in this section two Markov chains. The first is used by smart home sensors. It describes the activities of a given node n_j on its selected channel c_k. It estimates its average number of successfully transmitted data packets, i.e., $av_{j,k}$, that will be used to obtain the n_j's aggregate accumulative average data packets successfully sent ($s_j(t)$), as will be detailed later. The second Markov chain will be used by NAN sensors to obtain the probability $\pi(b,-1,-1)$ that a NAN user n_j has b buffered data packets during the data generation sub-period of the frame t where $b \in [1, B]$. Now, $s_i(t)$ and $\pi(b,-1,-1)$

will be used in smart homes and in NANs, respectively, to fairly share available spectrum resources among SG users. Therefore, given the two fairness metrics, we propose two channel allocation solutions: the Cooperative Spectrum Resource Allocation (CSRA) for smart homes and the Distributed Unselfish Spectrum Assignment (DUSA) for NANs. Both, CSRA and DUSA, are based on POMDPs, as we will detail in the two next sections.

3.5 Cooperative Spectrum Resource Allocation for Smart Homes: CSRA

We propose for one-hop CRSN-based smart home monitoring the Cooperative Spectrum Resource Allocation (CSRA) scheme. Based on a POMDP formulation that aims to follow every neighboring node's states during the time, every HAN node $n_i \in \mathcal{S}$ estimates the channels that will be assigned to its neighboring nodes $n_j \in \mathcal{N}_i$ where $\mathcal{S} = \mathcal{N}_i$.

3.5.1 Smart Home Users' Partially Observable Markov Decision Process

The CSRA's POMDP allows to follow a smart home node's states based on its selected channels during every frame. It can be formulated as follows:

1. State: Let $s_i(t)$ be the n_i's state. As we have introduced in Section 3.4.1, $s_i(t)$ is the approximation of the aggregate accumulative average data packets successfully sent by n_i by the end of the frame t.

2. Action: We denote by $a_i(t) \in \{-1\} \cup \mathcal{H}$ the action taken by n_i during the frame t. It represents the channel selected by n_i for data transmission. If $a_i(t) \in [c_1, \dots c_K]$, then n_i decides to transmit data on one channel. Otherwise, if $a_i(t)$ is equal to -1, then n_i decides to not transmit data during that frame.

3. Transition Matrix: Being in the state $s_i(t-1)$ at frame $(t-1)$, if $a_i(t) \neq -1$, then n_i transits to one of two possible states $s^1_{i,k}(t)$ and $s^2_{i,k}(t)$. $s^1_{i,k}(t)$ represents the n_i's aggregate accumulative average data packets successfully sent by the end of the frame t if n_i successfully sends at least one data packet during the frame t on the selected channel $a_i(t)$ where $a_i(t) = c_k$. $s^2_{i,k}(t)$ is the n_i's state if no data packet is successfully transmitted by n_i during the frame t. If n_i decides to postpone its data transmission, i.e., $a_i(t) = -1$, then it transits from the state $s_i(t-1)$ to the state $s^2_{i,-1}(t)$ where no data packet is transmitted. The transition probabilities between the different states are introduced in Equations (3.10) and (3.11). Moreover, Figure 3.7 depicts the different transitions between the n_i's node state.

$$P[s^1_{i,k}(t)/s_i(t-1), a_i(t)] = \begin{cases} \omega^i_k Pna^i_k(1 - Ploss_k) & a_i(t) = c_k \quad (3.10a) \\ 0 & a_i(t) = -1 \quad (3.10b) \end{cases}$$

$$P[s^2_{i,k}(t)/s_i(t-1), a_i(t)] = \begin{cases} 1 - \omega^i_k Pna^i_k(1 - Ploss_k) & a_i(t) = c_k \quad (3.11a) \\ 1 & a_i(t) = -1 \quad (3.11b) \end{cases}$$

The n_i's state is updated as introduced in Equations (3.12) and (3.13). $P_i(s_i(t))$ is the probability of being in the state $s_i(t)$. It is introduced in Equation (3.14) and is obtained by using the Baye's rule [102]. $S_i(t)$ denotes the possible states to which n_i belongs during the frame t.

$$s^1_{i,k}(t) = s_i(t-1) + P_i(s^1_{i,k}(t)) \times av_{i,k}, \; k \in [1, K] \tag{3.12}$$

$$s^2_{i,k}(t) = s_i(t-1), \; k \in \{-1\} \cup [1, K] \tag{3.13}$$

$$P_i(s_i(t)) = \frac{\sum_{s_i(t-1) \in S_i(t-1)} P_i(s_i(t-1)) P(s_i(t)/s_i(t-1), a_i(t)) O[s_i(t), a_i(t)]}{\sum_{s'_i(t) \in S_i(t)} O(s'_i(t), a_i(t)) \sum_{s_i(t-1) \in S_i(t-1)} P_i(s_i(t-1)) P(s'_i(t)/s_i(t-1), a_i(t))} \tag{3.14}$$

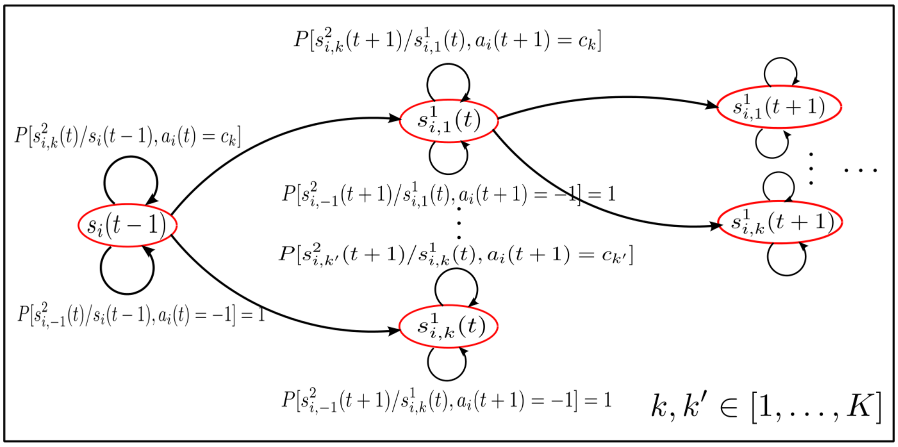

Figure 3.7: The CSRA partially observable Markov chain.

4. Observation probabilities: If n_i chooses the channel c_k ($a_i(t) = c_k$), then the observation probability is obtained by training the two-state Markov chain modeling the selected channel's states. If n_i decides to postpone its data transmission, i.e., $a_i(t) = -1$, then the probability of observing its state transits from the state $s_i(t-1)$ to the state $s^2_{i,-1}(t)$ is equal to 1.

   Thus, the probabilities of observing n_i transits from the state $s_i(t-1)$ to the state $s^1_{i,k}(t)$ and to the state $s^2_{i,k}(t)$ where $k \in \{-1\} \cup [1, K]$ are, respectively, introduced in Equations (3.15) and (3.16).

$$O[s^1_{i,k}(t), a_i(t)] = \begin{cases} \omega^i_k(t) & a_i(t) = c_k \quad (3.15a) \\ 0 & a_i(t) = -1, \quad (3.15b) \end{cases}$$

$$O[s^2_{i,k}(t), a_i(t)] = \begin{cases} 1 - \omega^i_k(t) Pna^i_k & a_i(t) = c_k \quad (3.16a) \\ 1 & a_i(t) = -1 \quad (3.16b) \end{cases}$$

5. The reward: We define the reward $r_i(t)$ as the aggregate accumulative average data packets successfully sent on the selected channels. It is expressed in Equation (3.17).

$$r_i(t) = \begin{cases} s^1_{i,k}(t) & a_i(t) = c_k \quad (3.17a) \\ s^2_{i,-1}(t) & a_i(t) = -1 \quad (3.17b) \end{cases}$$

Now, based on the states of the N nodes during the frame $(t-1)$, a SU n_i can predict at the beginning of the frame t the channel that may be allocated to every neighboring node.

3.5.2 Smart Home Users' Channel Allocation Policy

Using the POMDP formulation, all the nodes will determine, in a distributed way, the set $\mathcal{F}(t)$ of sensors n_j ($n_j \in S$) that will access to channels during the frame t. $\mathcal{F}(t)$ is obtained based on the number of packets successfully sent during the past frames. Thus, to achieve fairness in the channel access during t, the nodes belonging to $\mathcal{F}(t)$ are those nodes having the K smallest $s_j(t-1)$ values, i.e., the K nodes the least accessed to the spectrum during the $(t-1)$ previous frames. Thus, the channels' selection is performed in a way to maximize the quantity of data correctly sent during t. Let p be the channel's configuration that will attribute the channel c^p_j to the node n_j ($n_j \in F(t)$). $\mathcal{P} = \cup p$ represents the sets of all the possible channels' configurations during the frame t. Then, the configuration p^* that will achieve the fair spectrum allocation during t is obtained by the following Equation:

$$p^* = \underset{p \in \mathcal{P}}{\text{maximize}} \; (\sum_{n_j \in \mathcal{F}} r_j(t)) \quad (3.18)$$

The different steps of CSRA are summarized in Algorithm 1.

Algorithm 1 CSRA scheme.

Input: $\mathcal{F}$, $\omega_k^j(t)$, ω_k^j, $s_j(t-1)$, $\forall j \in [1, N]$ and $k \in [1, K]$

At the beginning of the frame t**:** Select p^*

if $n_i \in \mathcal{F}$ **then**

  if $a_i(t)$ is Idle **then**

    Start data transmission

  end if

end if

for $j = 1$ **to** N **do**

  for $k = 1$ **to** K **do**

    $\omega_k^j(t) \leftarrow (1 - \omega_k^j(t-1))\beta_k^j + \omega_k^j(t-1)(1 - \mu_k^j)$

  end for

  if $n_j \in \mathcal{F}$ **then**

    $s_j(t-1) \leftarrow s_{j,k}^1(t)$ $\{a_j(t) = c_k\}$

  else

    $s_j(t-1) \leftarrow s_{j,-1}^2(t)$ $\{a_j(t) = -1\}$

  end if

end for

3.6 Distributed Unselfish Spectrum Assignment for NANs: DUSA

In DUSA (the Distributed Unselfish Spectrum Assignment for NAN users) the SG sensor nodes have heterogeneous lists of neighboring nodes. Accordingly, every node $n_i \in \mathcal{S}$ predicts the channels that will be used by its neighbors. It predicts their channels based on their priorities. As used in CSRA, in the DUSA approach, every node avoids having a selfish behavior. If n_i has data to transmit and founds that its neighboring nodes are more prioritized to access to the spectrum, then n_i postpones its transmission to not interfere with them.

The NAN's sensors basically use a POMDP to distributively assign channels. The DUSA's POMDP is based on the three-dimensional Markov chain that estimates the probabilities that n_i has a given number of data packets, i.e., Section 3.4.2. The POMDP related to a node $n_i \in \mathcal{S}$ can be then described as follows:

1. State: The n_i's state is presented by the vector $\psi_i(t)$. $\psi_i(t)$ represents the list of the buffer occupancy probabilities, $\pi(b, -1, -1)(t+1)$ where $b \in [0, B]$, by the end of the data generation sub-period of the frame $t+1$. $\psi_i(t)$ is introduced in Equation (3.19).

$$\psi_i(t) = [\pi(0, -1, -1)(t+1), \ldots, \pi(B, -1, -1)(t+1)] \tag{3.19}$$

2. Action: At the beginning of the frame t, n_i selects the channel $a_i(t) \in A = \{-1\} \cup \mathcal{H}$. If $a_i(t)$ is equal to -1 then n_i postpones its data transmission. Otherwise, the node uses the selected channel to send its data.

3. Transition Matrix: After n_i takes action $a_i(t)$, the sensor n_i's state can transit from the state $\psi_i(t-1)$ to one of the two possible states $\psi^1_{i,k}(t)$ and $\psi^2_{i,k}(t)$ where $k \in \{-1\} \cup [1, K]$. If $a_i(t) \in \mathcal{H}$, then the state $\psi_i(t-1)$ can transmit to the state $\psi^1_{i,k}(t)$ if n_i sends at least one data packet on c_k during the frame t. Otherwise, if no data packet has been successfully sent on c_k, then n_i's state transmits to the state $\psi^2_{i,k}(t)$. Now, if $a_i(t) = -1$ then n_i's state will transit to the state $\psi^2_{i,-1}(t)$. The transition probabilities between the different states are introduced in Equations (3.20) and (3.21). Furthermore, the update of the n_i's state is obtained through the three-dimensional Markov chain (Figure 3.6).

$$P[\psi^1_{i,k}(t)/\psi_i(t-1), a_i(t)] = \begin{cases} \omega^i_k Pna^i_k(1 - Ploss_k) & a_i(t) = c_k \quad (3.20a) \\ 0 & a_i(t) = -1 \quad (3.20b) \end{cases}$$

$$P[\psi^2_{i,k}(t)/\psi_i(t-1), a_i(t)] = \begin{cases} 1 - \omega^i_k Pna^i_k(1 - Ploss_k) & a_i(t) = c_k \quad (3.21a) \\ 1 & a_i(t) = -1 \quad (3.21b) \end{cases}$$

4. Observation probability: As used in the CSRA's POMDP, the observation probabilities are basically obtained through the two-state Markov chain modeling the selected channel. Accordingly, the probability $O[[\psi^1_{i,k}(t), a_i(t)]$, i.e., the probability of observing the n_i's state transits from $\psi_i(t-1)$ to $\psi^1_{i,k}(t)$ while using $a_i(t)$ ($a_i(t) = c_k$), is introduced in Equation (3.22). However, the probability $O[\psi^2_{i,k}(t), a_i(t)]$, i.e., the probability of observing n_i's state transits from $\psi_i(t-1)$ to $\psi^2_{i,k}(t)$, is present in Equation (3.23). $O[\psi^2_{i,k}(t), a_i(t)]$ is based on the estimated value $\Omega^i_{-1}(t)$ (the probability that n_i senses the K channels busy during the frame t) due to the heterogeneous neighboring nodes and then the non-deterministic channel decisions.

$$O[\psi^1_{i,k}(t), a_i(t)] = \begin{cases} \omega^i_k(t) & a_i(t) = c_k \quad (3.22a) \\ 0 & a_i(t) = -1, \quad (3.22b) \end{cases}$$

$$O[\psi^2_{i,k}(t), a_i(t)] = \begin{cases} 1 - \omega^i_k(t)Pna^i_k & a_i(t) = c_k \quad (3.23a) \\ \Omega^i_{-1} & a_i(t) = -1 \quad (3.23b) \end{cases}$$

5. The reward: If n_i selects $a_i(t)$ where $a_i(t) \neq -1$ then the reward $R_i(t)$ is introduced in Equation (3.24). It represents the probability that $D-1$ data packets are successfully transmitted in the selected channel if the number of data packets stored is more than or equal to $D-1$, .i.e., the first sum, or that all the packets stored are successfully transmitted if the occupancy of the buffer is smaller than $D-1$, i.e., the second sum. If n_i does not allocate a channel, i.e., $a_{n_i} = -1$, then the reward is equal to

0. $P(\psi^1_{i,k}(t))$ is the probability of being in the state $\psi^1_{i,k}(t)$ where $a_i(t) = c_k$ and $k \in [1, K]$. It is obtained by using the Baye's rule.

$$R_i(t) = (\sum_{b=0}^{B-D+1} P[b, -1, D/b+1, a_i, D-1]\pi(b+1, a_i, D-1)(t) \tag{3.24}$$

$$+\sum_{d=2}^{D-1} P[0, -1, d/1, a_i, d-1]\pi(1, a_i, d-1)(t))P(\psi^1_{i,k}(t)),\ a_i(t) = c_k$$

As the probability that a node n_i has b ($b \geq 1$) buffered packets increases with the increase in its priority then one prioritized sensor node will have a high reward value. Thus, to achieve a fair channel allocation among prioritized sensor nodes, n_i selects the channel configuration p^* allocated to itself and to its neighbors that maximizes the sum of the rewards $R_j(t)$ ($n_j \in \mathcal{N}_i$), as introduced by Equation (3.25). The channels composing p^* are different to not cause interference between sensor nodes. If the channel allocated to n_i, i.e., $a_i(t) \in p^*$, is equal to -1 then n_i postpones its transmission. Otherwise, i.e., $a_i(t) \in [c_1, \ldots, c_K]$, it starts the transmission in $a_i(t)$.

$$\begin{aligned} &\underset{a_j \in [-1, c_1, \ldots, c_K]}{\text{Maximize}} && \sum_{n_j \in N_i} R_j(t) \\ &\text{subject to} && \forall n_j,\ n_l \in \mathcal{N}_i,\ \text{if } n_j \neq n_l \text{ and } a_j(t) \notin \{-1\}, \\ &&& \text{then } a_l(t)\ \neq\ a_j(t) \end{aligned} \tag{3.25}$$

The different steps executed by n_i to select $a_i(t)$ based on the optimization problem formulated by Equation (3.25) and by using DUSA are presented in Algorithm 2. We denote by $\mathcal{P}$, the list of the channel configurations ($\mathcal{P} = \cup p$).

3.7 Performance Evaluation

In this section, we evaluate the performances of the CSRA and the DUSA schemes using the OMNeT++/MiXiM network simulator. Both schemes are implemented based on the MiXiM Multi-channel model, i.e., Mac80211MultiChannel [103, 104]. We consider that every SG sensor is equipped with only one radio interface able to switch a list of channels. The sink nodes, i.e., HAN-Gs and NAN-Gs, are equipped with multiple radio-interfaces. In each monitored system, the SG sensors are uniformly deployed. The sink is placed at the center of the simulation area in a way to be directly reachable by the sensors in the networks. 3 PUs are deployed in each monitored area. As for the sink nodes, PUs are also equipped with multiple radio interfaces. PUs are placed in the simulation area in a way to ensure heterogeneous PU traffic environment for the sensor nodes placed in the HAN or NAN systems. This means that the list of PUs placed in the interference range of a node

Algorithm 2 DUSA scheme.

Input: $\omega_k^j(t),\ \omega_k^j,\ \lambda_k^j\ \forall n_j \in \mathcal{N}_i$

Channel Selection Policy: At t, n_i selects the channel $a_i(t) \in p^*$ ($p^* \in \mathcal{P}$: is the combination of channels maximizing the sum of the rewards associated to $\mathcal{N}_i$)
if $a_i(t) \in \{c_1, \ldots, c_K\}$ **then**
  if $a_i(t)$ is Idle **then**
    Start data transmission
  end if
end if
for $n_j \in \mathcal{N}_i$ **do**
  for $k = 1$ **to** K **do**
    $\omega_k^j(t) \leftarrow (1 - \omega_k^j(t-1))\beta_k^j + \omega_k^j(t-1)(1 - \mu_k^j)$
  end for
  if $a_j(t) \in [c_1, \ldots, c_K]$ **then**
    $\psi_j(t-1) \leftarrow \psi_{j,k}^1(t)\{a_j(t) = c_k\}$
  else
    $\psi_j(t-1) \leftarrow \psi_{j,-1}^2(t)\{a_j(t) = -1\}$
  end if
end for

n_i is different from the list of PUs placed in the n_j's interference range. The PUs arrive on every channel according to the Poisson distribution [105].
Table 3.1 lists the basic simulation parameters that we use in both simulations. In the following, we present in detail the simulation results of the CSRA and DUSA schemes in respectively monitoring one-hop HAN and NAN systems.

Table 3.1: Simulation Parameters.

Notation	Explanation
Simulator	OMNeT++ (4.6)/MiXiM (2.3)
Channels' occupancy	0.13/0.2/0.35/0.43/0.45/0.5/0.83
Channel bandwidth	20 MHz
δ	0.1 s
PUs' transmission range	30 m
D	4

3.7.1 CSRA Evaluation Results

The smart home area is represented by a $50m \times 50m$ square field. We first evaluate the impact of the frame size on CSRA's performance. For instance, the frame size substantially changes with the number D of micro-slots during the T_{tr} sub-period. Thus, we depict in Figure 3.8 the packet delivery ratio (PDR) as a function of D for different values of α (the SU's packet arrival rate which is the same for all the deployed smart home sensors) and for two different numbers of used channels K (with $N = 30$). Figure 3.8 shows that all curves shaped the same appearance (the PDR fluctuates for small D values and then keeps a constant increase from $D = 6$). Such behavior can be explained as follows: Initially, when D is in the interval $I_1 = [2, 4]$, T_{gen} and T_{ss} represent an important portion of the frame size ($> 25\%$). Thus, the high probability of a PU's appearance during these sub-periods partially protects SUs from PUs arrivals during the data transmission phase which increases PDR values during I_1. During $I_2 = [4, 6]$, however, the frame becomes more sensitive to PUs' arrivals. For instance, in I_2, the frequency of PU appearance during T_{tr} accordingly increases with D, resulting in a significant drop in PDR values. Finally, from $D = 6$, the frame sensitivity will be gradually alleviated as the probability of sending correct packets during the first micro-slots of the T_{tr} sub-period increases.

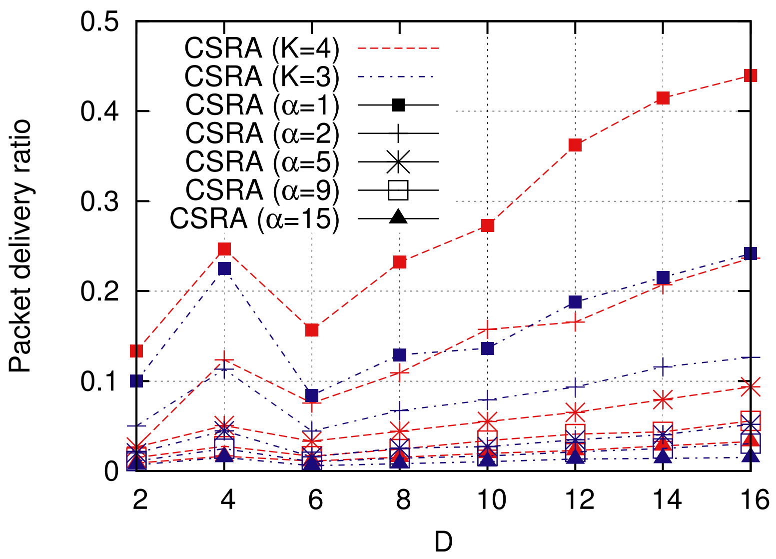

Figure 3.8: CSRA: Packet delivery ratio vs number of micro-slots D.

Now, we evaluate the efficiency of CSRA in achieving a fair channel allocation between SUs in smart homes. Thus, we compare CSRA to two other CCC-based centralized schemes [106] called *Ideal-Centralized* and *Non-Ideal-Centralized* schemes. With centralized algorithms, the HAN-G can achieve an optimal scheduling between the sensors given its perfect knowledge of the nodes' configurations and other network parameters. In the first *Ideal-Centralized* scheme, the HAN-G fairly assigns channels to SUs in each frame. One additional channel (considered as CCC) not in use by PUs is used to send control messages containing the channels' allocation. In the second *Non-Ideal-Centralized* approach, the CCC is one of the channels used to transmit data, i.e., the CCC can be accessed by PUs.

Figure 3.9 depicts the comparative PDR scenarios for different values of N (the number of SUs), where $D = 4$ and $\alpha = 3$. As shown in Figure 3.9, the PDR reversely decreases with N since the quantity of the generated data significantly increases with the number of SUs. Moreover, for all the values of N and K ($K = 3$ and $K = 7$), the PDR achieved by CSRA nearly approaches the one of the *Ideal-Centralized* scheme. Thus, with CSRA, the sensors are able to correctly predict the appropriate channels associated to prioritized nodes. Moreover, CSRA outperforms the *Non-Ideal-Centralized* scheme since, in this latter scheme if the CCC is sensed busy, the gateway can not use it to broadcast the channels' configuration.

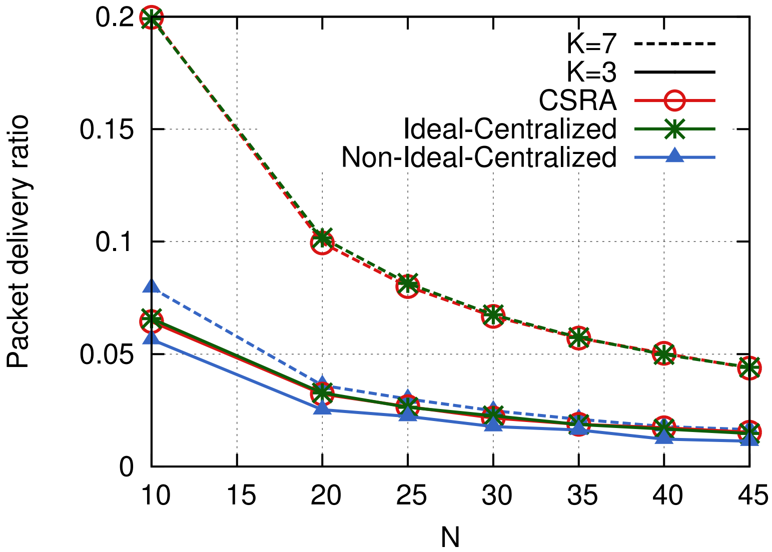

Figure 3.9: CSRA: Packet delivery ratio vs number of deployed sensors N.

In Figure 3.10, we evaluate the average packet delay of the three allocation approaches as a function of N, the number of SUs. The curves show that the average delay achieved by CSRA is almost the same as the *Ideal-Centralized* scheme's delay. However, a slight increase in the delay value occurs when N increases since the sensors have not an exact information about the interfering sensors and the channels' states. CSRA outperforms the *Non-Ideal-Centralized* scheme because of the potential CCC business by PUs.

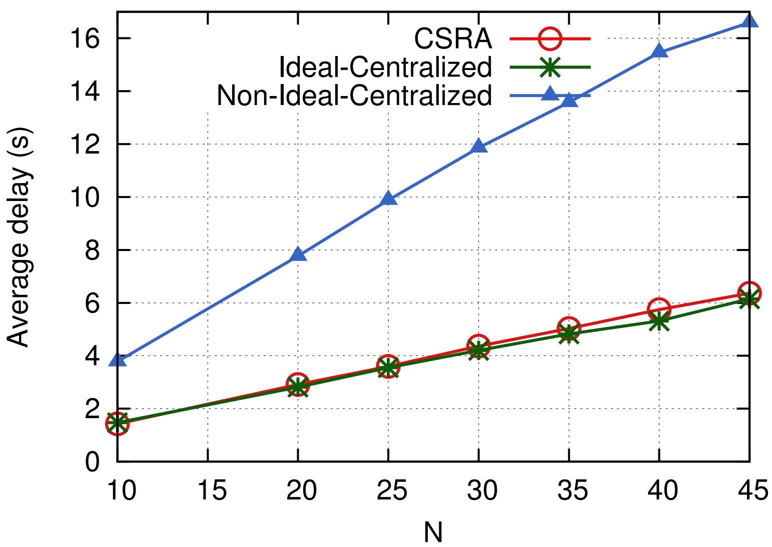

Figure 3.10: CSRA: Average packet delay vs number of deployed sensors N.

Finally, we evaluate the packet delivery ratio under different K values. The Figure 3.11 shows that the increase in K improves the spectrum utilization given the availability of a higher number of channels. However, since the *Non-Ideal-Centralized* scheme depends on the availability of the CCC channel, the increase in PDR for that scheme remains relatively low.

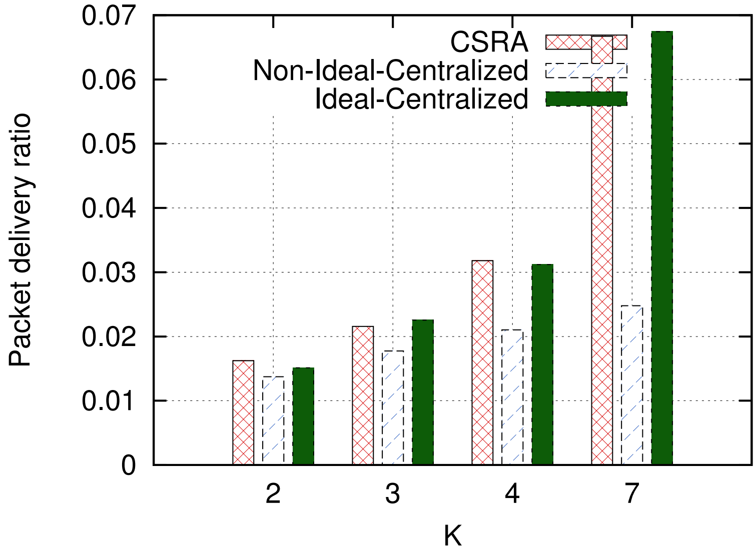

Figure 3.11: CSRA: Packet delivery ratio vs number of used channels K.

3.7.2 DUSA Evaluation Results

This section is dedicated to the performance evaluation of the DUSA scheme in the context of one-hop NAN systems. The NAN users (sensors) are deployed in a $100m \times 100m$ square field. We first propose to compare the DUSA approach to a CCC-based scheme, denoted in the following as *CCC-scheme* where the channel negotiation is performed through one of the licensed channels that can be used by PUs. Control messages are then exchanged with the *CCC-scheme* only in the case of vacuity of the related licensed channel.

We first focus on the comparison between DUSA and *CCC-scheme* in term of effective spectrum utilization. Then, we evaluate the DUSA efficiency in achieving a fair resource sharing between prioritized SUs.

3.7.2.1 Spectrum Utilization

To valuate the impact of the CCC avoidance by the DUSA scheme, we introduce the spectrum utilization ratio as the total number of bits successfully transmitted when using DUSA or *CCC-scheme* divided by the sum of the total number of bits successfully transmitted when using both schemes. Figure 3.12 shows that DUSA improves the spectrum utilization compared to the *CCC-scheme* (the number of NAN sensors=20). It also shows that when

DUSA is used, the spectrum utilization increases also with K. The difference between the two schemes is due to the cancellation of the data transmission if the CCC is sensed occupied by PU when using the *CCC-scheme*.

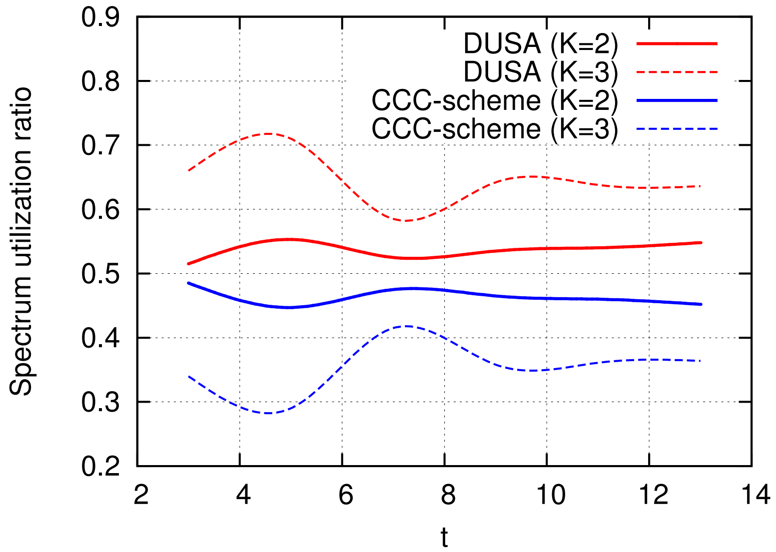

Figure 3.12: DUSA: Secondary network spectrum utilization ratio.

Additionally, to evaluate the fairness of DUSA and its adaptability to the sensors' priorities, we simulate the spectrum utilization ratio per class priority. Figure 3.13 shows that, when we use DUSA, the spectrum utilization increases with the node's priority. For the *CCC-scheme*, sensors with average packet arrival rate equals 1.5 packets/T_{gen} is more important than the spectrum utilization of SUs with average packet arrival rate equals 3 packets/T_{gen}. Hence, SUs with buffered data packets operate selfishly when using the *CCC-scheme*. By applying DUSA, even if some nodes have packets to transmit, they postpone their data transmission and allow prioritized nodes to access the spectrum. SUs with higher average packet arrival rates are more prioritized to access the spectrum and have higher spectrum utilization.

3.7.2.2 Average Packet Delay

Now, to ensure the unselfish behavior of the SUs, we evaluate the average packet delay per class priority. Figure 3.14 shows how the average packet delay reversely decreases with the SUs' priorities, i.e., packet arrival rates. On one side, data packet delay of SUs with the lower priorities is large when using DUSA. This is tolerated since their generated data packets are not prioritized to be transmitted to the sink. This traduce the SUs' unselfish sensor behavior. On the other side, the delay experienced by data packets originating from the nodes with higher priorities are significantly shorter because their generated data packets must be transmitted rapidly to the sink. DUSA clearly improves the average delays of prioritized sensors.

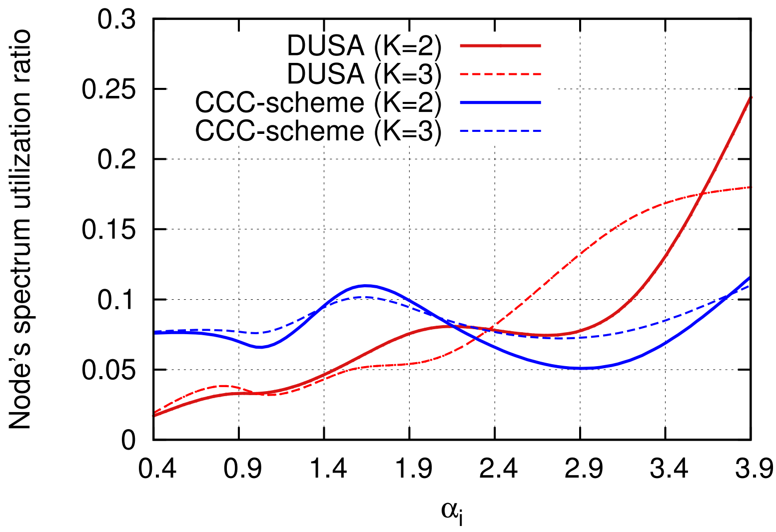

Figure 3.13: DUSA: Node's spectrum utilization ratio vs packet arrival rate.

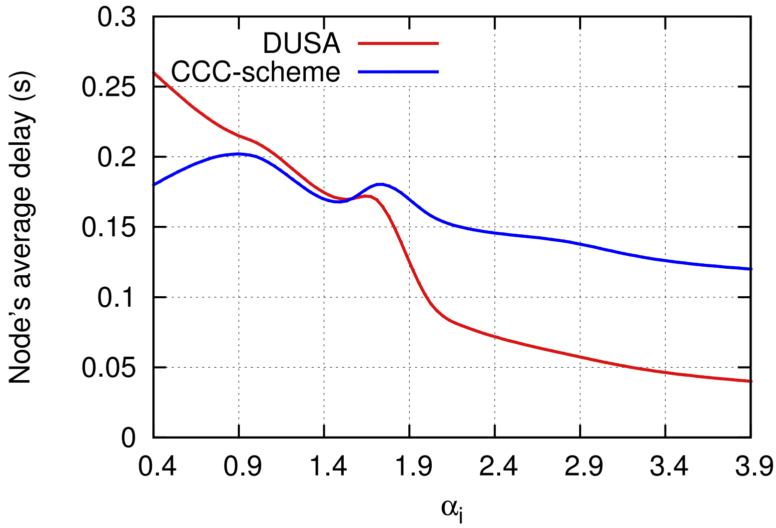

Figure 3.14: DUSA: The average packet delay vs packet arrival rate.

3.8 Discussion

All the above simulation results illustrate the proposed channel assignment schemes' capabilities to allow smart grid sensors to fairly share available spectrum resources with their neighbors based on local estimate:

- In smart homes, CSRA allow deployed sensors to use the aggregate accumulative average data packets successfully sent by every node in addition to the probabilities that the licensed channels are available inside the home to allocate the channels. Every smart home node predicts the channels' combination that maximizes the network spectrum utilization while responding to the prioritized nodes to send their data to the HAN-G. Based on the comparison between CSRA and the *Ideal-Centralized* scheme, simulation results demonstrated the ability of CSRA to achieve a fair channel allocation between SUs in smart homes. Simulation results showed that the packet delivery ratio (PDR) significantly increases with the frame size. Moreover, CSRA achieved nearly the same performances in terms of PDR and average delay as an ideal centralized fair scheduling. This definitely sustains the high efficiency and reliability of the CSRA scheme. Thus, the proposed probabilistic estimations of the smart home user's fairness metric and of the channels' states as sensed by every node represent a pertinent indicators for a distributed fair and probabilistic spectrum access decision, CSRA.

- In smart grid NANs, simulation results showed that the probabilities that a node has b stored data packets in addition to the channels' states estimation play an important role in achieving a prioritized spectrum sharing among NAN sensors with different priorities. The performance results revealed that unselfish behavior is achieved with DUSA (every sensor respects the needs of its neighboring nodes to transmit data and as a result it postpones its data transmission). The spectrum utilization of a given node increases with the increase of its priority (its queue length). Moreover, its average packet delay increases with the decrease of its priority. Furthermore, despite the absence of the CCC, the spectrum utilization is improved with the proposed solution.

3.9 Conclusion

In this chapter, we have investigated the application of one-hop CRSNs for two smart grid systems: smart homes and neighborhood area networks (NANs) segments. We focused on distributed and fair spectrum sharing in each system without using a common control channel. In smart homes, the SUs have the same priority to access to the spectrum. However, in NANs, the SUs have heterogeneous priorities. As a result, given the differences between both systems, we proposed two channel assignment schemes:

- **CSRA**: The Cooperative Spectrum Resource Allocation in CRSNs for smart homes.
- **DUSA**: The Distributed Unselfish Spectrum Assignment in CRSNs for NANs.

To achieve fairness with CSRA, each smart home node locally estimates the number of data packets successfully sent by all its interfering neighbors. This estimation allowed to select in each frame, the channels' configuration that maximizes the whole spectrum utilization using a Partially Observable Markov Decision Process (POMDP) formulation. Simulation results showed the efficiency of CSRA in achieving a fair channel allocation between SUs in smart homes. Moreover, the CSRA performances in terms PDR and average packet delay nearly approach an ideal centralized scheduling where a CCC free of any PU is used.

In DUSA, NAN SUs are prioritized according to their buffer occupancy. We have proposed a three-dimensional Markov chain to estimate the buffer occupancy variations of a SU based on its local spectrum available resources. Every SU selects the channel maximizing its local network spectrum utilization. This is achieved thanks to POMDP formulation. Simulation results revealed that DUSA achieves the two main objectives: the unselfish distributed spectrum access and the channel assignment without the use of a CCC.

In both schemes, we used a two-state Markov chain modeling a licensed channel to get an observation of neighboring nodes' selected frequency bands. Simulation results showed the efficiency of this tool. However, this may necessitate a frequent control message exchange in order to refresh the observation probabilities and the estimated fairness metrics, i.e., the real number of data packets successfully sent by every SU with CSRA and the buffer occupancy in every SU with DUSA. Moreover, both CSRA and DUSA are restricted to the one-hop CRSN topology. This may not be the case especially in an outdoor case, i.e., in NANs. Accordingly, in the next chapter, our target will be the improvement of the SUs' observation of their neighboring nodes' states and the extension of the DUSA scheme in order to take into consideration the sensors' short transmission range.

Chapter 4

Dual-Spectrum Assignment in Two-Stage CRSNs for Smart Grids

Contents

In the previous chapter, we focused on fair channel allocation in one-hop smart grids, as in the case of HAN and NAN systems. The proposed approaches allocate spectrum fractions as sensors need based on different criteria (traffic priorities, neighborhood properties and channels' availability). Both schemes proved their ability to achieve fairness in spectrum assignment in one-hop SG systems and without relying on a CCC. But, for both approaches, we assume that the gateway is always located at a distance from the sensors which may not be the case in some practical deployment scenarios or if some sensors have short transmission ranges.

To alleviate the above mentioned inconvenience, we investigate in this chapter a more general deployment scenario where sensor nodes can reach their gateway no matter their transmission range. This will be performed by using some particular nodes between deployed monitoring sensors and their gateway. These introduced nodes are called forwarding nodes. They are full functional nodes and have the ability to forward the sensors' traffic to their gateway. Therefore, we focus here on NAN smart grid systems where forwarding nodes will be powerful, long transmission range nodes. They will be in charge of collecting and forwarding the sensors traffic to a local control center (CC), i.e., to the NAN-G.

Thus, in accordance with prioritized SG sensors and the two-stage network topology that we will introduce, we propose in this chapter the Dual-Spectrum Assignment for NANs (D-SAN) approach. D-SAN is basically composed of two complementary channel assignment schemes. Each scheme is related to a communication in a stage of the NAN.

- The first approach executes channel assignment from the terminal nodes, the sensors, to the forwarding nodes. It is inspired from the DUSA scheme, introduced in the previous chapter and is designated as DUSA$^+$.
- The second approach is interested in the communication between the forwarding nodes and the NAN gateway. It allocates channels to forwarding nodes in order to transmit aggregated data to their associated NAN-G. It is called Balanced Spectrum Resource Allocation (BSRA).

D-SAN is based on POMDP formulations. It fairly allocates spectrum resources to deployed sensors, again without using a CCC.

The remainder of this chapter is organized as follows. We first highlight the different motivations behind our proposed D-SAN approach for NANs in Section 4.1. In Section 4.2, we introduce the two-stage CRSN topology and the network model. Thereafter, in Section 4.3, the two D-SAN's steps are detailed. We evaluate the efficiency of our proposed solution in Section 4.4 through extensive simulation and we discuss our contribution assessment in Section 4.5. Finally, in Section 4.6, we conclude the chapter.

4.1 Context and Motivations

In SG NANs, different topological scenarios may be considered to deploy wireless sensors [107]. In this context, the one-hop WSN is one of the widely recognized topology given its benefits, as we detailed in the previous chapter. However, this topology is adequate for small scale NANs. It represents a pertinent solution to monitor a NAN when the NAN-G is placed in the transmission range of all sensors. However, if sensors have short transmission ranges, then the use of a one-hop topology would not be possible for NANs. Accordingly, to tackle this problem while getting benefits from the advantages of the one-hop topology, several studies [47, 50, 108] proposed the division of a SG NAN into multiple sub-systems, named building area networks (BANs). Indeed, different gateways are deployed distributively in a NAN. Every gateway collects data from sensors deployed in its vicinity. Then, it transmits the collected data to the local CC, i.e., the NAN-G. Every BAN is considered as a power distribution network where a one-hop communication network is installed. However, these works basically focus on the architectural design of the SG communication network. Moreover, if a CRSN is assumed to be deployed to monitor a BAN, then one spectrum broker is generally assumed to be deployed [50]. The spectrum broker shares the available spectrum resources among the different deployed gateways. However, the existence of a spectrum broker rises the problems of a single point of failures. Moreover, its presence necessitates the use of a CCC for control messages exchange between the spectrum broker and the deployed gateways.

In order to avoid the above mentioned inconveniences, in this chapter, we are interested in distributed channel assignment in CRSNs to monitor SG NAN without using neither a CCC nor a BAN based o a spectrum broker. First, we propose a practical two-stage CRSN topology for NANs. Full-functional nodes, that we call forwarding nodes, are introduced in this context to extend the transmission range of SG monitoring sensors, named terminal nodes. Thereafter, we propose the Dual-Spectrum Assignment for NANs (D-SAN) approach. Based on the proposed two-stage topology, D-SAN is interested in the channel assignment process in each stage of the NAN. Thus, D-SAN is composed of two channel assignment policies. The first policy, DUSA$^+$, is executed by terminal nodes to communicate with forwarding nodes. The second policy, BSRA, allows every forwarding node to obtain its channel to forward its aggregated data (terminal nodes' data) to a NAN-G, i.e., a CC.

Performance evaluation of D-SAN through the OMNeT++ network simulator demonstrates its ability to share spectrum according to the terminal nodes' priorities. Moreover, it reveals that the developed system is a good candidate for independent, fair and distributed channel assignment in such prioritized SG systems.

4.2 Two-Stage NAN System Description

D-SAN is based on a two-stage CRSN topology. Thus, before introducing the D-SAN scheme, we present in this section the two-stage CRSN architecture we advocate to use here for NANs. First, we describe in Section 4.2.1 the two-stage topology of CRSN for NANs. Then, in Sections 4.2.2 and 4.2.3, we respectively introduce the terminal nodes and the forwarding nodes' activities. Finally, in Section 4.2.4, we detail how the two-stage CRSN will be organized to allow an efficient data transmission between deployed sensors.

4.2.1 Topology Presentation

To monitor and control the NAN's power infrastructure, we assume the existence of the list $\mathcal{S} = \{n_1, \ldots, n_N\}$ of N sensor nodes that we denote by Terminal Nodes (TNs). Every TN ($n_i \in \mathcal{S}$) is responsible of monitoring a NAN element/system such as smart homes, distribution substations and power storage systems. The monitored NAN elements/systems have heterogeneous impacts on the electricity distribution. As a result, the deployed TNs have not the same priorities to transmit their data. Generally, every TN has to send its data to the CC, i.e., sink or NAN-G. However, some TNs $n_i \in \mathcal{S}$ may be placed more than one-hop away from the CC. As a result, we propose the deployment of a list $\mathcal{R} = \{r_1, \ldots, r_F\}$

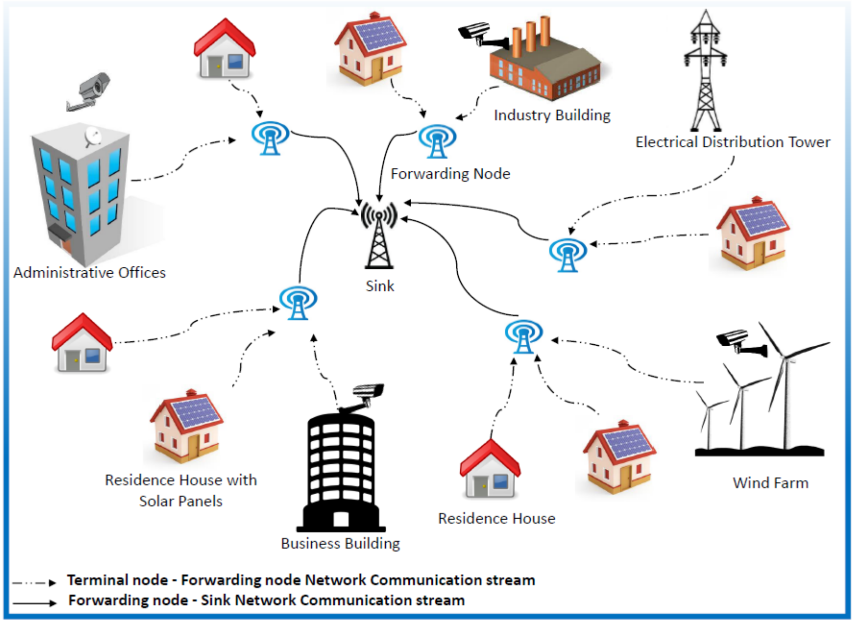

Figure 4.1: Two-stage CRSN topology for NANs.

of F full functional nodes that we call Forwarding Nodes (FNs). The list $\mathcal{R}$ will extend the TNs' coverage. As shown in Figure 4.1, FNs are placed between TNs and a sink. They receive SG data from TNs to, thereafter, send it to the sink node through one-hop transmissions. Accordingly, every TN ($n_i \in \mathcal{S}$) has at least one FN r_u ($r_u \in \mathcal{R}$) placed in its transmission range, in the sink direction. We denote by $\mathcal{R}_i$ the list of FNs that are able to receive data from n_i and to send it to the sink. Every TN will select only one FN r_u where $r_u \in \mathcal{R}_i$ to be its next-hop to the sink. r_u is called the n_i's associated FN. Now, we can conclude that the SG users network are composed of two sets of sensors: $\mathcal{R}$ and $\mathcal{S}$. Both kinds of sensors are cognitive radio-enabled. They communicate through a list of licensed channels $\mathcal{H} = \{c_1, \dots, c_K\}$ as we will explain in the following.

4.2.2 Terminal Nodes' Activity Description

To efficiently monitor a NAN, we assume that a TN $n_i \in \mathcal{S}$, is subject to the following assumptions:

- Given the prioritized NAN applications, n_i generates data packets according to a Poisson process with its own average packet arrival rate α_i.
- n_i has a finite buffer queue of size B to store its generated data packets waiting for transmission.
- At one point in time, n_i has one and only one associated FN $r_u \in \mathcal{R}_i$ that will always forward the n_i's data to the sink. Thus, if n_i wants to transmit, then it sends the data to r_u. Thereafter, r_u will send it to the sink.

- The communication between TNs and FNs takes place on the list $\mathcal{H}_1 = \{c_k, /k \in [1, \ldots, K_1]\}$ of K_1 licensed channels where $K_1 < K$ and $\mathcal{H}_1 \subset \mathcal{H}$.
- The TNs and the FNs are synchronized in time according to the frame structure introduced in the previous chapter (Subsection 3.3.2).
- Every TN n_i is equipped with one single radio interface able to switch a list $\mathcal{H}_1$ of licensed channels.

4.2.3 Forwarding Nodes' Activity Description

The FNs are placed in a monitored NAN to relay TNs' generated data to the sink. To better organize the communication in the NAN, we assume that:

- At one point in time, every FN, $r_u \in \mathcal{R}$, has its associated list of TNs $\mathcal{S}_u^*$ where:
  - For all $n_i \in \mathcal{S}_u^*$, r_u represents the n_i's associated node.
  - $\cup_{u=1}^{F} S_u^* = \mathcal{S}$.
- Every FN, $r_u \in \mathcal{R}$, is equipped with K radio interfaces:
  - K_1 interfaces are used to receive data from the list $\mathcal{S}_u^*$ of TNs.
  - K_2 radio interfaces are used to forward the TNs' received data to the sink node through the list $\mathcal{H}_2 = \{c_k/k \in [K_1 + 1, \ldots, K]\}$ of K_2 $(= K - K_1)$ channels.
- During the data transmission sub-period (T_{tr}) of a frame t, r_u can use more than one channel c_k to receive data from TNs and to forward data to the sink node.

As a matter of conclusion, the list of the licensed channels $\mathcal{H} = \{c_1, \ldots, c_K\}$ is divided into two sets of channels $\mathcal{H}_1$ and $\mathcal{H}_2$ used for communications between TNs and FNs and between FNs and a sink, respectively. We assume that:

- $K1 + K2 = K$
- $K1 < K$
- $\mathcal{H}_1 \cap \mathcal{H}_2 = \emptyset$
- $\mathcal{H}_1 \cup \mathcal{H}_2 = \mathcal{H}$

4.2.4 Spectrum-Driven Forwarding Node Selection

At each instant, every TN $n_i \in \mathcal{S}$ has only one associated FN $r_u \in \mathcal{R}$ that will be considered as its next-hop to the sink. However, n_i may have more than one FN $r_u \in \mathcal{R}_i$ that is able to receive and then to forward its data to the sink node. On another side, one of the major factors that impacts the SUs' access to a given frequency band is the channels' availability that depends on both time and location. Therefore, we propose n_i selects its associated FN $r_u \in \mathcal{R}_i$ based on a relative spectrum awareness. For this reason, we introduce in Equation (4.1) the spectrum rank parameter Δ_u:

$$\Delta_u = \frac{\frac{\sum_{n_i \in \mathcal{S}_u} \sum_{k=1}^{K_1} min(\omega_k^i, \omega_k^u)}{\sum_{n_i \in \mathcal{S}_u} \alpha_i}}{K_1 \times \|S_u\|} \tag{4.1}$$

Δ_u represents an estimated measure of the quantity of data that the FN r_u can receive from the TNs placed in its vicinity that we denote $\mathcal{S}_u$. Δ_u is a function of the steady state probabilities of the channels c_k's Idle states ($c_k \in \mathcal{H}_1$) and the average packet arrival rates α_i of the TNs n_i ($n_i \in \mathcal{S}_u$). Thus, as Δ_u increases, r_u becomes able to receive an important number of data packets through available frequency bands. As a consequence, we propose that every TN n_i chooses the FN r_u ($r_u \in \mathcal{R}_i$) having the highest Δ_u. Once every TN selects its associated FN $r_u \in \mathcal{R}_i$, r_u becomes the only n_i's next-hop to the sink. We denote by $\mathcal{S}_u^*$ the list of TNs n_i that have selected r_u as their associated FN.

After, the FN selection step, both FNs and TNs begin the channel assignment that will be repeated each frame as we will detail in the next section. Table 4.1 introduces the main notations used in our model.

For a sake of robustness, a reorganization of the TN-FN assignments will only be performed in case one FN disappears.

4.3 Dual-Spectrum Assignment for NAN-based Two-Stage CRSNs: D-SAN

Here, the network is well organized, i.e., every FN r_u has its own list of TNs $\mathcal{S}_u^*$. Thus, NAN data will be sent to the sink (NAN-G) through two-hops: from TNs $n_i \in \mathcal{S}_u^*$ to their associated FNs r_u and from FNs r_u to the sink. To this end, we propose a novel channel assignment approach that we call Dual-Spectrum Assignment for NANs (D-SAN). D-SAN consists of two channel allocation sub-policies. One first sub-policy, DUSA$^+$, is an extension of DUSA. It will be in charge of transmitting the data from TNs to FNs at the first network stage. The second sub-policy, Balanced Spectrum Resource Allocation (BSRA), is responsible of distributing channels to FNs to forward aggregated data to the

Table 4.1: Symbols and Notations.

Notation	Explanation
$\mathcal{S}$	The list of terminal nodes (TNs)
n_i	The TN number i ($i \in [1, N]$)
$\mathcal{R}$	The list of forwarding nodes (FNs)
r_u	The FN number u ($u \in [1, F]$)
$\mathcal{H}$	The list of licensed channels
$\mathcal{H}_1$	The list of licensed channels used by TNs
$\mathcal{H}_2$	The list of licensed channels used by FNs
α_i	The average packet arrival rate of n_i
B	The maximum buffer size
T_{gen}	The duration of the data generation period
T_{ss}	The duration of the sensing period
T_{tr}	The duration of the data transmission period
T_p	The micro-slot duration
λ_k^i	PU arrival rate in c_k according to n_i or r_i
β_k^i	The probability of channel c_k switching from Idle to Busy state
μ_k^j	The probability of channel c_k switching from Busy to Idle state
$\omega_k^i(t)$	The probability that n_i senses c_k idle during the frame t
ω_k^i	The steady-state probability of the channel c_k idle state
Pna_k^j	The probability of no PU reappearance in c_k during T_p
$D-1$	The maximum number of data packets to send during T_{tr}
$s_i(t)$	The aggregate accumulative average data packets successfully sent by n_i
$Ploss_k$	Packet loss probability in c_k
P_{gen}^i	The packet generation probability of n_i
δ	One channel sensing duration
$a_i(t)$	The channel estimated to be used by n_i during t
Δ_u	The r_u's spectrum rank parameter
$\mathcal{S}_u^*$	The list of TNs associated to the FN r_u
$a_i^*(t)$	The real channel used by n_i during t
γ_u	The r_u's weight to access to the spectrum
$\|S_u\|$	The number of TNs placed in the vicinity of r_u

sink at the second stage of the network. The main objective of D-SAN (both DUSA$^+$ and BSRA) is to perform a fair spectrum sharing that fits the TNs' prioritized traffic. In the following, we introduce in detail DUSA$^+$ and BSRA, respectively.

4.3.1 D-SAN's First Step: From Terminal Nodes to Forwarding Nodes

The TNs have different traffic priorities. Thus, DUSA$^+$ should achieve an access to the spectrum that fits the TNs' prioritized traffic. Accordingly, during every frame, each TN requires a local estimate of its neighboring nodes' transmission need. In the following, we introduce the solution we adopt to measure a TN's priority to access to the spectrum. Thereafter, we present the DUSA$^+$ policy we develop to share available frequency bands among TNs.

4.3.1.1 Terminal Nodes' Buffer Occupancy Estimation

Let n_i and n_j be two TNs associated with the same FN r_u ($n_i, n_j \in \mathcal{S}_u^*$). To allow n_i to properly estimate its neighbor n_j's requirements, i.e., n_j's spectrum access needs, we opt for the same strategy we adopted in the DUSA scheme and which we detailed in the previous chapter. Thus, n_i estimates the probabilities that n_j has b ($b \in [0, B]$) stored data packets waiting for transmission. We use the three-dimensional Markov chain depicted in Figure 4.2 to estimate each node buffer occupancy. This Markov chain is similar to the one used by DUSA and described in Chapter 3. But, compared to DUSA Markov chain, the one depicted in Figure 4.2 is related to only one frequency channel c_k where $k \in [1, K_1]$. Therefore, based on the n_i's selected channel during the frame t, the probability that n_i has a given number of data packets is obtained through the Markov chain related to this selected channel. Thus, the second dimension c of a given state (b, c, d) may have one of the two possible values, -1 or k. In the previously introduced Markov chain, the second dimension c can belong to K_1+1 values, i.e., K_1 values related to the K_1 licensed channels and the last value corresponds to the unavailability of the K_1 channels given their business by primary users.

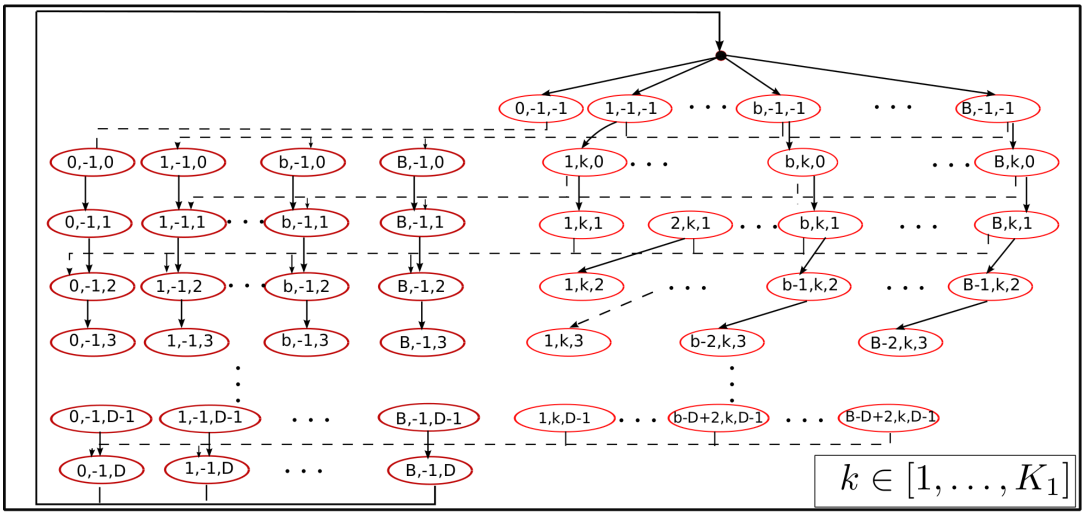

Figure 4.2: The DUSA$^+$ three-dimensional Markov chain.

The modification in the three-dimensional DUSA's Markov chain aims to provide a better estimation of a given node's states. In fact, we will not apply the estimated probability Ω_k^i (given by Equations (3.5) and (3.6) and which derivation is relatively fastidious) to determine channel c_k's availability. We rather use the probability that n_i senses c_k Idle (ω_k^i). Accordingly, the new transition probabilities $P[b, k, 0/b, -1, -1]$ and $P[b, -1, 0/b, -1, -1]$ are given as follows:

$$P[b, k, 0/b, -1, -1] = \omega_k^i \tag{4.2}$$

$$P[b, -1, 0/b, -1, -1] = 1 - \omega_k^i \tag{4.3}$$

The other Markov chain transition probabilities are the same as those introduced in the previous chapter (Subsection 3.4.2). Now, based on this three-dimensional Markov chain, we introduce, in the following, the way how the list of channels $\mathcal{H}_1$ is fairly and distributively assigned to the TNs.

4.3.1.2 Terminal Nodes' Decisions for Channel Selection

Let n_i and n_j be two TNs associated with the same FN r_u, i.e., $n_i,\ n_j \in \mathcal{S}_u^*$. Based on the probabilities $\pi(b, -1, -1)$ that n_i has b stored data packets waiting for transmission at the end of the generation sub-period T_{gen} of the frame t, n_j models the n_i's state as a partially observable Markov chain. Then, based on the estimated n_i's allocated channel, n_j updates the n_i's states. Accordingly, the access decision of n_i to the spectrum fits into a POMDP formulation. The POMDP modeling the state of n_i is defined as follows:

1. State: The n_i's state is presented by the vector $\psi_i(t)$ given by Equation (4.4) and is related to the node n_i's buffer occupancy probabilities $\pi(b, -1, -1)(t)$ where $b \in [0, B]$.

$$\psi_i(t) = [\pi(0, -1, -1)(t+1), \ldots, \pi(B, -1, -1)(t+1)] \tag{4.4}$$

2. Action: At the beginning of the frame t, n_i selects the channel $a_i(t) \in \{-1\} \cup \mathcal{H}_1$. If $a_i(t)$ is equal to -1 then n_i postpones its data transmission. Otherwise, n_i uses its estimated channel for data transmission.

3. Transition Matrix: The transition probabilities are the same as those previously introduced in Section 3.6 of the previous chapter (Equations (3.20) and (3.21)). Figure 4.3 depicts the different transitions between the node n_i's states.

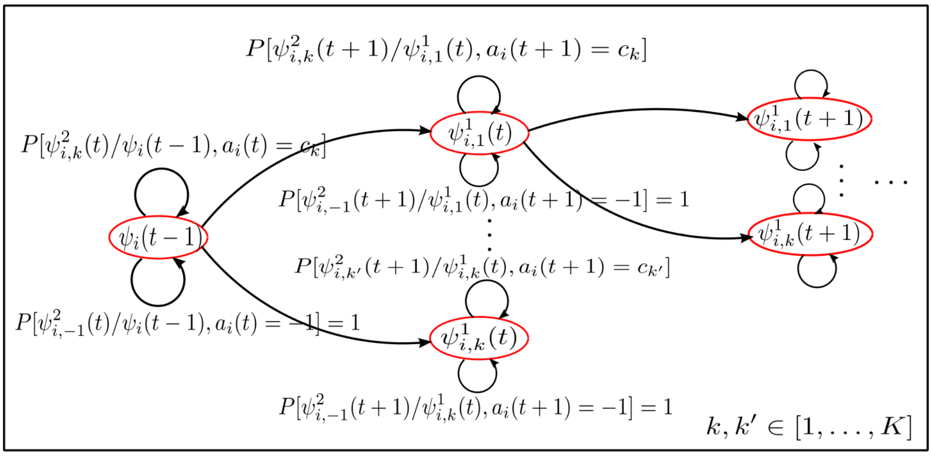

Figure 4.3: The DUSA$^+$ partially observable Markov chain.

4. Observation probability: In the DUSA's POMDPs, the respective probabilities that a given node n_j observes the node n_i transiting from one state to another are obtained

through the training of the two-state Markov chain modeling the selected channel (Subsection 3.3.3). Here, we propose to improve the observation probabilities of n_j concerning the states of the other TNs n_i. At every frame t, every FN r_u includes in its CTS and Ack packets the list Υ_u. As introduced in Equation (4.5) Υ_u is the list of couples $(n_i, a_i^*(t))$ where $n_i \in \mathcal{S}_u^*$. $a_i^*(t)$ represents the channel on which n_i has successfully sent a RTS to its associated FN r_u. If r_u does not receive an RTS from n_i, then $a_i^*(t)$ equals -1.

$$\Upsilon_u(t) = \{(n_i, a_i^*(t))/n_i \in \mathcal{S}_u^*,\ a_i^*(t) \in \{-1\} \cup \mathcal{H}_1\} \tag{4.5}$$

Accordingly, during the data transmission sub-period T_{tr} of the frame t, if for n_j one of the following conditions holds:

- n_j decides to postpone its data transmission, i.e., $a_j(t) = -1$,
- n_j senses its selected channel $a_j(t)$ Busy during T_{ss},
- n_j does not successfully receive an CTS from r_u,

then, during the remaining D micro-slots of T_{tr}, n_j switches the list of channels $c_k \in \mathcal{H}_1$ sensed available during T_{ss}. In every visited channel, n_j waits the reception of a CTS or an Ack sent by r_u. Based on the received message, n_j rectifies the estimated actions $a_i(t)$ and the channels' states probabilities $\omega_k^i(t)$ ($\forall n_i \in \mathcal{S}_u^*$). Here, we introduce the Boolean variable Φ_j. If n_j successfully received/sensed a CTS or an Ack from r_u then Φ_j equals 1. Otherwise, Φ_j is equal to 0. Algorithm 3 details how a node $n_j \in \mathcal{S}_u^*$ updates the actions $a_i(t)$ and their corresponding observation probabilities $O[\psi_{i,k}(t)^1, a_i(t)]$, $\forall n_i \in \mathcal{S}_u^*$.

5. Reward: As presented in the DUSA approach, the utility function computed by using Equation (3.24) is the probability that n_i transmits $D-1$ data packets, if its buffer occupancy is more than or equal to $D-1$, or if all the stored data packets will be successfully transmitted on the selected channel. $P_i(\psi_i(t))$, the probability that n_i is in the state $\psi_i(t)$. It is computed as in Equation (4.6). We denote by Λ the possible states that a node's states can belong to, i.e., $\psi_i(t) \in \Lambda$

$$P_i(\psi_i(t)) = \frac{\sum_{\psi_i(t-1)\in\Lambda} P_i(\psi_i(t-1))P(\psi_i(t)/\psi_i(t-1), a_i(t))O[\psi_i(t), a_i(t)]}{\sum_{\psi_i'(t)\in\Lambda} O(\psi_i'(t), a_i(t)) \sum_{\psi_i(t-1)\in\Lambda} P_i(\psi_i(t-1))P(\psi_i'(t)/\psi_i(t-1), a_i(t))} \tag{4.6}$$

Now, based on the states of n_i ($\forall n_i \in \mathcal{S}_u^*$), $n_j \in \mathcal{S}_u^*$ proceeds to assign the channels. By using (4.7), n_j predicts the channels' combination that will be used by the list of nodes $\mathcal{S}_u^*$ to maximize the sum of the rewards $R_i(t)$ ($\forall n_i \in \mathcal{S}_u^*$). Thereafter, if $a_j(t) \in \mathcal{H}_1$ then n_j starts its data transmission on the selected channel (if it is sensed free of PUs). If $a_j(t)$ equals -1 or n_j does not successfully receive a CTS then n_j switches the list of available channels to sense a CTS or an Ack and to rectify the estimated channels as presented in Algorithm 3.

$$\begin{aligned} \underset{a_i \in \{-1\} \cup \mathcal{H}_1}{\text{Maximize}} \quad & \sum_{n_i \in \mathcal{S}_u^*} R_i(t) \\ \text{subject to} \quad & \forall n_i,\ n_l \in \mathcal{S}_u^*,\ \text{if } n_i \neq n_l \text{ and } a_i(t) \neq -1, \\ & \text{then } a_l(t) \ \neq \ a_i(t) \end{aligned} \tag{4.7}$$

Algorithm 3 Observation probability update.

if $\Phi_j == 1$ **then**
  for $n_i \in \mathcal{S}_u^*$ **do**
    $a_i(t) \leftarrow a_i^*(t)\ \{n_i, n_j \in \mathcal{S}_u^*\}$
    for $c_k \in \mathcal{H}_1$ **do**
      if $(a_i(t) \in \mathcal{H}_1)$ and $(a_i(t) == c_k)$ **then**
        $\omega_k^i(t) \leftarrow 1$
      else
        $\omega_k^i(t) \leftarrow (1 - \omega_k^i(t-1))\beta_k^i + \omega_k^i(t-1)(1 - \mu_k^i)$
      end if
    end for
  end for
end if
for $n_i \in \mathcal{S}_u^*$ **do**
  if $a_i(t) \in \mathcal{H}_1$ **then**
    $O[\psi_{i,k}(t)^1, a_i(t)] \leftarrow \omega_k^i(t)\ \{a_i(t) = c_k\}$
    $O[\psi_{i,k}(t)^2, a_i(t)] \leftarrow 1 - \omega_k^i(t)$
  else if $a_i(t) = -1$ **then**
    $O[\psi_{i,-1}(t)^1, a_i(t)] \leftarrow 0$
    $O[\psi_{i,-1}(t)^2, a_i(t)] \leftarrow 1$
  end if
end for

4.3.2 D-SAN's Second Step: From Forwarding Nodes to The NAN-G

The deployed FNs do not generate data. They play the role of relay nodes. Every FN r_u receives data from its associated TNs $\mathcal{S}_u^*$. Then, it forwards the received data to the sink node on one-hop data transmission through the list of channels $\mathcal{H}_2$. Therefore, we introduce in this section the second sub-policy of D-SAN that we call Balanced Spectrum Resource Allocation (BSRA). BSRA is be executed by every FN. It is in charge of assigning the list of frequency bands $\mathcal{H}_2$ to the FNs. In BSRA, the FNs should use different channels during a frame t to not interfere on the sink side. Consequently, we propose that every FN r_u models its interfering FNs $r_v \in \mathcal{R}$ as a partially observable Markov chain. Moreover, to consider the prioritized deployed TNs, we introduce in Equation (4.8) the parameter γ_u.

$$\gamma_u = \sum_{n_i \in S_u^*} \alpha_i, \; r_u \in \mathcal{R} \tag{4.8}$$

γ_u represents the weight of r_u to access to the spectrum. The higher the r_u's weight is, the more chance r_u will have to access to the spectrum. Thus, we formulate the partially observable Markov chain, modeling the FN r_u, as follows:

1. State: During the frame t, r_u's state $s_u(t)$ is the approximation of the aggregate accumulative average number of packets successfully sent by r_u at the end of the frame t.

2. Action: An action $a_u(t)$ represents a channel allocated to r_u during t.

3. Transition Matrix: The transition probabilities are the same as those introduced in the CSRA approach (Equations (3.10) and (3.11)).

4. Observation probability: Here, to obtain the observation probabilities, the FNs follow the same strategy used in DUSA$^+$. The sink node includes in its CTS and Ack the list $\Gamma(t)$, introduced in Equation (4.9). $\Gamma(t)$ is similar to the list $\Upsilon_u(t)$, sent by r_u to its associated TNs $\mathcal{S}_u^*$ in DUSA$^+$ (Equation (4.5)). It contains the list of couples $(r_u, a_u^*(t))$ where $a_u^*(t)$ represents the effective channel on which r_u sends its data packets. Thus, every FN r_v proceeds to switch the channels $c_k \in \mathcal{H}_2$ sensed available if it decides to postpone its data transmission ($a_u(t) = -1$). Thus, r_v updates the state of r_u as used in Algorithm 3 where $r_u \in \mathcal{R}$.

$$\Gamma(t) = \{(r_u, a_i^*(t))/ \; r_i \in \mathcal{R}, \; a_u^*(t) \in \{-1\} \cup \mathcal{H}_2\} \tag{4.9}$$

5. Reward: As shown in Equation (4.10), the reward R_u^* obtained during the frame t is a measure of the r_u's priority to send data during the frame $t+1$. It measures the number of data packets successfully sent by r_u regarding the packet arrival rates of its associated TNs S_u^*, i.e., its weight γ_u. Thus, a given FN r_v ($r_v \in \mathcal{R}$) will update the reward R_u^* of its interfering FNs $r_u \in \mathcal{R}$ once it receives a CTS or an Ack.

$$R_u^*(t) = \frac{\gamma_u}{s_u^1(t)} \tag{4.10}$$

Now, during a frame t, every FN $r_u \in \mathcal{R}$ uses the BSRA sub-policy. It proceeds to allocate the channels $\mathcal{H}_2$, distributively. It sorts the list $\{R_v^*(t-1), \; r_v \in \mathcal{R}\}$ in decreasing order. Then, it, sequentially, proceeds to allocate the channel to each FN r_v in a way to minimize its reward value $R_v^*(t)$. The FNs should use different channels to not interfere with each other in the sink side.

4.4 Performance Evaluation

In this section, we first propose to evaluate the performance of the first stage D-SAN process, the DUSA$^+$ algorithm and compare its results to those obtained by the DUSA scheme introduced in Chapter 3. The objective of this comparison is to evaluate the effect of the observation probabilities' update through the channel hopping process and the parameter $\Upsilon_u(t)$ introduced in Equation (4.5) on the spectrum utilization. Then, in the second step, we study the full D-SAN approach capabilities. Simulation results are obtained through the OMNeT++/MiXiM network simulator [103, 104].

4.4.1 DUSA vs DUSA$^+$

The extension of DUSA, DUSA$^+$, basically aims to improve the SUs' observations related to their neighbors' decisions regarding channels' selection. So, in order to evaluate the effects of such improvement, N terminal nodes are uniformly deployed one-hop away from one FN in a $100m \times 100m$ square field. The FN is deployed in the center of the monitored area and 3 PUs are also installed. The TNs' average packet arrival rates (α_i) are randomly generated and assigned to the TNs at the beginning of every simulation ($\alpha_i \in \{0.4,\ 1.4,\ 2.4,\ 3.4\}$). Table 4.2 lists the basic parameters used in both simulations.

Table 4.2: Simulation Parameters.

Notation	Explanation
Simulator	OMNeT++ (4.6)/MiXiM (2.3)
Channel occupancy	0.13/0.2/0.35/0.43/0.45/0.5/0.83
Channel bandwidth	20 MHz
δ	0.1 s
PU's transmission range	30 m
D	4

First, we evaluate the effect of varying the number N of SUs on the total packet delivery ratio (PDR). Figure 4.4 shows that DUSA$^+$ outperforms DUSA in terms of PDR for $K = 3$ and $K = 4$ (where K is the number of channels used by the deployed nodes to send their data to the sink). For both schemes, the PDR reversely decreases with N. The decrease in PDR results from the increase in the data volume with the number of SUs N. However, for different values of N and K, DUSA$^+$ always achieves better PDR than DUSA. In fact, thanks to the update of the observation probabilities via the parameter $\Upsilon_u(t)$ included in CTS or Ack frames sent by the FN, the TNs are able to refine their channel allocation decisions. In fact, they will consider the actual frequency band allocated to their neighbors rather than locally estimated selected channels. As a result, the probability that a TN finds its allocated channel available is higher with DUSA$^+$ than with DUSA.

The ability of DUSA$^+$ to allocate available channels to the appropriate/adequate nodes is further illustrated in Figure 4.4.2. Figure 4.4.2 depicts the PDR variation with the

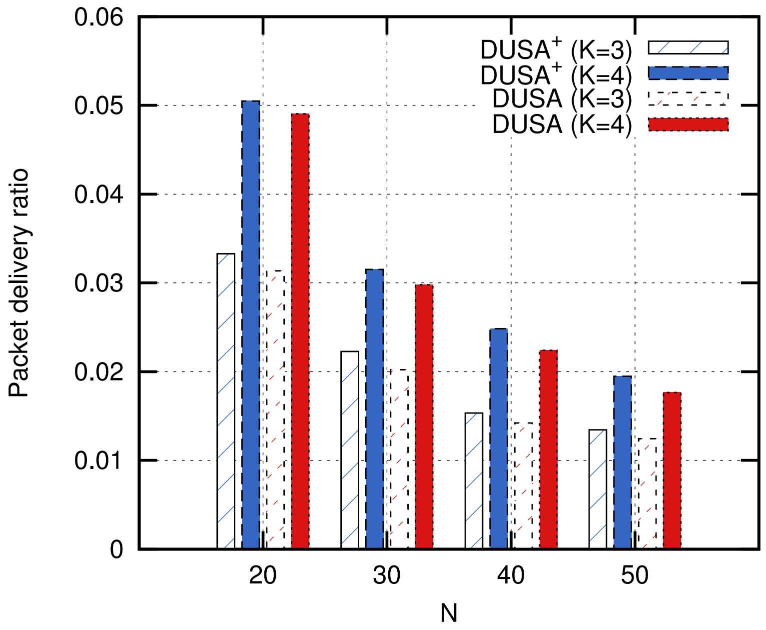

Figure 4.4: Packet delivery ratio vs terminal nodes' number N.

sensors' priorities, i.e., average packet arrival rates, for two different values of K ($K = 3$ and $K = 4$) when N equals 20. DUSA$^+$ allows a prioritized spectrum sharing. This figure clearly depicts the PDR increases with the TNs' priorities. Furthermore, one can note that DUSA$^+$ improves the PDR for the different nodes' priorities compared to the DUSA approach. We can thus conclude that, DUSA$^+$ outperforms DUSA in terms of spectrum utilization.

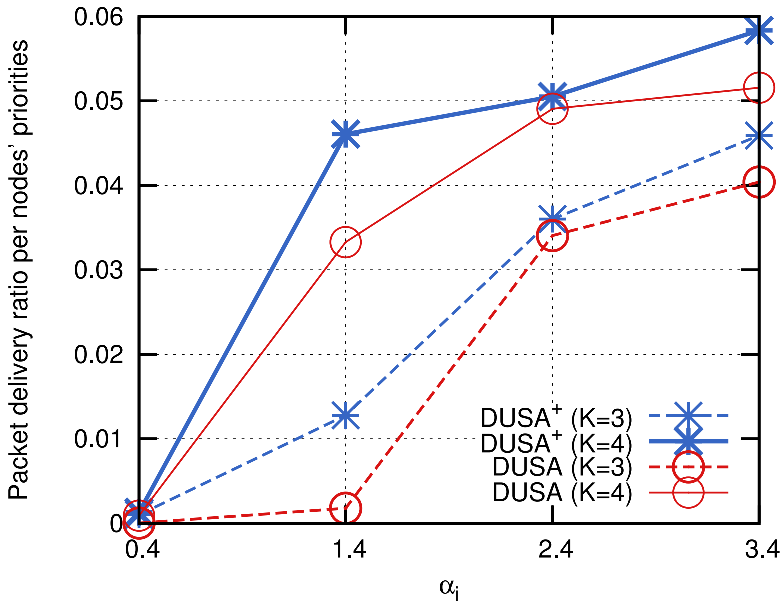

Figure 4.5: Packet delivery ratio per nodes' priorities.

4.4.2 Full D-SAN Scheme Evaluation

In the second step of the simulation, we are interested in the performance evaluation of the full D-SAN approach adopted in the two stage CRSN to monitor NAN systems. We deploy N TNs and 3 FNs in a $200m \times 200m$ square field. $(100, 0)$ represents the sink coordinates. The deployed FNs are able to reach the sink through one-hop data transmissions.

In D-SAN, every TN is interested in the channel allocation to itself and to the TNs that have selected the same FN to send their generated data. Therefore, TNs that share different FNs opportunistically access to the same list of channels. Thence, we first focus on the successful TN-FN rendezvous ratio. We denote by a successful rendezvous, the successful RTS/CTS exchange between a TN and its associated FN on a given selected channel. A failed rendezvous occurs if one of the following events holds:

- The selected channel is sensed occupied by a PU during T_{ss}.
- A PU arrives during the first micro-slot of T_{tr}.
- An RTS/CTS collision occurs.
- Either RTS or CTS packets are lost given the non-perfect channel condition.

Figure 4.6 shows the successful rendezvous ratio as a function of TNs' priorities. The successful rendezvous ratio reversely decreases with the number of deployed PUs. In fact, as the number of deployed PUs increases the licensed channels become more and more scarce. However, the successful rendezvous ratio increases with the TNs' priorities. Hence, we conclude that at the first stage, D-SAN achieves an efficient channel allocation while considering TNs' traffic rewards.

During the channel allocation between TNs and FNs and between FNs and the sink, the probability that a PU arrives during the data transmission sub-period (T_{tr}) is considered during the channel allocation processes. In Figure 4.7, we evaluate the link reliability of TNs and FNs for different numbers of deployed PUs. We define the link reliability as the probability that the allocated channel between a TN and its corresponding FN or between a FN and the sink reminds available during T_{tr}. Thus, if the link is reliable, then the emitter node can transmit $D - 1$ data packets. As shown in Figure 4.7, for each scenario, D-SAN achieves reliable links. Indeed, the FNs' link reliability approaches 1 and the link reliability values of the TNs slightly decrease reversely with the number of deployed PUs. Despite the slight degradation in the TNs' link reliability with the increase in the number of deployed PUs, all its values are still high (> 0.74).

Finally, we compare D-SAN to the distributed channel allocation scheme-based on the use of CCC. Figure 4.8 depicts the number of successful received data packets by the sink for different values of N and K_2 ($K_2 = 3$ and $K_2 = 4$). For both compared schemes the

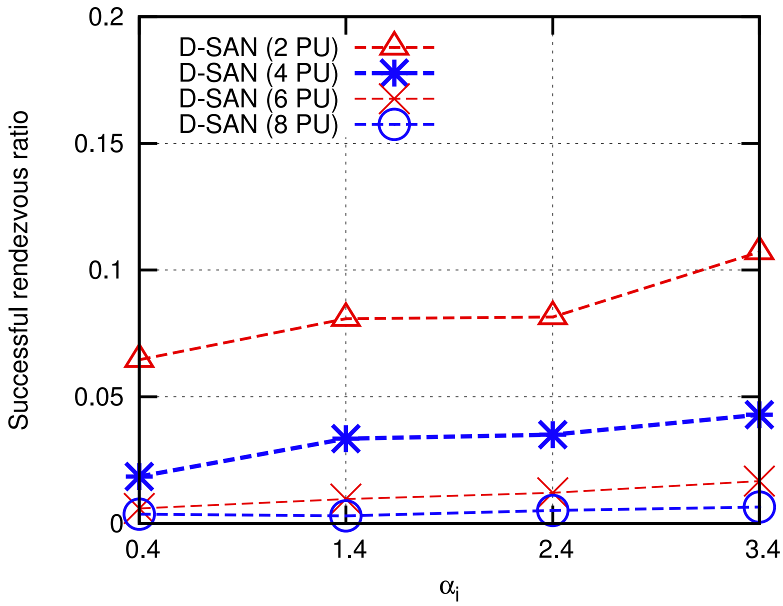

Figure 4.6: Successful rendezvous ratio per nodes' priorities.

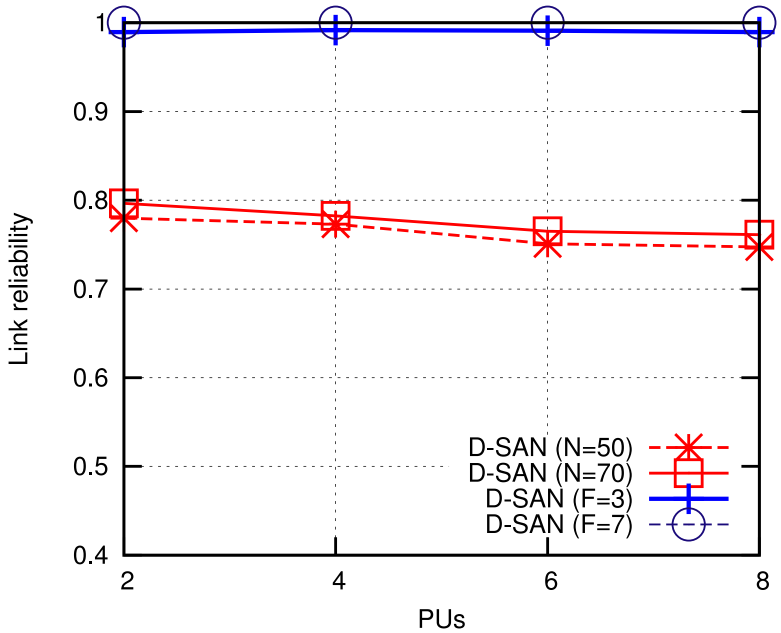

Figure 4.7: Link reliability vs number of PUs.

number of successful transmitted data packets increases with K_2. However, it decreases with the increase in N. In D-SAN, the degradation in the number of successful transmitted data packets is due to the collisions among TNs associated to different FNs. In the CCC-based scheme, the successful received data packets decrease with the increase in N due to the congestion of the CCC. As the number of contenders increases, the CCC becomes a bottleneck. For different values of N, D-SAN outperforms the CCC-based scheme. D-SAN does not use a CCC. It exploits all the available channels. However, the CCC-based scheme depends on the CCC's states (Idle, Busy).

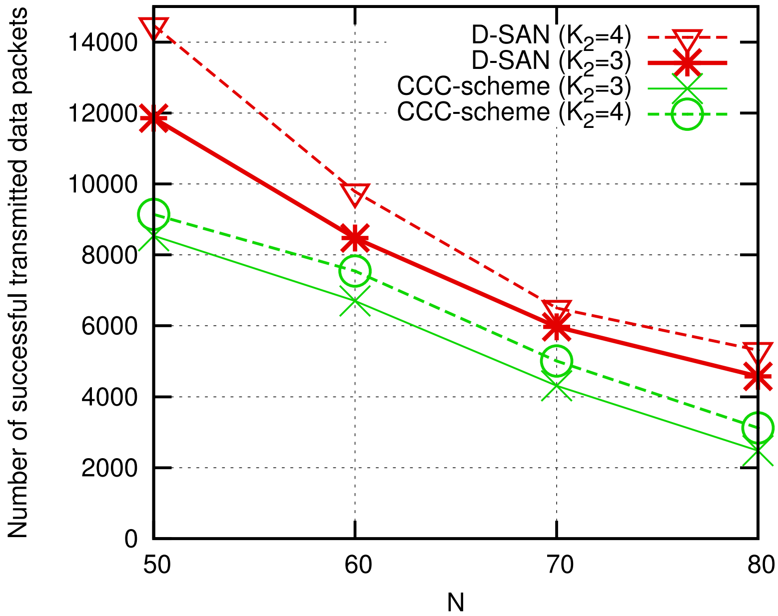

Figure 4.8: Successful transmitted data packets vs terminal nodes' number N.

4.5 Discussion

In the previous section, we presented the performance evaluation of D-SAN. We mainly focused on the evaluation of the proposed scheme capabilities to efficiently allocate idle channels to prioritized SUs, i.e., the SUs in need to transmit data. The simulation results basically showed that:

- The update of the observation probabilities of interfering nodes' states through the exploitation of the parameter $\Upsilon_u(t)$ or Γ's content improves the network spectrum utilization. It allows the SUs, i.e., the TNs and/or the FNs, to obtain an observation of neighboring nodes' states and available channels that approaches the reality.

- In D-SAN, the spectrum sharing fits the prioritized deployment of terminal nodes. The probabilistic channel assignments allow the TNs and the FNs, respectively, to get a correct estimation of neighboring nodes' priorities and needs to access to the spectrum.

- D-SAN outperforms a CCC-based scheme since the later is based on the availability of one CCC which is challenging especially when the number of contending nodes increases. However, our proposed scheme exploits all the available channels without being dependent on one central unit.

4.6 Conclusion

In this chapter, we focused on multi-hop data transmission in CRSNs for SG NAN. To deal with the SG sensors' short transmission range, we proposed the introduction of forwarding nodes (FNs), i.e., full functional nodes. They are able to reach the sink in one-hop data transmission. The FNs extend the NAN monitoring sensors' coverage. The main contributions of this chapter can be summarized as follows:

- A two-stage topology for CRSNs in SG NAN: The deployed network is composed of two sets of SUs: a list of TNs and a set of FNs. Based on the prioritized deployment of TNs and the licensed channel availability, every TN selects its associated FN to achieve a better network organization. FNs forward the aggregated TNs' data to the sink.
- A Dual-Spectrum Assignment for NANs (D-SAN) approach: To prevent the use of a CCC during the two-stage communication, from TNs to FNs and from FNs to the sink, we proposed D-SAN. D-SAN is composed of two channel assignment sub-policies:
  - A first scheme represents an extension of the Distributed Unselfish Spectrum Assignment approach (DUSA), that we have introduced in the previous chapter. Thus, we call this first scheme DUSA$^+$. DUSA$^+$ allows a distributed channel allocation to TNs in order to send their generated data to FNs. Compared to DUSA, DUSA$^+$ allows TNs to refresh their observations of interfering TNs to obtain a more significant estimation of interfering TNs need to access to the spectrum.
  - The second channel assignment scheme is the Balanced Spectrum Resource Allocation (BSRA) approach. It is executed by the FNs to forward their received data from TNs to the sink node. Every FN estimates the needs of its interfering FNs to access to the spectrum. Then, it uses a POMDP formulation to assign the channels distributively.
- We have evaluated D-SAN through extensive simulation. Simulation results showed that the D-SAN channel assignment fits the prioritized deployed TNs. This is achieved thanks to the fact that, in D-SAN, the deployed SUs are able to estimate efficiently their neighboring nodes needs to access to the spectrum. Moreover, Simulation results revealed that D-SAN outperforms existing channel allocation works.

In this chapter, we introduced the deployment of FNs in the NAN to ensure the connectivity between the monitoring sensors, i.e., TNs and a sink. However, if the TNs' density is high, then the use of full functional nodes can be completely avoided as these FNs' cost may be relatively high compared to the native sensor devices. Thus, the native sensor nodes can be used to allow nodes to transmit TNs' data to the sink. In this context, data may reach the sink through multi-hop. On the other side, performance evaluation of D-SAN revealed that the number of successful transmitted data packets reversely decreases with the number of deployed terminal nodes. This problem can be avoided if we coordinate the access to the frequency bands between TNs associated to different FNs to avoid collisions. Therefore, this will be the focus of the next chapter where hierarchical multi-hop communications will be conducted in CRSNs to monitor SGs.

Chapter 5

Channel Assignment for Hierarchical Multi-Hop CRSN-based Smart Grid Systems

Contents

Smart Grid NANs represent the distribution SG segment. Several last mile technologies had been proposed to monitor this part of the grid. In this context and as state earlier, CRSNs are considered as one of the communication networks that mostly suits the SG characteristics. But, depending on the networks size and density, different CRSN topologies can be deployed to achieve an efficient SG monitoring in this part of the network. For instance, in Chapter 3, a simple one-hop CRSN topology was adopted to monitor a NAN system. Chapter 4, however, tackled the short transmission range of NAN sensors by introducing Forwarding Nodes. Now, in this chapter, we are interested in multi-hop CRSNs for SG NANs where the network density is high. In this context, forwarding nodes are no more needed as some NAN sensors can be used to forward other nodes' data through multi-hop communications. Moreover, we opt for hierarchical transmission to efficiently schedule the transmission coming from various monitoring nodes. As for the two previous chapters, the common control channel will be avoided in all data transmissions. Whereas the traffic in the network will be prioritized.

In the first part of the chapter, we propose a new clustering algorithm to auto-organize the deployed network into clusters without using a CCC. Then, we design a novel Predictive Hierarchical Spectrum Assignment (PHSA) scheme. Finally, as an extension of PHSA, we introduce the Routing-based PHSA (R-PHSA) approach. R-PHSA is a joint channel assignment and data routing scheme for hierarchical CRSNs while deployed in NANs. R-PHSA assigns channels distributively to NAN sensors while taking into consideration the routing aspects, i.e., the sensors' need to send data in the sink direction. Performance evaluation reveals that PHSA and R-PHSA achieve a balanced spectrum sharing among sensors and that both schemes outperform existing clustering works.

5.1 Context and Motivations

In SG NANs with large populations, the network density increases. Furthermore, in such area, a number of sensors may be placed more than one-hop away from the NAN gateway, i.e., a local control center or the sink. Thus, data can be sent to the sink in a multi-hop manner. In this context, a hierarchical network organization represents an encouraging topology to be considered in NANs. It allows a better network organization. Moreover, it adds robustness to the monitoring system against topological changes or faults. Thus, sensors will be divided into clusters. Every cluster is composed of one cluster head (CH) and several cluster members (CMs). Each CH is directly reachable from all its associated members. It collects their data. Thereafter, it proceeds to forward the collected data to the sink, through multi-hop transmission. Several works [109–114] recognize the use of clustered topologies for WSN monitoring SG power distribution areas. Moreover, multiple research works focus on the channel allocation in hierarchical CRNs. The main goal of these studies is to deal with the temporal and spatial availability of spectrum resources. They don't consider the differentiated priorities between SG sensors. Given this background, in this chapter, we intend to tackle the fair channel assignment in hierarchical CRSN for NANs. We will prevent the use of a CCC before every access to the spectrum. The main contributions of the chapter are the following:

- We propose a new spectrum-aware clustering algorithm. It divides the SG users into clusters without using a CCC ,while considering the prioritization within the deployed network.
- We develop the Predictive Hierarchical Spectrum Assignment (PHSA) scheme. In PHSA, licensed channels are affected to the SUs distributively based on local estimates of their neighbors' priorities. Channels are assigned through a POMDP since SUs have not a full observation of their neighborhoods' priorities.

- We develop the Routing-based Predictive Hierarchical Spectrum Assignment (R-PHSA) scheme. As an extension of PHSA, R-PHSA considers the routing aspects jointly with the channel assignment in CRSNs for NANs.

5.2 Related Work

The clustering was early integrated in traditional WSNs for many purposes routing, data aggregation, energy conservation, to name a few. A comprehensive survey of the most popular clustering schemes is discussed in [115]. Furthermore, the WSN clustered topologies use for smart grid applications has also been considered in the literature in [109–111]. These works are interested in prioritized SG traffics. The authors proposed cluster-based MAC protocols for WSNs to accelerate the transmission of prioritized data in SGs.

In cognitive radio networks, the vacuity of licensed bands fluctuates over the time depending on the primary signal arrivals, thus constraining SUs to achieve a permanent sensing of the available spectrum resources. In flat CRSNs, SUs may have different opportunities to access to the spectrum due the diversity of the neighboring environment (neighborhood degree, PUs arrival rates, etc.). In hierarchical topologies, the problem is accentuated since cluster heads (CHs) have to consider their members' diversity when allocating the channels. Several works have been proposed to deal with the heterogeneous spectrum opportunities between the SUs when forming clusters. In [116], the authors presented Cognitive Low-Energy Adaptive Clustering Hierarchy (CogLEACH), an extension of the LEACH routing protocol initially proposed for WSNs. Compared to LEACH, CogLEACH accounts for the number of vacant channels, available for each sensor node, when calculating its probability of being a CH. As a result, both throughput and network lifetime are improved. CHs selection and channel allocation are performed based on the channels' availability before forming the clusters. Thus, licensed channels are implicitly assumed to keep the same states during a long period of time. In [117, 118], efficient energy consumption schemes combining dynamic spectrum access to hierarchical routing in CRSNs are presented. Despite providing promising results for hierarchical CRSNs, [117] and [118] assume the permanent availability of a CCC. In [119], a cluster-based spectrum allocation scheme is presented. Sensors are divided into clusters based on their mutual interference degree (i.e., the number of channels shared between SUs belonging to the same cluster). [119] assumes the existence of a central unit to control SUs transmissions and the licensed channels' states which requires a permanent communication between the SUs and this central node. This cannot be guaranteed in CRNs where the access to licensed channels is conditioned by their vacuity of PUs. In [120], the authors proposed a clustering and a routing solution for CRNs where the radio resources are allocated based on a machine-learning algorithm. Clusters are partially reconstructed whenever the states of the channels change. This solution does not fit environments where channel states change rapidly. In [121], a dynamic cluster formation algorithm triggered by events occurrence is proposed. Clusters cover the region between the detected event and the sink's position. This work is not suitable for SG systems where multiple events may be detected consecutively or even at the same time (within very short time interval). In fact, every time an event is detected, sensors have to reconstruct clusters.

In the opposite of [121], [122] introduces a clustering algorithm where multiple control channels are used. Within every cluster, one local CCC is assigned. All the assigned control channels may be sensed occupied by primary signal. Accordingly, to efficiently allocate channels, SUs have to be always aware of these control channels' states which depend on the PUs activities.

Finally, we can conclude that all the above discussed works are based either on one or multiple CCCs. Moreover, they don't consider the prioritized aspects of deployed networks. Thus, to the best of our knowledge, no work has considered cluster-based solutions in prioritized CRSNs for SGs and without using CCCs before every access to the spectrum, which we argue is crucial throughout this thesis. Therefore, we propose in this chapter the PHSA and the R-PHSA schemes that don't use a CCC. They deal with prioritized SG in hierarchical CRSNs.

5.3 Hierarchical Multi-hop NAN Model

This section is dedicated to the presentation of the basic assumptions and the SU's medium access control we opt for our work. Furthermore, in this section, we introduce the workflow of the framework PHSA.

To this end, we model a NAN by the list $\mathcal{S} = \{n_1, \dots, n_N\}$ of N synchronized wireless sensors. Every sensor $n_i \in \mathcal{S}$ is deployed to monitor one NAN application/system. n_i is equipped with one radio interface able to switch a list of K licensed channels $\mathcal{H} = \{c_1, \dots, c_K\}$. The sink node, i.e., the local CC, has K radio interfaces to simultaneously receive data from multiple nodes on different available frequency bands. Furthermore, the sink communicates with the smart grid central control center through a high data rate technology. As previously used, every sensor n_i has its own average data packet arrival rate α_i. As n_i's average packet arrival rate α_i, is higher than n_j's average packet arrival rate α_j, i.e., $\alpha_i > \alpha_j$, n_i's controlled system has a more important impact on the NAN than the n_j's monitored system ($n_i, n_j \in \mathcal{S}$) [123].

Now, to efficiently transmit data to the sink, the deployed network is divided into clusters. We denote by $\mathcal{C}_i$ the list of CMs belonging to the cluster having as CH the node n_i. During an intra-cluster communication, a CH n_i collects the data from its associated CMs n_j ($n_j \in \mathcal{C}_i$). Thereafter, during the inter-cluster communication, CHs cooperate to forward the generated/received data to the sink node in a multi-hop manner.

5.3.1 Basic Assumptions

To efficiently transmit data to the sink, we consider the following assumptions:

- To get an estimation of a channel $c_k \in \mathcal{H}$ occupancy, we characterize the licensed signal activities. We model the occupancy of each channel by a two-state Markov chain (Busy, Idle) [101], as we used in the previous two chapters (Section 3.3.3).
- To transmit data to the sink, every CH n_i knows the hop count to the sink using the transmission range R_h [124].
- As shown in Figure 5.1, in order to control the network topology, every SU has two transmission ranges [124]:
  - R_m: the intra-cluster transmission range used between a CH and its corresponding members.
  - R_h: the inter-cluster transmission range used between CHs to forward data to the sink ($R_h \geq 2R_m$).

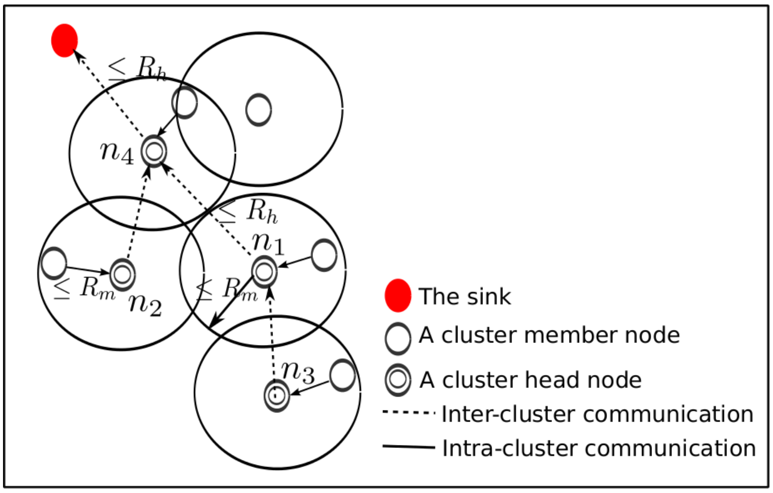

Figure 5.1: The hierarchical NAN structure.

- Each node $n_i \in \mathcal{S}$ is aware of all its neighbors $\mathcal{N}_h^i$ and $\mathcal{N}_m^i$ where:
  - $\mathcal{N}_m^i$: If $n_j \in \mathcal{N}_m^i$, then $d(n_i, n_j) \leq R_m$. $d(n_i, n_j)$ is the Euclidean distance between n_i and n_j.
  - $\mathcal{N}_h^i$: The set of the CH n_i' neighbors. If $n_j \in \mathcal{N}_h^i$ then $d(n_i, n_j) \leq R_h$.
- To transmit data to the sink, every CH knows the hop count to the sink using R_h [125].

5.3.2 Medium Access Scheme

To enable the smart grid sensors organized hierarchically to access the spectrum, we organize the SU's communications into super-frames. As depicted in Figure 5.2, a super-frame T' is composed of M_1 frames used for intra-cluster communications, i.e., to allow a given CH to collect data from its associated CMs. Thereafter, M_2 frames are dedicated to the inter-cluster data transmission, i.e., every CH forwards the received/generated data in the sink direction. If a given CH n_i is placed more than one hop (R_h) away from the sink, then it transmits data to one of its neighboring CH n_j ($n_j \in N_h^i$) placed closer to the sink.

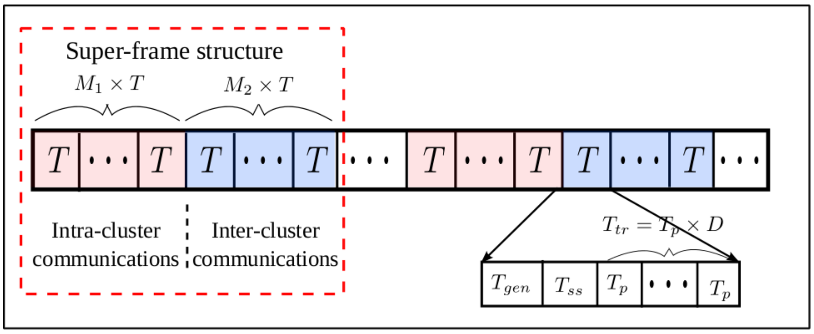

Figure 5.2: Super-frame structure.

The frame represents the basic time unit. It has a fixed duration $\mathcal{T}$ that is divided into three sub-periods: data generation (T_{gen}), sensing (T_{ss}) and transmission (T_{tr}), respectively. T_{gen} allows a given SU n_i ($n_i \in \mathcal{S}$) to, periodically, collect the physical measures on its monitored system/application with an average arrival rate α_i. The generated data packets are stored in a buffer queue. We denote by $Q_i(t)$, the node n_i's buffer occupancy during the frame t. During T_{ss}, each node checks the vacuity of the channels. Finally, data is transmitted during the T_{tr} sub-period. T_{tr} is composed of D micro-slots. The access to a given channel during T_{tr} is based on the CSMA/CA algorithm, as we have explained in the third chapter (in Section 3.3.2).

5.3.3 Predictive Hierarchical Spectrum Assignment Scheme Workflow

In Figure 5.3, we depict the PHSA approach workflow. This approach executes in 4 steps. The first step is dedicated to the cluster formation. Thereafter, to avoid the use of a CCC before each transmission, each CH locally estimates the channels to use for the M coming super-frames while considering its neighbors' priorities.

Only CHs are involved in the channel prediction for the intra/inter-cluster communications. Thus, every CH should inform its CMs of their assigned channels. Also, to coordinate their transmissions, CHs exchange their local decisions through the communication range R_h every M super-frames.

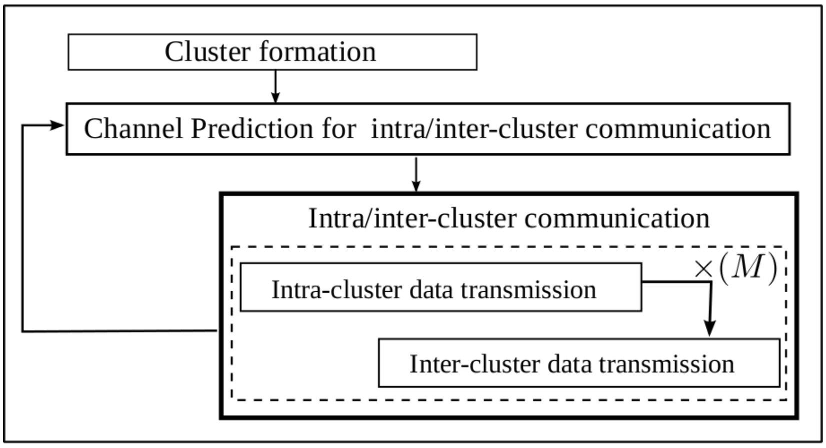

Figure 5.3: Hierarchical data transmission workflow.

Once channels are assigned, communications actually begin. During M super-frames, every SU turns its radio interface to its corresponding allocated channel and starts communicating. All kinds of control messages used during the cluster formation and the channel prediction are sent through a channel hopping process via the list of channels $\mathcal{H}$. The channel hopping mechanism is introduced in Algorithm 4.

Algorithm 4 Control message exchange.

Output: c_k

```
for d = 1 to D do
    Switch to the channel c_k
    if n_i has a control messages to send then
        if c_k is Idle then
            Broadcast the control message
        end if
    end if k ← k + 1 {if(k > K) then k ← 1}
end for
```

Now, based on our network model and the PHSA workflow, we present in the following the cluster formation process.

5.4 Cluster Formation Process

The cluster formation is the first execution step of the PHSA approach. It is composed of three phases: *the CH election, the CH announcement and the cluster join processes.*

5.4.1 Cluster Head Election

In a smart power distribution segment based CRSN, the CH election has to take into consideration:

- The available joint channels between the CHs and their associated CMs, i.e., the set of available channels shared between CHs and their members (to allow CHs to efficiently collect data during the intra-cluster communications).
- The heterogeneity of the NAN traffic (the CMs $n_i \in \mathcal{S}$ have to be fairly distributed between clusters according to their priorities α_i).

To this end, we introduce the CH cumulative spectrum rank parameter Υ_i related to a given node n_i ($i \in [1, N]$). Υ_i is introduced in (5.1):

$$\Upsilon_i = \frac{\sum_{n_j \in \mathcal{N}_m^i} \frac{\sum_{k=1}^{K} min(\omega_{ki}, \omega_{kj})}{\alpha_j}}{K \times \|\mathcal{N}_m^i\|} \tag{5.1}$$

Υ_i measures the capacity of the available spectrum resources shared between the prioritized SUs ($n_j \in \mathcal{N}_m^i$) and n_i to succeed the intra-cluster communications (if n_i is selected as a CH). Accordingly, sensors $n_i \in \mathcal{S}$, having the highest values of Υ_i are able to collect a higher amount of data from their neighbors $\mathcal{N}_m^i$.

If $n_i \in \mathcal{S}$ finds its Υ_i among the R highest CH cumulative spectrum rank values of its neighbors $\mathcal{N}_m^i$, then it elects itself as a temporary CH.

5.4.2 Cluster Head Announcement Process

Due to the heterogeneous neighboring nodes, for a given node $n_i \in \mathcal{S}$ elected as a temporary CH, we propose the following strategy to announce its election as temporary CH:
Let r_i be the rank of Υ_i among the R values of Υ_j where $n_j \in \mathcal{N}_m^i$.

- If $r_i = 1$, then n_i sequentially broadcasts a CH *announcement* message on each idle channel in the set $\mathcal{H}$ using the communication range R_m. n_i switches the sequence of channels $\mathcal{H}$ W rounds to be sure that all its neighbors are aware of its new CH status.
- If $r_i \geq 2$, then if n_i did not received a CH *announcement* message during the $r_i \times W$ previous rounds, it starts sending its own CH *announcement* message at the beginning of the $(r_i \times W + 1)^{th}$ round.

At the end of the CH *announcement* phase, the cluster join process begins.

5.4.3 Cluster Join Process

Every node $n_j \in S$, neither elected as a temporary CH nor having sent a CH *announcement* message, elects its corresponding CH as follows:

- If n_j has received a number of CH *announcement* messages (≥ 1), then it becomes the CM of the CH n_i having the smallest distance $d(n_i, n_j)$, i.e., the best received signal strength, to improve the intra-cluster data transmission.
- If no CH *announcement* message is received by n_j, then it elects itself as a CH.

Once sensors have determined their associated CHs, they execute the Algorithm 4 to send cluster *join* messages to their corresponding CHs, thus to become their effective members.

The cluster formation process is performed based on the information related to the neighboring nodes. Once clusters are formed, every CH n_i broadcasts through the transmission range R_h the list of its associated CMs ($\mathcal{C}_i$). Therefore, every CH n_i obtains the list of its neighboring CH $\mathcal{N}_h^i$ and the lists of their associated CMs $\mathcal{C}_j$ ($\forall n_j \in \mathcal{N}_h^i$). Then, every CH n_i broadcasts via R_h the list of its neighboring nodes $\mathcal{N}_h^i$. Thus, based on the list of these broadcast control messages, the channel assignment tasks are performed as will be detailed in the next section.

5.5 Predictive Hierarchical Spectrum Assignment for NANs

As we have previously introduced, CHs are responsible of the channel assignment in PHSA. Both CMs and CHs will be modeled as Partially Observable Markov chains. Then, based on these Markov models, every CH assigns channels for the intra-cluster and the inter-cluster communication to its own and to its neighboring clusters. However, due to the heterogeneous cluster neighborhoods, channel assignment decisions will be scheduled among CHs. Thus, in this section before introducing how channels will be assigned, we present in the following the technique we use to organize the channel decisions between CHs. Thereafter, we present in detail the intra and the inter-cluster channel assignment processes.

5.5.1 Channels' Decision Scheduling

To organize the decision making among CHs, we characterize every CH n_i by $\mathcal{E}_i$. $\mathcal{E}_i$ is the list of couples $(e, \|\mathcal{N}_h^e\|)$ where e is the index of the CH n_e ($n_e \in \mathcal{S}$) and $\|\mathcal{N}_h^e\|$ is the number of n_e's neighboring clusters. To define the list $\mathcal{E}_i$, we introduce the following relation $\gg$ to sort neighboring CHs according to their locations in the network.

Definition: Let n_i and n_j be two CHs where $n_i \in \mathcal{N}_h^j$, i.e. $n_j \in \mathcal{N}_h^i$, n_j is greater than n_i ($n_j \gg n_i$):

- if $\exists n_u \in \mathcal{N}_h^j$ where $\forall n_v \in \mathcal{N}_h^i$ $n_u \gg n_v$

- else if $\|\mathcal{N}_h^j\| > \|\mathcal{N}_h^i\|$,
- else if $\|\mathcal{N}_h^j\| = \|\mathcal{N}_h^i\|$ and $j > i$.

$\mathcal{E}_i$ is then composed of the couples $(e, \|\mathcal{N}_h^e\|)$ where $n_e \gg n_i$. A given CH n_i cannot start the channel assignment for the intra and the inter-cluster communication while it has not received its neighboring CH n_j's decisions where $n_j \gg n_i$, i.e., $(j, \|\mathcal{N}_h^j\|) \in \mathcal{E}_i$.

The organization of CHs according to the relation $\gg$ takes place after the cluster formation. In fact, CHs exchange control messages through the transmission range R_h to allow every CHs n_i to obtain the lists $\mathcal{E}_j$ that characterize neighboring CHs n_j ($\forall n_j \in \mathcal{N}_h^e$). Figure 5.4 presents an example of a network organized into 6 clusters.

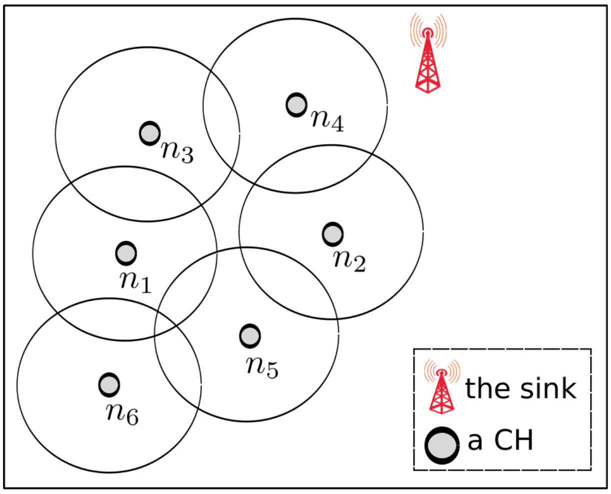

Figure 5.4: Example of hierarchical NAN.

The lists $\mathcal{E}_i$ associated to the different CHs n_i ($i \in [1, \ldots, 6]$) are the following:

- $\mathcal{E}_1 = \{(5,3); (3,2)\}$
- $\mathcal{E}_2 = \{(5,3)\}$
- $\mathcal{E}_3 = \{(4,2)\}$
- $\mathcal{E}_4 = \{(2,2)\}$
- $\mathcal{E}_5 = \emptyset$
- $\mathcal{E}_6 = \{(5,3); (1,3)\}$

As depicted in Figure 5.4, n_5 is the first CH that will start the channel assignment. Once n_2 receives the n_5's decisions, it starts taking its own decision concerning the channels to be used by its associated and neighbor cluster having as CH the node n_4. Thus, n_4 will wait the n_2's decisions since $n_2 \gg n_4$. Moreover, n_3 will start its channel assignment process once it receives the n_4's decisions. The n_1 decision making is conditioned on the n_5 and the n_3's channel allocations ($n_3 \gg n_1$ and $n_5 \gg n_1$). Finally, once n_6 receives the n_5 and the n_1's decisions, it starts its channel allocation process. n_5 and n_1 are bigger than n_6 since n_5 and n_1 have more neighbor clusters than n_6.

Given this background, we conclude that in every NAN, one CH n_i that is considered the greater among all its neighbor CHs will initiate the PHSA process, the channel assignment for M super-frames. Then, every time one CH n_j finishes its channel assignment, it proceeds to the channel hopping process and broadcasts on every visited idle frequency band an *allocation* message within the R_h range. The broadcast *allocation* message contains the channel assigned to n_j and to its neighboring nodes. When the CH n_v receives a broadcast *allocation* message, it updates its own and its neighboring clusters' states according to the content of the received messages. When n_v becomes able to start its channel assignment process, it proceeds to the intra and the inter channel assignment. Its decision includes its own and its neighboring clusters n_j where $n_v \gg n_j$.

PHSA aims to allow hierarchically deployed sensors to access to the available spectrum according to their priorities. Therefore, in the following, we introduce in detail the intra-cluster and the inter-cluster spectrum assignment approaches used by the CHs to achieve a fair distributed channel allocation.

5.5.2 Intra-cluster Channel Allocation

During the intra-cluster communication, every CH n_i allocates channels to its CMs and to the CMs of its neighboring clusters having n_j as CHs where $n_i \gg n_j$. Thus, we develop a POMDP modeling CM's states. Thereafter, based on this Markov chain, n_i allocates channels. In the following, we introduce the POMDP modeling a CM. Then, we present the intra-cluster channel allocation policy based on this POMDP modeling.

5.5.2.1 Cluster Member's State Model

For the CM $n_l \in \mathcal{C}_i$, i.e., $n_i \in \mathcal{S}$ is its associated CH, the POMDP is defined as follows:

- State: At the frame t, n_l's state ($s_l(t)$) is the approximation of the aggregate accumulative average data packets successfully transmitted by n_l during the frame t.
- Action: The action $a_l(t)$ is defined as the channel assigned to n_l to send data to its CH during the frame t if $a_l(t) \in \mathcal{H}$. Otherwise, if $a_l(t) = -1$ then no channel will be allocated to n_l to transmit data during t.
- Transition Probabilities: Being in the state $s_l(t-1)$, n_l's state can transit to the state $s^1_{l,k}(t)$ with the probability $P[s^1_l(t)/s_l(t-1), a_l(t)]$ if it successfully sends at least one

data packet through $a_l(t)$ where $a_l(t) = c_k$ and $c_k \in \mathcal{H}$. n_l's state can also transit to the state $s^2_{l,k}(t)$ with the probability $P[s^2_{l,k}(t)/s_l(t-1), a_l(t)]$ if no data packet is correctly sent through $a_l(t) \in \mathcal{H}$ where $s^2_{l,k}(t) = s_l(t-1)$, i.e., $a_l(t) = c_k$. If no channel is assigned to n_l, i.e., $a_l(t) = -1$, then n_l's state transits to the state $s^2_{l,-1}(t)$ with the probability $P[s^2_{l,-1}(t)/s_l(t-1), a_l(t) = -1]$ that is equal to 1. $P[s^1_{l,k}(t)/s_l(t-1), a_l(t)]$ and $P[s^2_{l,k}(t)/s_l(t-1), a_l(t)]$ are respectively introduced in Equations (5.2) and (5.3) where $\overline{Ploss_k} = 1 - Ploss_k$.

$$P[s^1_{l,k}(t)/s_l(t-1), a_l(t)] = \begin{cases} \omega^l_k Pna^l_k \overline{Ploss_k} & a_l(t) = c_k \quad (5.2a) \\ 0 & a_l(t) = -1 \quad (5.2b) \end{cases}$$

$$P[s^2_{l,k}(t)/s_l(t-1), a_l(t)] = \begin{cases} 1 - \omega^l_k Pna^l_k(1 - Ploss_k) & a_l(t) = c_k \quad (5.3a) \\ 1 & a_l(t) = -1 \quad (5.3b) \end{cases}$$

- Observation Probabilities: If n_l selects the channel c_k, i.e., $a_l(t) = c_k$, and its state transits to the state $s^1_{l,k}(t)$ then its observation probability, $O[s^1_{l,k}(t), a_l(t)]$, is defined as the probability that n_l senses c_k free of PUs during the frame t. Otherwise, the observation probability $O[s_{l,k}(t)^2, a_i(t)]$ is defined as the estimation of the probability that n_l senses c_k busy where $a_l(t) = c_k$ or that at least one PU arrives during the first micro-slot. If $a_l(t) \in \mathcal{H}$, i.e., $c_k = a_l(t)$, then $O[s_{l,k}(t)^1, a_i(t)]$ and $O[s_{l,k}(t)^2, a_l(t)]$ are obtained by the training of the two-state Markov chain modeling the occupancy of c_k by a PU. Otherwise, if $a_l(t) = -1$ then $O[s_{l,-1}(t)^1, a_l(t)]$ and $O[s_{l,-1}(t)^2, a_l(t)]$ are respectively equal to 1 and 0. $O[s_{l,k}(t)^1, a_l(t)]$ and $O[s_{l,k}(t)^2, a_l(t)]$ are introduced in Equations (5.4) and (5.5), respectively.

$$O[s^1_{l,k}(t), a_l(t)] = \begin{cases} \omega^l_k(t) & a_l(t) = c_k \quad (5.4a) \\ 0 & a_l(t) = -1, \quad (5.4b) \end{cases}$$

$$O[s_{l,k}(t)^2, a_l(t)] = \begin{cases} 1 - \omega^l_k(t) Pna^l_k & a_l(t) = c_k \quad (5.5a) \\ 1 & a_l(t) = -1 \quad (5.5b) \end{cases}$$

- Reward: As introduced in Equation (5.6), the reward $R^l_{intra}(t)$ measures the number of data packets successfully sent by n_l regarding its priority (α_l). It will be used as an indicator for the considered CM's priority to transmit data during the frame t.

$$R^l_{intra}(t) = \begin{cases} \dfrac{\alpha_l}{s^1_{l,k}(t)} & a_l(t) = c_k \quad (5.6a) \\ \dfrac{\alpha_l}{s^2_{l,-1}(t)} & a_l(t) = -1, \quad (5.6b) \end{cases}$$

$s^1_l(t)$ and $s^2_l(t)$ are introduced in Equations (5.7) and (5.8), respectively. $P_l(s^1_l(t))$ is the probability of being in the state $s^1_l(t)$. It is calculated by using the Baye's rule [102].

$$s^1_{l,k}(t) = s_l(t-1) + P_l(s^1_{l,k}(t))\omega^l_k[(D-1).((1-Ploss_k)Pna^l_k)^D + \sum_{d=1}^{D-2} d.((1-Ploss_k)Pna^i_k)^{d+1}(1-(1-Ploss_k)Pna^l_k))],\ k \in [1,K] \quad (5.7)$$

$$s^2_{l,k}(t) = s_l(t-1),\ k \in \{-1\} \cup \{1,K\} \quad (5.8)$$

5.5.2.2 Intra-Cluster Decision Policy

Based on the previously presented POMDP, we note that high $R^l_{intra}(t-1)$ values indicate that CMs $n_l \in \mathcal{C}_i$ did not gained enough access to the spectrum in the previous frames. Thus, the intra-cluster channel allocation will target the minimization of nodes n_l' rewards by decreasing the number of data packets successfully sent by these CMs during t.

Accordingly, at a frame t, the CHs $n_u \in \mathcal{N}^i_h$, $n_i \gg n_u$ are sorted by decreasing order of their $R^{u-\max}_{intra}(t-1)$, where $R^{u-\max}_{intra}(t-1) = \max\limits_{n_l \in \mathcal{C}_u} \left\{R^l_{intra}(t-1)\right\}$, is the maximum intra-cluster reward value among the CH n_u's members as given by the Equation (5.6). The node n_i, then, sequentially proceeds to the channel allocation, within each of its neighbors clusters, in a way to minimize the reward values in the cluster for the subsequent frames and to avoid interferences with the neighboring SUs.

As we have previously discussed, the CH n_i takes into consideration the decision of neighboring CHs broadcast on *allocation* messages within the R_h range. Algorithm 5 introduces how the CH n_i updates its CMs' states.

5.5.3 Inter-cluster Channel Allocation

Once the CHs collect the data sent by their associated CMs during the intra-cluster transmission, they start the transmission of their generated and collected data towards the sink through the neighboring CHs placed closer to the sink. Accordingly, we model every CH as a POMDP. Thereafter, based on this model, CHs assign channels.

Algorithm 5 Neighboring CMs' states update.

Input: *allocation* message sent by $n_q \in \mathcal{N}_h^i$

for $b = 1 \dots M$ **do**
  for $y = 1 \dots M_1$ **do**
    for $n_l \in \mathcal{C}_j$ **do**
      if $a_l(t) \in \mathcal{H}$ **then**
        $s_l(t) \leftarrow s^1_{l,k}(t)$ $\{n_j \in \mathcal{N}_h^i$ and $a_l(t) = c_k\}$
        Update($Q_j(t), R^l_{intra}(t)$) $\{n_j$ is the n_l's CH$\}$
      end if
    end for
  end for
end for

5.5.4 Cluster Head's State Model

The POMDP modeling a given CH n_i is defined as follows:

- State: At the frame t, n_i's state, $S_i(t)$ is defined by the couple $(s_i(t), Q_i(t))$. $s_i(t)$ is the approximation of the aggregate accumulative average data packets successfully transmitted. $Q_i(t)$ is the n_i's buffer occupancy by the end of the frame t.
- Action: The action $a_i(t)$ is defined as the channel allocated to n_i, $a_i(t)$, to transmit its data as well as the selected next-hop CH to which n_i's data will be forwarded.
- Transition Probabilities: If the selected channel is c_k, then n_i's state $S_i(t-1)$ can transit to the state $S_{i,k}(t)^1 = (s^1_{i,k}(t), Q^1_{i,k}(t))$ if at least one data packet is successfully transmitted. n_i's buffer occupancy update to $Q^1_{i,k}(t)$ is introduced in Equation (5.9) where $a_i(t) = c_k$. $s^1_{i,k}(t)$ is previously introduced in Equation (5.7). If no data packet is correctly sent through c_k or if no channel is assigned to n_i then $S_i(t-1)$ transits to $S_{i,k}(t)^2 = (s^2_{i,k}(t), Q^2_{i,k}(t))$, i.e., $s^2_{i,k}(t) = s_i(t-1)$. As shown in Equation (5.10), the buffer size $Q^2_{i,k}(t)$ is the n_i's generated data packets added to its buffer size during the frame $t-1$.

$$
\begin{aligned}
Q^1_{i,k}(t) = \mathrm{Max}(0\ ,\ & Q_i(t-1) + \alpha_i - P_i(s^1_{i,k}(t))\omega^i_k[(D-1)((1-Ploss_k)Pna^i_k)^D \\
&+ \sum_{d=1}^{D-2} d((1-Ploss_k)Pna^i_k)^{d+1}(1-(1-Ploss_k)Pna^i_k))]) \qquad (5.9)
\end{aligned}
$$

$$
Q^2_{i,k}(t) = Q_i(t-1) + \alpha_i, \text{ if } a_i(t) \in \mathcal{H} \cup \{-1\} \qquad (5.10)
$$

The transition probabilities from one state to another is mainly dependent on the selected channel $a_i(t) \in \{-1\} \cup \mathcal{H}$. Thus, the probabilities that n_i's state transits from $(s_i(t-1), Q_i(t-1))$ to $(s_{i,k}(t)^1, Q^1_{i,k}(t))$ and from $(s_i(t-1), Q_i(t-1))$ to $(s_{i,k}(t)^2, Q^2_{i,k}(t))$ are the same than those introduced in Equations (5.2) and (5.3).

- Observation Probabilities: The observation probabilities are defined as for the intra-cluster allocation, described in the previous section.
- Reward: As introduced in Equation (5.11), the reward measures the number of packets successfully transmitted on the selected channel regarding the node n_i's buffer occupancy.

$$R^i_{inter}(t) = \begin{cases} \dfrac{Q^1_{i,k}(t)}{s^1_{i,k}(t)} & a_l(t) = c_k \quad (5.11a) \\ \dfrac{Q^2_{i,-1}(t)}{s^2_{i,-1}(t)} & a_l(t) = -1, \quad (5.11b) \end{cases}$$

5.5.4.1 Inter-Cluster Decision Policy

Based on $R^i_{inter}(t-1)$ already obtained in the frame $t-1$, channels will be assigned during the frame t of the inter-cluster communication period. Thus, $\frac{Q_i(t-1)}{s_i(t-1)}$ represents an indicator to determine how n_i is prioritized to transmit data in the current frame t.

At a frame t, n_i sorts the CHs $n_u \in N^i_h$, where $n_i \gg n_u$, according to $R^u_{inter}(t-1)$'s values introduced in Equation (5.11). The CH n^*_u, having the highest inter-cluster reward $R^*_{inter}(t-1)$, among the other n_u's CH neighbors, is considered as the most prioritized CH to access to the spectrum. Thus, n_i allocates to n_u the channel minimizing its reward without causing interferences to the other CHs. Moreover, n_i also selects n^*_j, the node n_u's next-hop to the sink. Once a given CH is selected as a receiver during the frame t, then it cannot transmit its data at the same time. In fact, as all the nodes are equipped with a unique transceiver, they can only forward one another CH traffic in a given frame.

In Algorithm 6, we introduce how a CH n_i updates the states of neighboring CHs.

Algorithm 6 Neighboring CHs' states update.

Input: *allocation* message sent by $n_q \in \mathcal{N}^i_h$

for $b = 1 \ldots M$ **do**
  for $z = 1 \ldots M_2$ **do**
    for $n_j \in \mathcal{N}^i_h$ **do**
      if $a_j(t) \in \mathcal{H}$ **then**
        $s_j(t) \leftarrow s^1_j(t)$
        Update($Q_j(t), Q_p(t), R^j_{inter}(t)$) {$n_p$ is n_j's receiver}
      end if
    end for
  end for
end for

In PHSA, every CH assigns channels for intra and for inter-data transmission to its own and to its neighboring clusters. The channel allocation task takes place according to an order, i.e., $\gg$, that basically considers the number of neighboring clusters associated to every CH. Furthermore, the inter-cluster channel assignment is based on the approximation of the aggregate accumulative average data packets successfully transmitted by a given CH compared to the number of stored data packets waiting to be transmitted. During the PHSA inter-cluster channel assignment, if a CH is placed more than one-hop away from the sink then its next-hop will be selected randomly. Accordingly, the next-hop selection in PHSA does not consider the need of a selected CH as a receiver to transmit data, i.e., to be an emitter. Thence, we introduce in the following the Routing-based PHSA scheme (R-PHSA) that investigates this latter part. As an extension of PHSA, R-PHSA provides a distributed data routing adapted to hierarchical smart grid network topology.

5.6 Routing-based Predictive Hierarchical Spectrum Assignment for NANs

Here, we propose to integrate the need of every CH to forward its stored data to the sink, i.e., to be considered as an emitter and not a receiver. In PHSA, we introduced the relation bigger, i.e., $\gg$. $\gg$ orders of the channel assignment decisions for the intra and the inter-cluster communication among the CHs based on the number of their neighboring clusters. However, this scheduling results in a long channel assignment process. Accordingly, every CH n_i has to wait the reception of *allocation* messages sent by neighboring CHs n_j where $n_j \gg n_i$. As a result, to alleviate the PHSA's channel assignment process while considering every CHs' need to transmit its data to the sink, the hierarchical multi-hop model introduced in Section 5.3 will be subject to some additional hypotheses:

- The monitored network is virtually divided into Y consecutive rows. The height of every row is equal to $2 \times R_h$. Figure 5.5 illustrates an example of such a network where Y equals 3.
- Every row is characterized by its index $y \in [1, Y]$. The sink is placed at row 1. As the row is far away from the sink as its index increments.
- A local central unit (CU), i.e., a full functional node, is deployed in every range. We denote by f_y the CU that is deployed in the row y, i.e., the row whose index is y.
- Every CU is equipped with K radio interfaces.
- The CU f_y is aware of the list of CHs placed in its row y that we denote by ζ_y, their associated CMs $\mathcal{C}_i$ where the CH $n_i \in \zeta_y$ and their next-hops.
- Every CU f_y assigns channels to the list of CMs $\mathcal{C}_i$ where the CH $n_i \in \zeta_y$ during the intra-cluster communication and to the list of CH ζ_y during their inter-cluster communications.

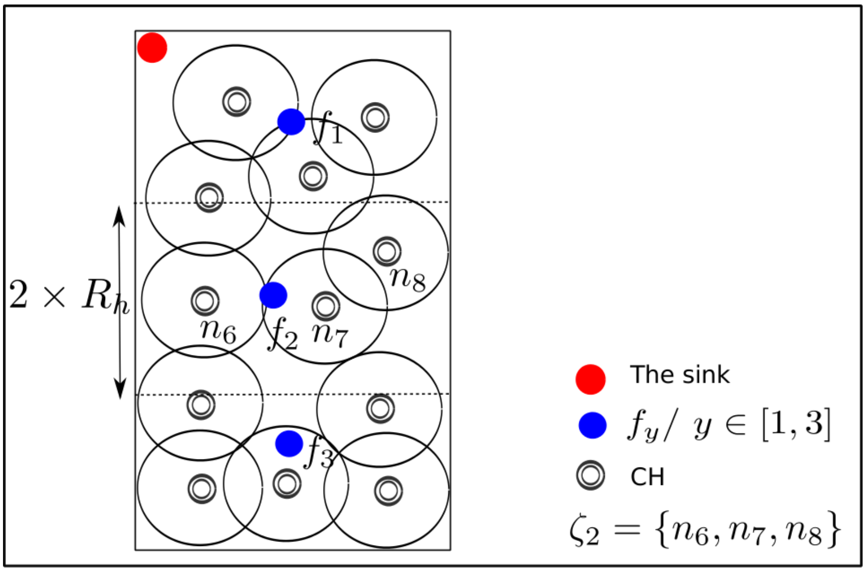

Figure 5.5: Hierarchical NAN for R-PHSA.

In R-PHSA, the channel assignment processes will be centralized in f_y ($y \in [1, Y]$). The CU f_Y, placed the farthest away from the sink, represents the first CU to start the channel assignment. Then, once a CU f_y receives an allocation message from f_{y+1}, then it becomes able to start its channel allocation. During the intra-cluster channel assignment, f_y uses the same Partially Observable Markov chain introduced in Section 5.5.2 to obtain the CMs' states. However, to model a given CH n_i's states ($n_i \in \zeta_y$), we introduce the following POMDP.

5.6.1 Cluster Head's State Model in R-PHSA

As an extension of PHSA, R-PHSA considers the need of a CH to be an emitter and not a receiver to accelerate the transmission of its stored data. Accordingly, we introduce in the following a Partially Observable Markov chain that models CH's states. This Partially Observable Markov chain is based on the previously introduced PHSA chain, in Section 5.5.3.

- State: At the frame t, n_i's state $S_i^*(t)$, is a three dimensional state $(s_i(t), Q_i(t), \eta_i(t))$. $s_i(t)$ and $Q_i(t)$ are the same than those introduced in Section 5.5.3, i.e. the approximation of the aggregate accumulative average data packets that have been successfully transmitted and the n_i's buffer occupancy by the end of the frame t. The third dimension $\eta_i(t) \in \{-1, 0, 1\}$ represents the role affected to n_i during the frame t. If $\eta_i(t)$ equals 1 then n_i will transmit data on the channel $a_i(t) \in \mathcal{H}$ in the sink direction. Otherwise, if $\eta_i(t)$ equals -1, then n_i will be a receiver. It will receive data from another CH in order to forward it to the sink in the coming frames. Finally, if $\eta_i(t)$ equals 0 then no channel is affected to n_j, neither to transmit nor to receive the data, i.e., $a_i(t) = -1$.

- Action: The action affected to a CH n_i ($A_i(t)$) is defined by the three dimension $(\eta_i(t), a_i(t), n_l(t))$. $\eta_i(t) \in \{-1, 0, 1\}$ represents the n_i's role. If $\eta_i(t)$ equals -1 than n_i will be a receiver during t. If $\eta_i(t)$ equals 1 then it will be an emitter. Otherwise, if $\eta_i(t)$ is equal to 0, then n_i will be neither a receiver nor an emitter. The second dimension $a_i(t)$ represents the channel assigned to n_i to receive data, i.e., if $\eta_i(t) = -1$, or to transmit data, i.e., if $\eta_i(t) = 1$. Moreover, based on the value of $\eta_i(t)$, the third dimension n_l models the n_i's next-hop (if $\eta_i(t) = 1$) or the emitter that will send data to n_i (if $\eta_i(t) = -1$). If $\eta_i(t)$ equals 0 then $a_i(t) = -1$ and $n_l(t) = -1$.

- Transition Probabilities: Let $A_i(t) = (\eta_i(t), a_i(i), n_l)$ be the action affected to n_i. If $a_i(t) \in \mathcal{H}$, i.e., $a_i(t) = c_k$, then n_i's state $S_i^*(t-1)$ can transit to the state $S_{i,k}(t)^{+1*} = (s_{i,k}^1(t), Q_{i,k}^1(t), 1)$ or to the state $S_{i,k}(t)^{-1*} = (s_{i,k}^{-1}(t), Q_{i,k}^{-1}(t), -1)$ if at least one data packet is successfully transmitted or received, respectively, on c_k. If no data packet is correctly sent or received through c_k, then $S_i^*(t-1)$ transits to $S_{i,k}(t)^{2*} = (s_{i,k}^2(t), Q_{i,k}^2(t), \eta_i(t))$ where $\eta_i(t) \in \{-1, 1\}$. The transition to $S_{i,k}(t)^{2*}$ can also take place if no channel is allocated to n_i to transmit or to receive, i.e., $a_i(t) = -1$. The aggregate accumulative average data packets $s_{i,k}^1(t)$ and $s_{i,k}^2(t)$ have been previously introduced in Equations (5.7) and (5.8), respectively. Moreover, $Q_{i,k}^1(t)$ and $Q_{i,k}^2(t)$ have been introduced in Equations (5.9) and (5.10), respectively. Now, $Q_{i,k}^{-1*}(t)$ is introduced in Equation (5.12). $P_i(S_{i,k}(t)^{-1*})$ is the probability of being in the state $s_l^1(t)$. It is calculated by using the Baye's rule [102].

$$Q_{j,k}^{-1*}(t) = Q_j(t-1) + \alpha_j + P_j(S_{i,k}(t)^{-1*})\omega_k^j[(D-1)((1-Ploss_k)Pna_k^j)^D + \sum_{d=1}^{D-2} d((1-Ploss_k)Pna_k^j)^{d+1}(1-(1-Ploss_k)Pna_k^j))] \tag{5.12}$$

The transition probabilities between the different states are introduced in Equations (5.13) and (5.14) where $\overline{Ploss_k} = 1 - Ploss_k$.

$$P[S_{i,k}(t)^{\pm 1*}/S_i^*(t-1), a_i(t)] = \begin{cases} \omega_k^i Pna_k^i \overline{Ploss_k} & a_i(t) = c_k \quad (5.13a) \\ 0 & a_i(t) = -1 \quad (5.13b) \end{cases}$$

$$P[S_{i,k}(t)^{\pm 2*}/S_i^*(t-1), a_i(t)] = \begin{cases} 1 - \omega_k^i Pna_k^i \overline{Ploss_k} & a_i(t) = c_k \quad (5.14a) \\ 1 & a_i(t) = -1 \quad (5.14b) \end{cases}$$

- Observation Probabilities: They are defined as for the intra-cluster allocation, described in Section 5.5.2.

- Reward: If n_i is an emitter, i.e., $\eta_i(t) = 1$, then as introduced in Equation (5.11), the reward measures the number of packets successfully transmitted on the selected channel regarding the node n_i's buffer queue size. If n_i is a receiver, i.e., $\eta_i(t) = -1$, then its reward is equal to 0, i.e., $R^i_{inter}(t) = 0$.

5.6.2 Channel Allocation Policy

The R-PHSA channel assignment is executed by the Y deployed CUs in a sequential manner. A CU f_y cannot start its channel allocation for the CHs ζ_y and their associated CMs until it receives the CU f_{y+1}'s decisions. In fact, the f_y's decisions are based on the decisions of f_{y+1}. For example, if a CH n_j is placed at row $y+1$ where the CU f_{y+1} is deployed, i.e., $n_j \in \zeta_{y+1}$, then its next-hop n_i may be placed at row y closer to the sink, i.e., $n_i \in \zeta_y$. In this case, the n_i's role would be decided by f_{y+1} if it is selected as the n_j's next-hop during a given frame t. Thus, f_y should wait for an *allocation* message sent by f_{y+1} to take into consideration the n_i's role during its channel assignment. Given this background, f_Y represents the first CU to start the channel assignment process.

5.6.2.1 Intra-Cluster Channel Allocation

The R-PHSA intra-cluster channel allocation policy is almost the same then the strategy presented in Section 5.5.2.2. However, here it is the CU f_y placed in the virtual row number y that allocates channels to the CMs associated to the CH n_i where $n_i \in \zeta_y$.

5.6.2.2 Inter-Cluster Channel Allocation

At a frame t, f_u sorts the CHs $n_u \in \zeta_y$ that have been receivers during the frame $t-1$, i.e., $\eta_u(t-1) = -1$, according to their reward $R^u_{inter}(t-1)$ introduced in Equation (5.11). The CH n^*_u having the highest inter-cluster reward $R^*_{inter}(t-1)$, among the other n_u's CH neighbors, is considered as the most prioritized CH to access to the spectrum. Once the CH having played the role of receivers during $t-1$ get their assigned channels, f_y considers in a next step the CHs n_u that have not gained access to the spectrum during the frame $t-1$, i.e., $\eta_u(t-1) = 0$. Finally, f_y focus on the CHs n_u that have accessed to the spectrum during $t-1$, i.e., $\eta_u = 1$. Now, if a CH n_u is placed more than one-hop away from the sink, then it next-hop n_l should not be a receiver during the frame $t-1$, i.e., $\eta_l(t-1) \neq -1$.

So, R-PHSA prioritizes the receivers CHs during the frame $t-1$ to be emitters during the frame t. The goal of this prioritization is to quickly forward the received and generated data to sink.

5.7 Performance Evaluation

In this section, we evaluate the performance of both PHSA and R-PHSA. We proceed using simulations under the OMNeT++ network simulator and through the MiXiM framework. First, the simulation aims to evaluate how the different PHSA parameters impact its behavior in terms of:

- Number of formed clusters ($\mathcal{F}$).
- Number of successfully transmitted data packets (Θ).

Then, it illustrates the PHSA and the R-PHSA's capabilities to:

- Allocate channels according to the SUs' priorities.
- Allow the SUs to get benefit from the available channels despite the probabilistic channel assignment.

In the same context, it aims to demonstrate the R-PHSA abilities to achieve a better data routing compared to PHSA.

Thus, SUs are uniformly deployed in the simulation field. The sink is installed in one of its corners. As illustrated in Table 5.1, different SUs' priorities are considered in the network. Each node's packet arrival rate represents its weight to transmit its data. Table 5.1 lists the basic parameters used in our simulations.

Table 5.1: Simulation Parameters.

Parameter	Value
Number of nodes	115
Channels' occupancy	0.35/ 0.45/ 0.5/ 0.83
R_m/R_h	30/60 m
$M_1/M_2/D$	3/3/5
PU transmission range	30 m
Area range	300×100 m^2
Data packet size	166 bytes
L	10 super-frames
α_i	$\{2.5, 5, 7.5, 10\}$
Number of PUs	2
Number of CUs	3

5.7.1 Evaluation of PHSA parameters

We first evaluate the impact of PHSA parameters on the cluster formation process (Section 5.4). Figure 5.6 depicts the variations of $\mathcal{F}$, the number of clusters, with R, the number of sensors with the highest cumulative spectrum rank values in a CH's neighborhood. As shown in Figure 5.6, $\mathcal{F}$ increases with R. Indeed, as R increases as the number of elected CHs increases too and henceforth $\mathcal{F}$ does. Moreover, Figure 5.6 shows that $\mathcal{F}$ reversely decreases with W, the number of times that an elected CH switches the list of channels to broadcast its *announcement* message. In fact, as W increases, an elected CH will get more opportunities to send its *announcement* message on idle channels. Accordingly, SUs non elected as CHs will correctly receive this message. This aspect is further illustrated in Figure 5.7 where we show that $\mathcal{F}$ decreases with W. It also shows that when W reaches a given value ($W \geq 14$ when $N = 210$ and $W \geq 9$ when $N = 115$) the value of $\mathcal{F}$ becomes constant for the different numbers of channels, i.e., $K = 3$ and $K = 4$.

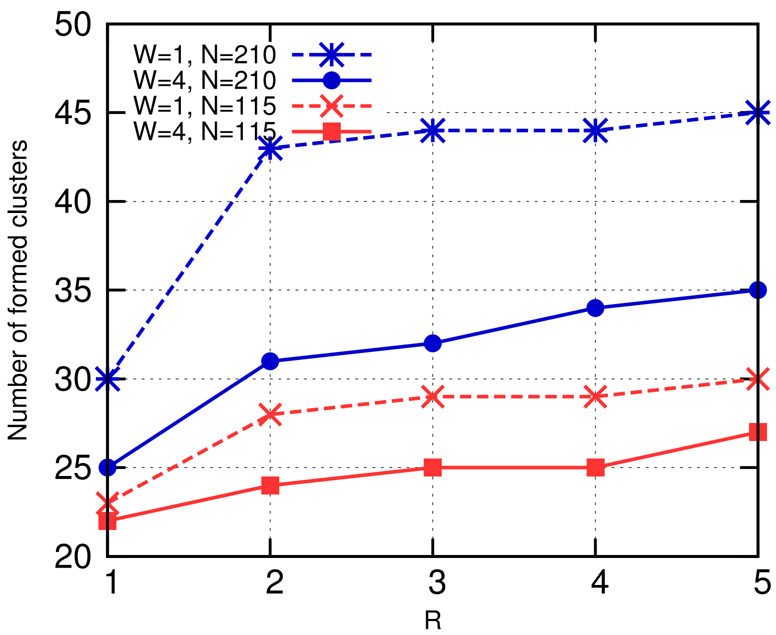

Figure 5.6: Number of formed clusters vs R.

Now, we evaluate the different parameters that impact the super-frame duration. In Figure 5.8, we evaluate the number of data packets successfully received by the sink (Θ) according to the frame size (D), i.e., the number of micro-slots composing the data transmission period of a frame T. Figure 5.8 shows that Θ reaches a maximum value at $D = 11$ for both values of N ($N = 115$ and $N = 210$). Thus, when $D > 11$, the frame becomes more sensitive to PUs' arrivals, i.e., high probability of a PU's appearance.

Finally, Figure 5.9 depicts the variation of Θ for different M_1 and M_2 values. It shows that the increase of M_1 negatively impacts Θ and that the increase of M_2 positively impacts Θ. In fact, when M_1 increases, CHs will get a short duration to send data during the inter-cluster communications compared to the time used for the intra-cluster communications.

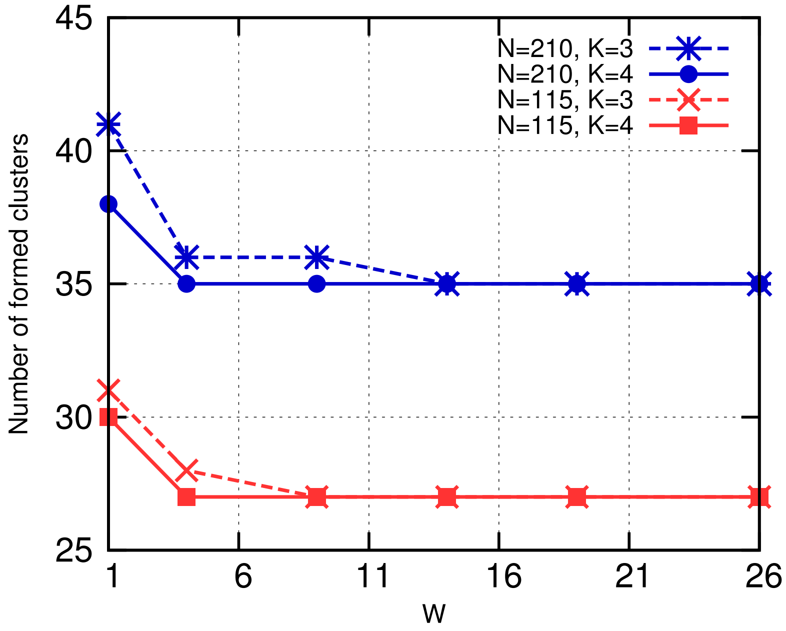

Figure 5.7: Number of formed clusters vs W.

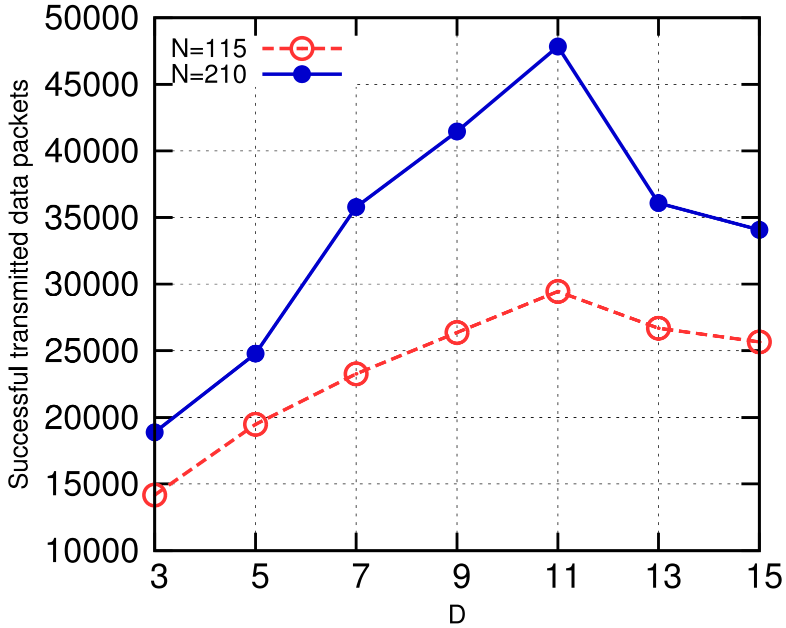

Figure 5.8: Successful transmitted data vs number of micro-slots D.

5.7.2 Fairness of PHSA and R-PHSA

Both PHSA and R-PHSA schemes are proposed to achieve transmissions to the sink per nodes' priorities. Figure 5.10 depicts the number of data successfully transmitted to the sink per node's priorities. It shows that for both PHSA and R-PHSA schemes the quantity of data successfully transmitted to the sink increases per nodes' priorities. Furthermore, R-PHSA achieves a better spectrum utilization per node's priority compared to PHSA.

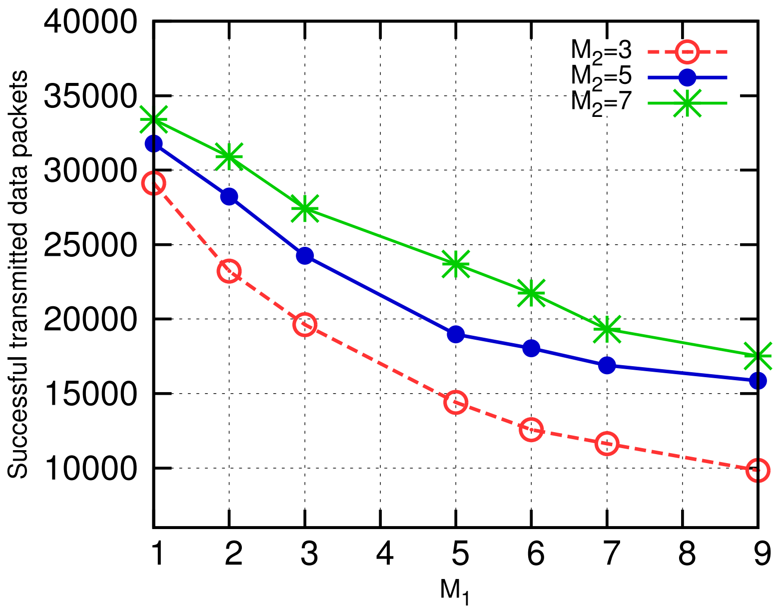

Figure 5.9: Quantity of packets successfully received by the sink vs M_1.

For instance, in R-PHSA, channels for intra-cluster communications are allocated by CUs placed in the different rows. Thus, the inter-cluster channel allocation achieved with R-PHSA is more pertinent than PHSA since every CU is completely aware of the spectrum needs of its clusters (the CHs and the CMs placed in its row).

Figure 5.11 evaluates the delay (packet waiting time + transmission time) per node's priority for PHSA and R-PHSA. It indicates that for both schemes, PHSA and R-PHSA, sensors with the highest priorities ($\lambda = 10$) experience short delays (respectively 9.3s and 7.6s when $K = 3$ and respectively 4.6s and 3.9s when $K = 4$). The increase in the SU's priority involves the decrease in its delay. Sensors non prioritized to transmit data have a long delay due to the control messages exchanged every L super-frames (messages containing the predicted channels). This can be authorized since a delayed transmission of these non-prioritized sensors' data will have less negative impact on the SG compared to delaying more prioritized sensors' data. This behavior clearly illustrates how PHSA and R-PHSA achieve service differentiation between SUs in SG NANs based on their priorities (traffic arrival rates). From another side, Figure 5.11 shows that, compared to PHSA, R-PHSA achieves a better delay per node's priority. For instance, R-PHSA prioritizes during the frame t CHs that have received data during $t-1$, thus decreasing the transmission delay compared to PHSA.

Finally, since in both PHSA and R-PHSA, the CHs forward the data to the sink in a multi-hop manner, we evaluate the data routing performances of PHSA and R-PHSA during the inter-clusters data transmission. In Figure 5.12, we compare the two proposed schemes to the well known spectrum-aware cluster-based routing for CRSNs (SCR) [117] framework for different numbers of SUs. The results clearly show that PHSA and R-PHSA outperform

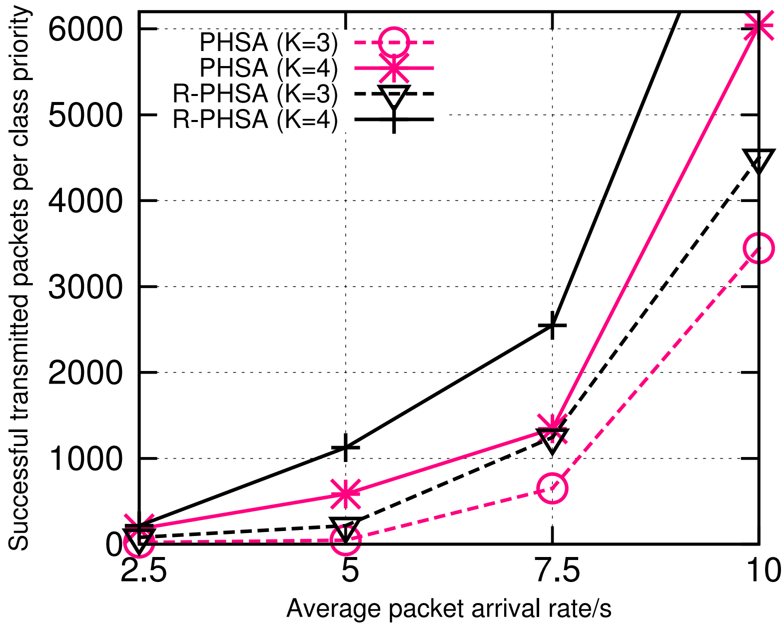

Figure 5.10: Transmitted data per node's priority.

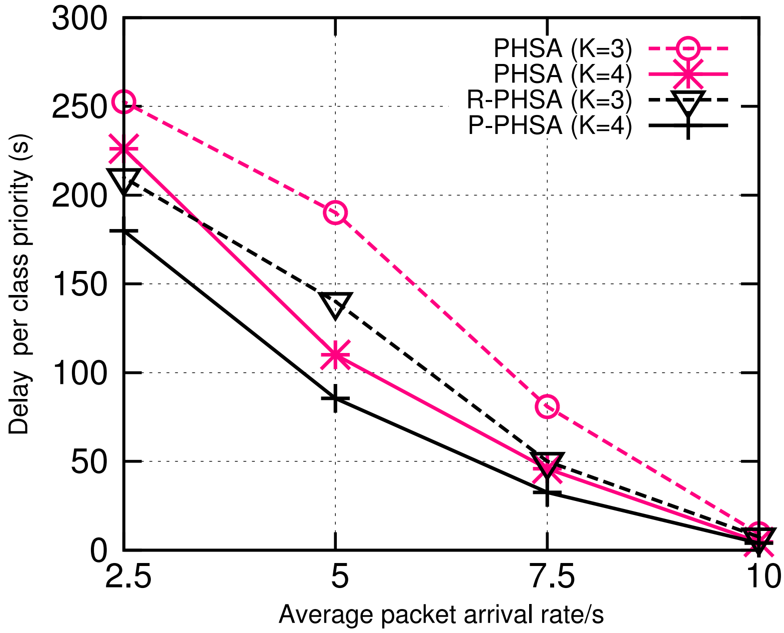

Figure 5.11: Delay per node's priority.

SCR since this latter scheme completely relays on the CCC availability, i.e., if the CCC is sensed occupied by licensed users than the SUs postpone their data transmissions even if different other channels are sensed in the idle state. Moreover, SCR assumes the existence of a negligible number of active nodes, i.e. sensors that can generate data. However, PHSA and R-PHSA takes into consideration the large number of active sensors (sensors with data to transmit). Additionally, Figure 5.12 shows that R-PHSA outperforms PHSA for the different numbers of deployed sensors (N). In fact, the use of different CUs in R-PHSA to allocate the channels for the intra and the inter-cluster communications allows a global transmission scheduling which henceforth improves the network spectrum utilization.

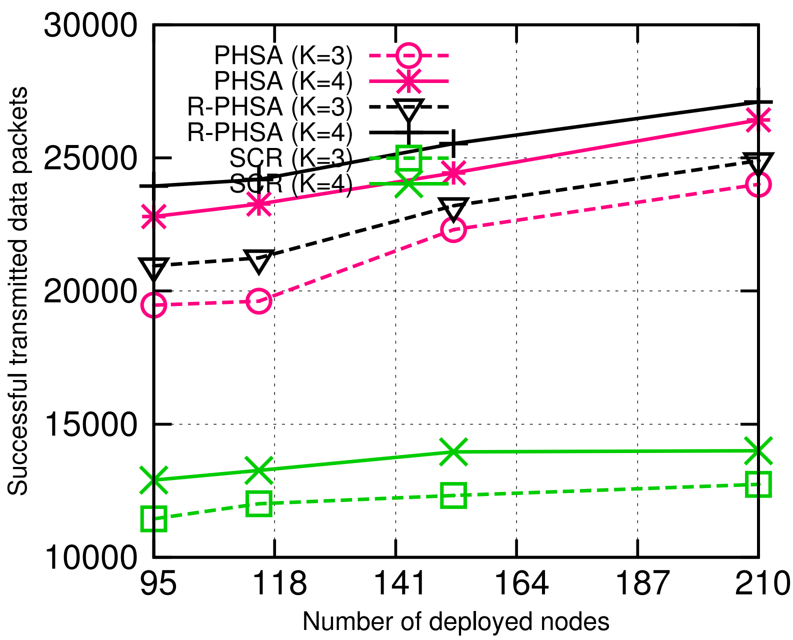

Figure 5.12: Quantity of packets successfully received by the sink vs N.

5.8 Discussion

In the previous section, dedicated to the performance evaluation of both PHSA and R-PHSA, we evaluated the impact of the different parameters that we have considered in both, PHSA and R-PHSA schemes as a first step. Simulation results showed that these parameters largely impact the number of formed clusters. Then, as a second step, we focus our efforts on the evaluation of PHSA and R-PHSA capabilities to achieve an efficient and fair spectrum sharing. Accordingly, simulation results showed that:

- Both PHSA and R-PHSA outperform the SCR scheme in term of total spectrum utilization. Thus, our two proposed schemes succeed to get benefits from the available frequency bands distributively.
- Our solutions achieve a spectrum sharing that fits NAN's prioritized traffic. In fact, when using PHSA or R-PHSA, the packet delay reversely increases with nodes' priorities. In the opposite, spectrum utilization increases with nodes' priorities. We can conclude that the predictive models that we developed can be considered as good estimates of nodes' priorities that properly capture SUs' needs to transmit their data.
- R-PHSA outperforms PHSA in terms of spectrum utilization and data packet delays. Moreover, simulation results illustrate R-PHSA efficiency in routing data to the sink.

In fact, in addition to the prioritization of the frame $t-1$'s non-emitters CH during the upcoming frame t, the use of CUs for the channel allocation process allowed a better consideration of SUs' needs to transmit their prioritized data.

5.9 Conclusion

In this chapter, we concentrated our efforts on multi-hop data transmission in smart grid NANs. We opted for a hierarchical CRSN communication network to ensure the SG monitoring. In fact, hierarchical topology allows a better network organization and adds robustness against topological changes or faults in a smart grid environment. Accordingly, to organize the network into clusters, we proposed a CCC-free clustering algorithm that considers heterogeneous NAN traffic. Then, we developed a novel distributed predictive hierarchical spectrum assignment scheme (PHSA) for multi-hop CRSNs deployed in smart grid NANs. PHSA presents a channel assignment strategy that does not use a CCC before every data transmission. With PHSA, channels are assigned by CHs based on the estimation of their neighboring nodes' priorities and their associated available channels. Intra-cluster and inter-cluster channel allocations are achieved by CHs in a distributed manner through Partially Observable Markov Decision Processes (POMDPs). Thereafter, based on PHSA, we proposed the Routing-based PHSA (R-PHSA). Compared to PHSA, R-PHSA takes into consideration the routing aspects during the inter-cluster channel assignment. In R-PHSA, we divided the NAN area into virtual rows. In every row, one central unit (CU) is deployed to allocate the channels for all clusters belonging to its row. R-PHSA is also based on POMDPs. During the inter-cluster channel assignment, at a frame t, a CH prioritizes previous frames' non emitter CHs to properly transmit their stored data to the sink, i.e., NAN-G.

Simulation results illustrated the adaptability of both PHSA and R-PHSA regarding the traffic priority variation in the NAN. In fact, the quantity of data packets successfully received by the sink and the data packet delay depend on the sensors' priorities. Moreover, simulation illustrates that PHSA and R-PHSA outperform existing clustering approaches in terms of the amount of successfully received data by the sink since our predictive schemes do not rely on a CCC. Finally, simulation revealed that R-PHSA outperforms PHSA since R-PHSA accounts for the routing aspect during the inter-cluster channel allocation.

In this chapter, as well a in the two previous chapters, data is periodically transmitted to the sink. In SGs, a second kind of data may exist. It is the event-based traffic. This later type of traffic is generated once an abnormal event occurs in the monitored field. To avoid the CCC limitations, the next chapter will be dedicated to the channel allocation for event-based traffic transmission in SGs.

Chapter 6

Distributed Channel Allocation for Event-driven Smart Grid Traffic

Contents

In the previous chapters, we mainly focused on prioritized smart grid traffic where smart grid sensors periodically obtain information of monitored electrical applications. Thus, we concentrated our effort on achieving fair channel assignments in CRSNs for periodically controlled smart grid applications. However, the smart grid communication traffic in wireless access network can be periodic and can also be event-driven. An event driven traffic is generated once an abnormal event takes place. One of the most critical systems where randomly traffic is frequently generated are the distribution substations. They have to be in a continuous control to be aware of unpredictable events that may damage the systems. Thus, in this chapter, we propose to fully get benefits from the cognitive radio sensor network (CRSN) technology to control electrical distribution substations and more precisely coping with the event-driven traffic they generate. More precisely, we use CRSNs for early-warning from unexpected events in electrical substations. We focus on allowing deployed cognitive sensors to efficiently aggregate and report data in substations upon unexpected events' detection. Our approach, called Distributed Event-driven data Aggregation and constrained multipath Reporting (DEAR), also completely emancipate from the common control channel (CCC) limitations. DEAR assigns channels distributively based on the graph coloring paradigm.

The remainder of this chapter is organized as follows. First, in Section 6.1, we discuss the motivations behind the DEAR scheme. In Section 6.2, we present the major related work. The substation network model is described in Section 6.3. In Section 6.4, we introduce the channel allocation during the data aggregation phase. Section 6.5 presents the DEAR data reporting strategy. Performance evaluation results are introduced in Section 6.6. Finally, conclusion is given in Section 6.7.

6.1 Context and Motivations

In smart grids, substations are fundamental systems [61]. They can operate at different parts of the smart grid (transmission or distribution) to transform voltage and to ensure safe and reliable delivery of power. But as depicted in Figure 6.1, a particular attention should be paid to the distribution substations due to their proximity to the consumers' homes. For instance, unpredictable failures within such systems will directly impact the power supply at the consumers. Thus, an efficient monitoring within these substations is required to prevent/recover from such events in a timely manner.

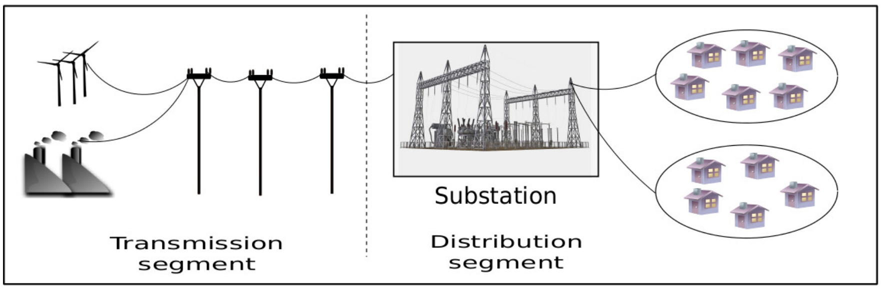

Figure 6.1: Distribution substation position in a smart grid.

Nowadays, WSNs have become mature enough to be one of the candidate technologies for undesirable event early warning systems [126]. They are privileged for events' detection and supervision in the monitored systems due to the ability of the sensor devices to collect data from numerous phenomena (temperature, fire, pressure, humidity, etc.) [127]. However, to deal with the ISM frequency band crowdedness in smart grid distribution area, the dynamic spectrum access (DSA) technology has emerged as an intelligent solution for randomly occurred events' detection and then for event-driven traffic transmission [128,129]

Thus, we focus in this chapter on the early events' detection in substations using CRSNs in suburban environments. The early events' detection in substations consists in detecting unexpected events (such as fire, equipment malfunctioning or single phase current grounded by hurricane) and reporting them to a central node (sink) through multi-hop communications. This task should be done before the usual event's detection time.

The cognitive network, in charge of the substation monitoring, consists of a number of sensors scattered in the substation yard to instantly detect impromptu/abnormal events. Once the measured values are collected, the sensors generally proceed to data aggregation to avoid erroneous and redundant data transmissions and to produce consistent mean values that will be reported to the sink [127]. The sensor nodes, known as secondary users (SUs), will then proceed to an opportunistic access to the licensed bands to forward (report) the collected data to the sink via multi-hop transmissions.

Different nodes may be involved in the data aggregation and reporting phases. Here again, the CRSN's channel assignment process for these tasks is achieved through one common control channel (CCC) to prevent interferences between SUs. However, as states earlier, using a channel allocation approach based on a CCC is not a safe solution given the CCC's inconveniences.

To avoid the CCC limitations, we introduce in this chapter a new channel allocation scheme for CRSNs, called Distributed Event-driven data Aggregation and constrained multipath Reporting (DEAR), to monitor distribution substations in suburban areas. To perform an efficient data processing, DEAR uses clustering during the data aggregation phase. Hence, the measured values sensed and detected by sensors belonging to the same cluster are aggregated by their cluster head. Then, DEAR performs the data reporting through a constrained multi-hop "Beam" routing. In both phases, the channel allocation is achieved based on the graph coloring paradigm.

6.2 Related Work

Several approaches in the literature proposed to use WSNs for the substations' monitoring in smart grids [34, 61, 130]. Most of these approaches exploit common wireless technologies such as Wifi or Zigbee for sensor nodes' communications. Thank to the abundance of spectrum resources in the under-utilized licensed bands, some recent works suggested the cognitive radio technology as a good alternative for the data exchange between the sensors in WSNs to monitor electrical systems' entities [2, 98]. Such systems' surveillance is even more efficient when cluster-based solutions are adopted in CRSNs [127]. Indeed, among the set of advantages it offers, the clustering increases the network robustness against topological changes, preforms an efficient data transmission by removing redundant information between the collected values, restores lost data by exploiting the samples' correlation.

Regarding the path construction in a multi-hop data transmission, [117] proposes a cluster-based spectrum aware routing protocol (SCR). During the path formation process, the number of nodes involved in the data transmission to the sink is minimized to reduce the energy consumption in the network. Path establishment and channel allocation processes are essentially based on the continuous CCC availability. In [131], a cluster based QoS routing adapted to the multimedia traffic is proposed. Authors take into consideration a multi-channel data transmission in WSNs, but did not consider the channel occupancy by primary signals. In [118], a routing framework for multimedia traffic in a cluster-based CRSN has been also proposed. Works in [117], [131] and [118] all rely on CCC for channels' allocation.

On the other side, as far as event-driven solutions are concerned, few works [132] [128] [133] focused on data transmissions triggered by random events in CRSNs. The primary focus of these works is the reactive cluster formation following events' detection. In [128], the event-driven spectrum-aware clustering (ESAC) aims to minimize the number of nodes participating in clusters' formation between the sink and the event locations. Moreover, [133] aims to construct clusters in a reactive way upon an event detection to minimize the energy consumption.

To transmit data to the sink, these works use existing protocols such as SCR [117]. Accordingly, data is aggregated by the cluster heads then forwarded to the sink node. The channel assignment for data aggregation and forwarding always rely on CCC and is achieved in a way to minimize energy consumption.

In the present chapter, our purpose is to provide a reliable data transmission for event-driven CRSNs to monitor distribution substations in smart grids. Hence, we propose a novel distributed channel allocation scheme, DEAR, that completely avoids the use of a CCC.

6.3 Substation Network Model

The distributed channel allocation using the DEAR approach is expected to be executed in two steps: a data aggregation phase aiming to collect data upon an event detection within the substation and a reporting phase aiming to report (forward) the aggregated data via multi-hop transmissions to the sink.

First, we consider that the substation area is geographically divided into G clusters called virtual grids [127] (c.f. Figure 6.2) where a set $\mathcal{S} = \{n_1, \ldots, n_N\}$ of cognitive wireless sensors are scattered.

We denote by (x_i, y_i) the coordinates of a given node n_i and $(0, 0)$ are the sink coordinates. We denote by $\mathcal{G}_y$ the list of sensors placed inside the virtual grid y ($y \in [1, G]$). In each virtual grid $y \in [1, G]$, a unique sensor node $n_i \in \mathcal{G}_y$ is responsible of the data aggregation. This node is called the reporting node r_y.

Thus, once a node $n_i \in \mathcal{G}_y$ detects an unexpected event, it sends its measured values to its associated reporting node r_y. r_y aggregates the received data and produces a local report that is sent via multi-hop communications to the sink using the available licensed channels. Let $\mathcal{H} = \{c_1, \ldots, c_K\}$ be the list of the licensed frequency bands used to transmit

Table 6.1: Symbols and Notations.

Notation	Explanation
$\mathcal{S}$	The list of monitoring sensors
n_i	The sensor number i ($i \in [1, N]$)
(x_i, y_i)	The coordinates of n_i
$\mathcal{G}_y$	The list of sensors placed inside the virtual grid y
r_y	The reporting node placed inside the virtual grid y
$\mathcal{H}$	The list of licensed channels
c_k	The licensed channel number k ($k \in [1, K]$)
$Ploss_k$	Packet loss probability in c_k
R_{tr}	sensors' transmission range
R_{int}	Sensors' interfernce range
R_{ss}	Sensors' sensing range
$\overline{\omega_k^i}$	The steady-state probability of the channel c_k Busy state
ω_k^i	The steady-state probability of the channel c_k Idle state
$d(n_i, n_j)$	The Euclidean distance between n_i and n_j
T_{ss}	The spectrum sensing sub-period
T_{tr}	The data transmission sub-period
$F(t)$	The frame stating at time instant t
ev	A detected event
Z_1	The number of frames used to aggregate data
Z_2	The number of frames used to forward a report to next-hops
H_0	The number of hops between the sink and the detected event
$\mathcal{N}(ev)$	The list of sensors that can detect ev
$\mathcal{A}$	The data aggreation communication graph
V_a	The set of vertices in $\mathcal{A}$
E_a	The set of edges (n_i, n_j) in $\mathcal{A}$
Col_{t_p}	The color affected to the vertex n_i
$Pf_i(t_p)$	The probability of failed data aggregation during $F(t_p)$
$\mathcal{Q}_i^*$	The list of n_i's next-hops that can be involved in the data forwarding to the sink
$\mathcal{R}$	The data aggreation communication graph
V_r	The set of vertices in $\mathcal{R}$
E_r	The set of edges in $\mathcal{R}$
$v_{i,j}^x$	The vertex composed of nodes n_i and n_j in relation to the report generated by r_x
$(v_{i,j}^x, v_{p,q}^y)$	An adge of the set E_r
f_1	An Objective function
δ	A boolean function

data. $Ploss_k$ denotes the packet loss probability of the channel c_k caused by obstructions or electromagnetic interferences due to the harsh environment in which substations are generally deployed [34].

6.3.1 Basic Assumptions

To achieve a distributed channel allocation during the data aggregation and reporting phases upon an event detection, we consider the following assumptions:

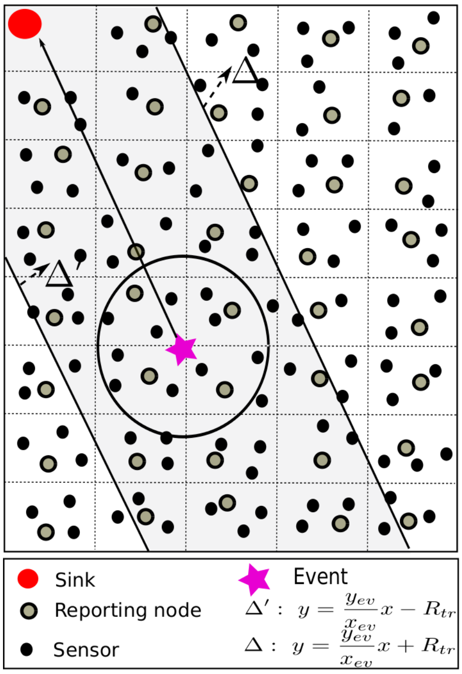

Figure 6.2: Controlled system model.

- A reporting node r_y is placed one-hop away from the nodes n_i where $n_i \in \mathcal{G}_y$.
- $n_i \in \mathcal{S}$ is aware of its location using either a GPS or any other localization technique [127].
- Each sensor $n_i \in \mathcal{S}$ is characterized by transmission (R_{tr}), interference (R_{int}) and sensing (R_{ss}) ranges where $R_{ss} \leq R_{tr}$ and $R_{int} = \beta \times R_{tr}$ ($\beta \geq 2$) [134].
- To ensure a better exploitation of the multiple channels' availability in the licensed spectrum, each node n_i has K radio interfaces [131]. Thus, at any time instant t, n_i can send and receive data on different idle channels.
- As in [135], within each node n_i, the licensed traffic is modeled as a two-state Markov chain (Busy, Idle) where the "Busy" state (respectively the "Idle" state) represents the channel state occupied by a PU (respectively, free of PUs) as it is sensed by the node n_i. $\overline{\omega_k^i}$ and ω_k^i are the respective Busy/Idle states' probabilities.
- A node n_i is aware of all its 2-hops neighbors n_j such as $d(n_i, n_j) \leq 2 \times R_{tr}$. $d(n_i, n_j)$ is the Euclidean distance between n_i and n_j.

6.3.2 SU's Spectrum Access for Data Aggregation and Reporting

To ensure reliable communications between SUs in the cognitive radio context where the spectrum access is conditioned on the absence of PUs on licensed channels, we adopt the following considerations:

- The time is synchronized and divided into frames $F(t)$ with fixed duration. Every frame begins with a spectrum sensing sub-period T_{ss} followed by a data transmission sub-period T_{tr} as shown in Figure 6.3.

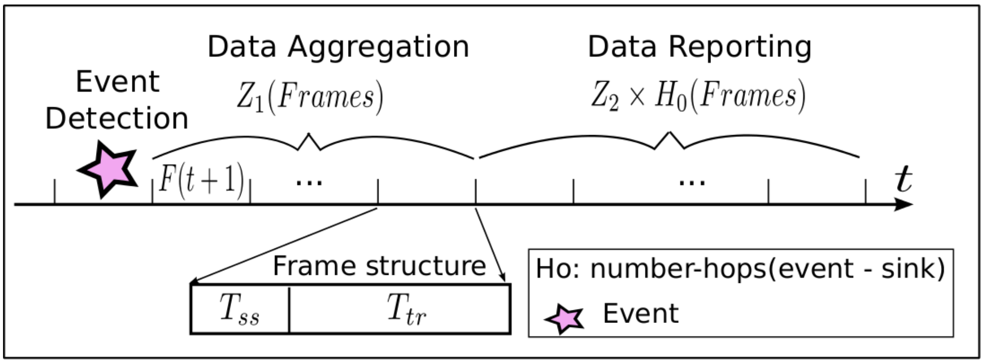

Figure 6.3: Frame structure for event detection.

- If a node $n_i \in \mathcal{S}$ detects an event ev during $F(t)$, it sends the measured values to its associated reporting node r_y during the following Z_1 frames. Thus, if n_i fails to transmit its data to r_y during the z first attempts, due to licensed channels' occupancy, it can repeat its transmission during the remaining $Z_1 - z$ frames. At the end of the data aggregation phase, all the reporting nodes within the event's vicinity will generate a report that will be transferred to the sink.

- In the same way, at the frame $F(t + Z_1 + 1)$, each reporting node r_y will forward its report to its next-hops during the upcoming Z_2 frames. Hence, the data reporting phase lasts a maximum of $Z_2 \times H_0$. H_0 represents the number of hops between the event and the sink.

- Finally, to prevent packets' loss along the path to the sink during the reporting phase, we opt for a constrained multipath "Beam" data routing where the nodes involved in the routing process are only those situated within the "Beam" (c.f. the grey zone in Figure 6.2). The "Beam" routing will be detailed in Section 6.5.

Based on the above system description, we present in the following sections how the DEAR approach allocates the licensed channels during the data aggregation and reporting phases.

6.4 Channel Allocation for Data Aggregation

During the data aggregation phase, all the nodes within the event's vicinity will send their data to their reporting nodes. Therefore, the channel allocation process should be done in a way to limit or even avoid the conflicts (collisions/interferences) between concurrent transmissions. To propose an adequate solution to this problem, we formulate it as a graph coloring problem (GCP) where vertices' colors will correspond to the prospective allocated channels.

6.4.1 Data Aggregation Communication Graph

Let ev be an event occurred at the frame $F(t)$. $\mathcal{N}(ev)$ is the list of sensors n_i that can detect ev, i.e., $d(ev, n_i) < R_{ss}$. Using the vertex coloring paradigm, each node n_i in $\mathcal{N}(ev)$ obtains a sequence of channels to send its data to its reporting node without disturbing its interfering nodes (one-hop and two-hops neighbors in $\mathcal{N}(ev)$). Let $\mathcal{A} = (V_a, E_a)$ be an undirected graph. V_a is the set of vertices composed of the non-reporting nodes able to detect the event (ev). We have:

$$V_a = \mathcal{N}(ev)/\ r_y,\ y \in [1, G] \tag{6.1}$$

E_a is the set of edges. An edge (n_i, n_j) exists if one of the following conditions is true:

- n_i and n_j have the same reporting node r_y $(n_i, n_j \in \mathcal{G}_y)$.
- $n_i \in \mathcal{G}_x$ and $n_j \in \mathcal{G}_y$ $(x \neq y)$ where $d(n_i, r_y) \leq R_{int}$. For instance, if n_j and n_i transmit data to their corresponding reporting nodes r_x and r_y then a collision may occur at r_y.

Figure 6.4 represents an example of a graph $\mathcal{A}$ construction.

- As depicted in Figure 6.4, the set of nodes $\mathcal{N}(ev)$ that have detected ev are n_6, n_7, n_8, n_9 and r_x. The list of vertices V_a are the non reporting nodes $n_i \in \mathcal{N}(ev)$. So, V_a equals $\{n_6, n_7, n_8, n_9\}$. Now, based on V_a, we construct the list of edges E_a. In fact, n_6 and n_7, respectively n_8 and n_9, have the same reporting node r_x, respectively r_y $(n_6, n_7 \in \mathcal{G}_x$ and $n_8, n_9 \in \mathcal{G}_y)$. Thus, (n_6, n_7), $(n_8, n_9) \in E_a$. Moreover n_9 is in the r_x's interference range. Thus, (n_6, n_9) and $(n_7, n_9) \in E_a$.

We also consider the set $\mathcal{H} = \{c_1, \ldots, c_K\}$ of channels (colors) to be used for the vertices' coloring. We have $|\mathcal{H}| = K$. Thus, for a given frame $F(t_p)$ of the data aggregation phase, $t_p \in [t+1, t+Z_1]$, the function $Col_{t_p} : V_a \to \mathcal{H}$ can be defined as $Col_{t_p}(n_i) = c_k$, which means that the vertex n_i is colored by the color (channel) c_k.

Therefore, we say that n_i and $n_j \in V_a$ are two conflicting vertices if an edge exists between n_i and n_j $((n_i, n_j) \in E_a)$ and n_i and n_j have the same color (channel) c_k during the considered frame $F(t_p)$, i.e., $Col_{t_p}(n_i) = Col_{t_p}(n_j)$.

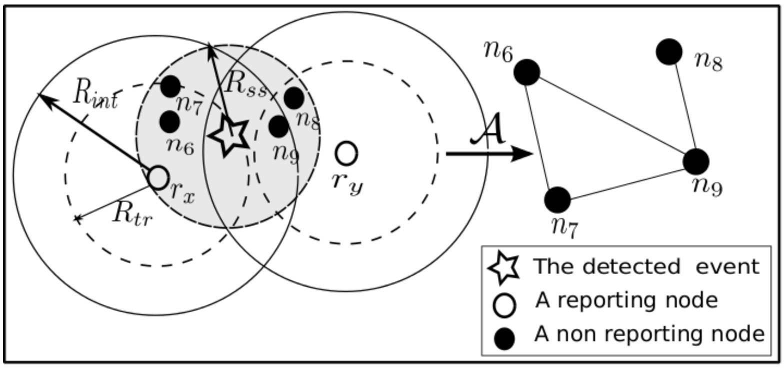

Figure 6.4: Graph $\mathcal{A}$ construction.

Hence, we define the function $\delta : V_a \times V_a \longmapsto [0, 1]$ as:

$$\delta(n_i, n_j) = \begin{cases} 1 & \text{if } (n_i, n_j) \in E_a \bigwedge Col_{t_p}(n_i) = Col_{t_p}(n_j) \\ 0 & \text{otherwise.} \end{cases} \tag{6.2}$$

Thus, a correct channel allocation between the nodes of the set $\mathcal{N}(ev)$ during a frame $F(t_p)$ consists in minimizing the number of conflicts within the graph $\mathcal{A}$, i.e., minimizing the number of adjacent vertices with the same color.

We can formulate this problem as:

$$\begin{gathered} \mathit{minimize} \left(f_1 = \sum_{n_i, n_j \in V_a} \delta(n_i, n_j) \right) \\ \text{subject to } Col_{t_p}(n_i) \in \mathcal{H}, \ \forall n_i \in V_a \end{gathered} \tag{6.3}$$

From the above formulation, we can conclude that the channel allocation process during the whole data aggregation phase consists in solving the above system, given by the Equation (6.3), during Z_1 subsequent frames, where the Z_1 is the number of frames used during the data aggregation phase.

6.4.2 Channel Allocation Process

As a well known NP-hard problem, the GCP is generally solved through heuristics such as DSATUR or Tabu-search [136]. Moreover, it has been widely used for the fixed channel assignment problem. But, in the cognitive radio context, the problem is slightly different since the channel allocation is a dynamic process that completely depends on PUs arrivals. Thus, a graph recoloring is continuously performed to achieve an efficient channel access. Several approaches, referred in [137], attempted to adapt the GCP to the cognitive radio context. Most of these approaches consider that the neighboring nodes are exchanging their decisions based on a CCC. As we consider a fully distributed channel allocation scheme, each node will make its own decisions based on its local view of the network obtained by the graph $\mathcal{A}$.

Therefore, we propose a cognitive decentralized graph coloring (Cognitive-DGC) based on a simple nevertheless accurate local search heuristic, as introduced in [138], to minimize the edge conflicts in a graph. The heuristic proposed in [138] is efficient since every node uses its local information to minimize the number of conflicts in its vicinity. The local search minimum conflict heuristic in [138] is adapted to the particular cognitive radio context as follows:

Cog-min-conflicts heuristic: Every vertex n_i selects the color $c_k \in \mathcal{H}$ that minimizes the number of conflicts with its neighbors. If at least two colors (channels) achieve the same minimum number of conflicts, then n_i selects the channel c_k^* with the highest availability value ω_k^{i*}.

Algorithm 7 details the execution steps of the *Cog-min-conflicts heuristic.*

Algorithm 7 Cog-min-conflicts.

Input: n_j, tp, $\mathcal{A}$
Output: $Col_{tp}(n_j)$

conflict-array$[1,\ldots,K] \leftarrow [0,\ldots,0]$
for $k = 1$ *to* K **do**
  for $n_l \in V_a$ **do**
    if $(Col_{tp}(n_l) = c_k)$ and $((n_j, n_l) \in E_a)$ **then**
      conflict-array$[k] \leftarrow$ conflict-array$[k] + 1$;
    end if
  end for
end for
$Col_{tp}(n_j) \leftarrow \underset{c_k/\ k\in[1,K]}{\arg} (\min\ (\text{conflict-array}[k]))$

The *Cog-min-conflicts heuristic* only minimizes the number of conflicts among neighboring vertices. But, since the data aggregation phase executes during Z_1 frames, we can ensure that during a given frame $F(t_p)$, $t_p \in [t+1, t+Z_1]$, nodes can send data to their reporting nodes without collision on any transmitting channel, i.e., the set of vertices E_a can be colored with zero conflicts.

Thus, we introduce $Pf_i(t_p)$ as the probability of failed data aggregation during the frame $F(t_p)$. $Pf_i(t_p)$ is evaluated as a function of the channel occupancy $\overline{\omega_k^i} = 1 - \omega_k^i$ and the packet loss $Ploss_k$ values on the channel c_k. To ensure fairness among the nodes and in the case of conflicts during $F(t_p)$, the vertices n_i with the highest $Pf_i(t_p)$ probabilities will be prioritized to transmit their data during this frame. The other vertices will postpone their transmissions to the next frames. To this end, we propose a new heuristic *Graph-based-zero-conflict* that aims to eliminate, during a given frame $F(t_p)$ all the conflicts in the graph $\mathcal{A}$ based on the probabilistic successful/failed data transmission aspect.

Graph-based-zero-conflict heuristic: Iteratively, during the frame $F(tp)$, $tp \in [t+1, t+Z_2]$, the vertices n_i in E_a having the smallest $Pf_i(t_p)$ probabilities and causing conflicts to their neighbors convert their colors to c_{K+1}. c_{K+1} indicates that the colored vertex will not transmit data during $F(tp)$.

The Algorithm 8 explicits the execution steps of the *Graph-based-zero-conflict heuristic*.

Algorithm 8 Graph-based-zero-conflict.

Input: n_j, tp, $\mathcal{A}$
Output: $Col_{tp}(n_j)$

```
1: n_i ∈ V_a are sorted according to Pf_i in descending order
2: for n_i ∈ V_a do
3:     if (∑_{n_j ∈ V_a} δ(n_i, n_j) ≠ 0) then
4:         Col_tp(n_i) ← c_{K+1}
5:     end if
6: end for
```

Thus, from the above two heuristics, we can introduce in Algorithm 9 the whole Cognitive-DGC process. Initially, every vertex $n_j \in V_a$ is colored with c_k^*, the channel with the highest availability value ω_k^{i*} in the set $\mathcal{H}$. Then, iteratively, the *Cog-min-conflicts heuristic is* executed during a number of iterations equal to $\|V_a\| \times K + \|E_a\|$, as in [138], to obtain a graph $\mathcal{A}$ with a minimum number of conflicts. Thereafter, the *Graph-based-zero-conflict heuristic* is executed during $F(t_p)$ to allow vertices with highest $Pf_i(t_p)$ values to access the spectrum in the case of conflicts. The other conflicting vertices n_j will have their colors changed to c_{K+1} and would not transmit in the current frame. At the end of $F(t_p)$, all the vertices that received a color different from c_{K+1} will reevaluate their probabilities $Pf_i(t_p+1)$, for the next frame $F(t_p+1)$. The vertices n_j that did not transmit during $F(t_p)$, such as $Col_{t_p}(n_i) = c_{K+1}$, will keep their probabilities $Pf_j(t_p+1)$ for the next frame unchanged. This will increase their opportunities to access the spectrum in subsequent frames.

Once the Z_1 data aggregation frames elapses, the data reporting process can then start.

6.5 Channel Allocation for Data Reporting

During the data reporting phase, the reporting are in charge of forwarding the collected data through multi-hop transmissions to the sink. We opt for multipath data routing to avoid the single path failures given the substations' harsh environment conditions [2]. Moreover, to reduce the amount of exchanged information during the reporting phase, we adopt a constrained multipath routing called "Beam" data routing (c.f. Figure 6.5).

Algorithm 9 Cognitive DGC.

Input: $\mathcal{A} = (V_a, E_a)$;
$Ite \leftarrow \|V_a\| \times K + \|E_a\|$
Output: $[Col_{t+1}(n_i), \ldots, Col_{t+Z_1}(n_i)]$

$\forall n_j \in V_a$, $Pf_j \leftarrow 1$;
for $tp = t + 1$ *to* $t + Z_1$ **do**
  $it \leftarrow Ite$
  for $n_j \in V_a$ **do**
    $Col_{tp}(n_j) \leftarrow \arg\max_{c_k/\ k\in[1,K]} \omega_k^j$
  end for
  while $(it \geq 1)$ **do**
    for $n_j \in V_a$ **do**
      Cog-min-conflicts$(n_j, tp, \mathcal{A})$
    end for
    $it \leftarrow it - 1$;
  end while
  Graph-based-zero-conflict$(n_j, tp, \mathcal{A})$;
  for $n_j \in V_a$ **do**
    if $(Col_{tp}(n_j) \neq c_{K+1})$ **then**
      $Pf_j \leftarrow Pf_j \times (\overline{\omega_k^j}) \times Ploss_k\ \{Col_{tp}(n_j) = c_k\}$
    end if
  end for
end for

Multipath beam data routing: Let n_i be a sending node, i.e., it has reports to forward to the sink. n_i may be either a reporting node that has aggregated the data or another sensor closer to the sink than the reporting node. We denote by $\mathcal{Q}_i^*$ the list of n_i's next-hops that can be involved in the data forwarding to the sink. $n_j \in \mathcal{Q}_i^*$ if n_j is closer to the sink than n_i $(d(sink, n_j) < d(sink, n_i))$ and it is placed in the area limited by Δ and Δ'. Δ and Δ' are defined by the detected event ev coordinates (x_{ev}, y_{ev}) and the sink coordinates $(0, 0)$:

- $\Delta : y = \frac{y_{ev}}{x_{ev}} x + R_{tr}$
- $\Delta' : y = \frac{y_{ev}}{x_{ev}} x - R_{tr}$

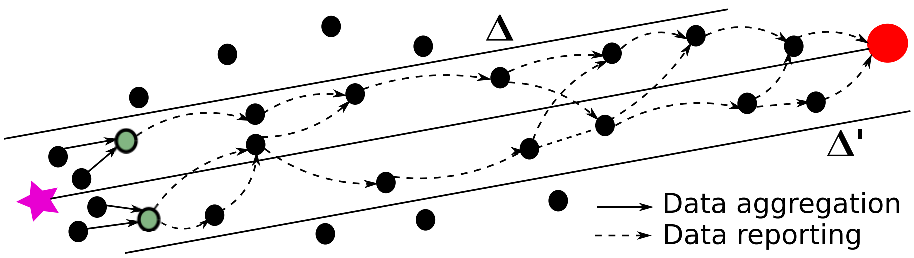

Figure 6.5: Multipath beam data routing.

Given the opportunistic access to the licensed spectrum, each hop along the path to the sink waits for Z_2 frames to receive data from its predecessors. Indeed, if n_i starts forwarding data to the sink at the frame $F(t_p)$, its next-hop $n_j \in \mathcal{Q}_i^*$ starts the transmission of the received data at the frame $F(t_p + Z_2)$. This allows sensor nodes with simultaneous data transmissions to make the same decisions regarding their channels' selection.

Therefore, as for the data aggregation phase, we adopt the graph coloring paradigm for the spectrum assignment during the DEAR reporting phase. Thus, every node in the "Beam" with reports to send toward the sink direction constructs an undirected graph $\mathcal{R} = (V_r, E_r)$. $\mathcal{R}$ is constructed based on the sensors involved in simultaneous transmissions that may concur for the same radio resources. Accordingly, V_r, representing the set of vertices is defined as follows:

- If a node n_i along the path to the sink has to forward data, originally generated by r_x, to its next hop $n_j \in \mathcal{Q}_i^*$, then we have: $v_{i,j}^x \in V_r$. $v_{i,j}^x$ denotes the vertex composed of nodes n_i and n_j in relation to the data report originally generated by r_x.

E_r is the set of edges. An edge $(v_{i,j}^x, v_{p,q}^y)$ exists, i.e., $(v_{i,j}^x, v_{p,q}^y) \in E_r$, if one of the following conditions holds:

- The same node is involved in the transmission of two different reports, i.e., $(i = p) \bigvee (i = q) \bigvee (j = p) \bigvee (j = q)$.
- n_q is in the n_i's interference range, i.e., $d(n_i, n_q) \leq R_{int}$.

Figure 6.6 represents an example of a graph $\mathcal{R}$ construction:

- As shown in Figure 6.6, two reports are generated after the data aggregation phase. They should be sent to the sink node. These reports are generated by respectively r_x, i.e., n_5, and r_y, i.e., n_8. Let n_6 be the next-hop of r_x, i.e., $\mathcal{Q}_5^* = \{n_6\}$, and n_7 represents the r_y's next-hop, i.e., $\mathcal{Q}_8^* = \{n_7\}$. Thus, the list of vertices V_r is composed of: $v_{5,6}^x$ and $v_{8,7}^y$. Now, since n_7 is placed in the n_5's interference range, i.e., $d(n_5, n_7) < R_{int}$, then $(V_{5,6}^x, V_{8,7}^y) \in E_r$.

The two vertices $v_{i,j}^x, v_{p,q}^y \in E_r$ are called two conflicting vertices if the two following conditions hold:

- $v_{i,j}^x, v_{p,q}^y \in E_r$
- $Col_{tp}(v_{i,j}^x) = Col_{tp}(v_{p,q}^y)$, where the $Col_{tp}()$ function is the one previously introduced in Section 6.4.

Hence, by using the same objective function f_1 defined in Equation (6.3) applied to the graph $\mathcal{R}$, every node proceeds to the graph $\mathcal{R}$ coloring through the Cognitive DGC algorithm during Z_2 frames.

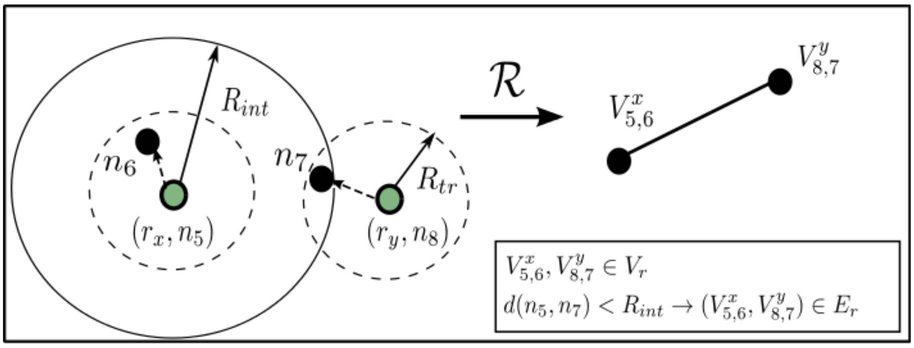

Figure 6.6: Graph $\mathcal{R}$ construction.

6.6 Performance Evaluation

This Section is dedicated to the performance evaluation of the DEAR approach. We first evaluate how the different parameters of DEAR impact its behavior in terms of efficient data transmission. Thereafter, we compare it to the well known cluster-based SCR routing [117] and another existing CCC-based multipath routing [139] for CRSNs.

We carried out simulations under the OMNeT++ network simulator through the MiXiM framework. the SUs are uniformly deployed in the field area and divided into G virtual grids. Table 6.2 lists the basic parameters used in our simulation.

Table 6.2: Simulation Parameters.

Parameter	Value
Number of nodes	150
Channel occupancy	0.35/ 0.83/ 0.5/ 0.45
$R_{ss}/R_{tr}/R_{int}$	$30/30/60m$
Number of PUs	4
Area range	$200 \times 200\ m^2$
G	16

6.6.1 Data Aggregation Efficiency

We first evaluate the ability of DEAR to efficiently aggregate data once an event is detected. In DEAR, the data aggregation efficiency is dependent on the parameter Z_1. Thus, in Figure 6.7, we evaluate the failed data aggregation ratio for different Z_1 values. We compare DEAR to SCR where one channel is opportunistically accessed to assign channels. The percentage of sensors that fail to transmit their data to their associated reporting nodes decreases with the increase in Z_1 and in the number of used channels (K). DEAR outperforms SCR since the latter depends on the availability of the control channel. In fact, in the opposite to SCR, DEAR don't use a CCC, sensors can get benefit from available channels without relying on the availability of one channel.

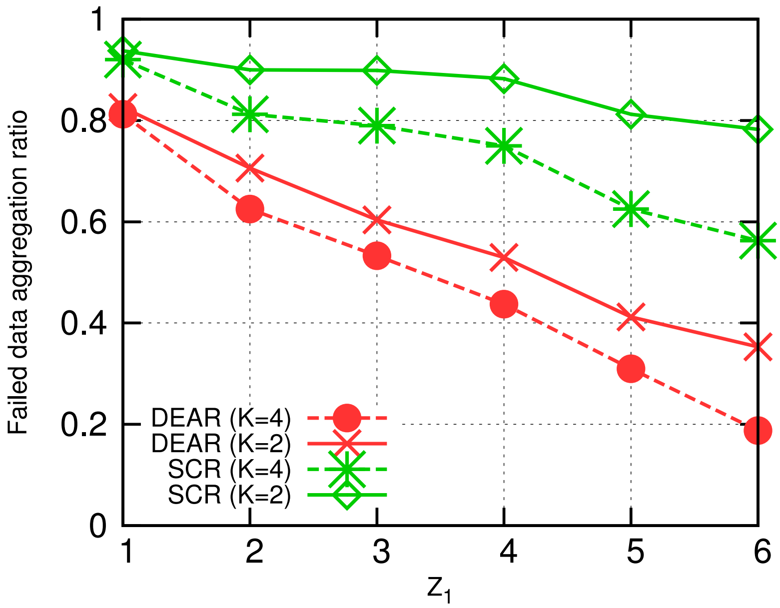

Figure 6.7: Failed data aggregation ratio vs Z_1.

6.6.2 Report Forwarding Efficiency

Now, to measure the DEAR efficiency to forward the different generated reports to the sink, we evaluate the impact of the reporting frame number Z_2 on the successful data reporting ratio "Θ". As shown in Figure 6.8, the increase in Z_2 positively impacts (improves) Θ (the successfully transmitted data by a sender per the total number of transmissions during the reporting phase). The Θ value reaches 0.78 when $K = 4$. We also evaluate our constrained multipath "Beam" routing and compare it to the *non constrained DEAR* where all the next-hops will be involved in the data reporting. As depicted in Figure 6.8, with DEAR, Θ increases with Z_2 and with the number of the used channels K ($K \in \{2, 4\}$). However, with the non-constrained DEAR, Θ starts to increase to thereafter decrease with highest Z_2 values. In fact, as Z_2 increases, a large number of nodes will be involved during the data routing. As messages get closer to the sink, the number of forwarding nodes increases too resulting in an important set of conflicting nodes concurring for the same resources.

Furthermore, we evaluate Θ for different values of N, corresponding to the number of SUs. As depicted in Figure 6.9, Θ remains almost constant ($\simeq 0.65$) with a slow increase when N increases. Thus, despite the nodes' number, DEAR achieves a correct channel allocation between SUs to efficiently aggregate and report data to the sink.

6.6.3 Report Transmission Delay Evaluation

DEAR is dedicated for an early critical event's detection. Thus, the locally generated reports have to be rapidly sent to the sink. However, the data transmission delay in DEAR

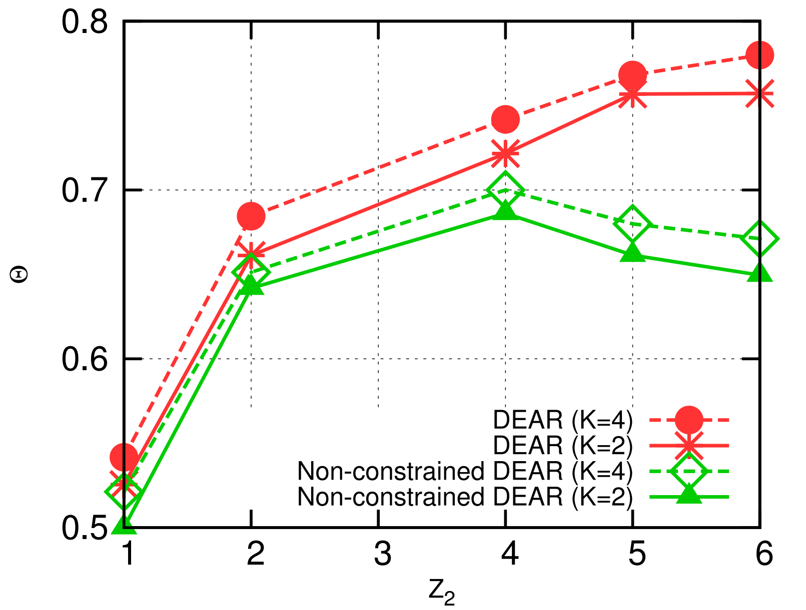

Figure 6.8: Successful data reporting ratio (Θ) while varying Z_2.

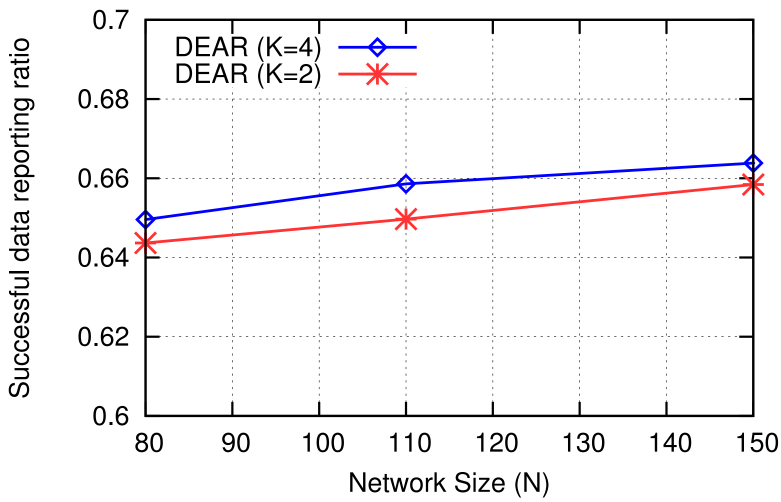

Figure 6.9: Successful data reporting ratio (Θ) vs the network size N.

is impacted by different parameters. We first evaluate the impact of the reporting frame number Z_2, on the delay ($\mathcal{D}$) between the event detection and the reports' reception by the sink. Figure 6.10 depicts the variation of $\mathcal{D}$ for different Z_2 values. $\mathcal{D}$ is measured for multiple events occurred at different positions in the network. Figure 6.10 shows that $\mathcal{D}$ gradually increases with Z_2. Indeed, increasing Z_2 may slightly slow the transmissions, but the nodes will have more chances to faster reach the sink (as a large number of conflicting nodes could transmit during Z_2).

Figure 6.11 depicts the delay $\mathcal{D}$ variation according to the distance between the detected event and the sink. The results show that $\mathcal{D}$ increases with the distance to the sink as the number of hops to reach the sink increases.

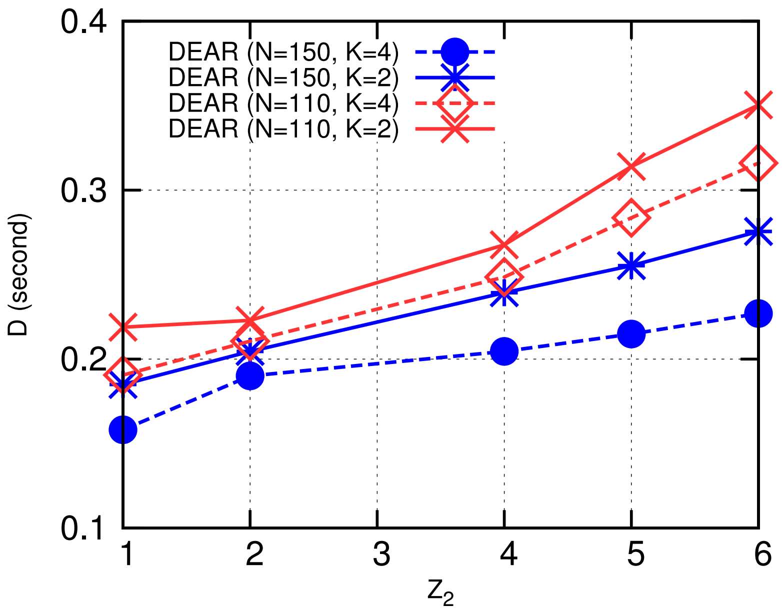

Figure 6.10: Time spent by the sink to receive the reports vs Z_2.

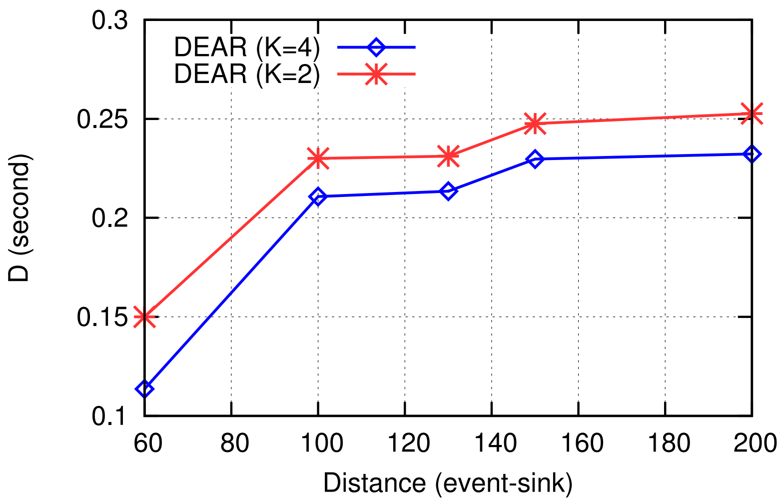

Figure 6.11: Time spent by the sink to receive the reports vs $d(event, sink)$.

Finally, we vary the number of virtual-grids G in the network and we study its effect on $\mathcal{D}$. In fact an increase in G leads to a large number of produced reports when an event is occurred. We compare DEAR to SCR and to the CCC-based multipath data routing. As depicted in Figure 6.12, when using SCR and the CCC-based multipath routing, $\mathcal{D}$ increases with G. For instance, as G increases, the number of reporting nodes increases too leading to an important contention on the CCC which peduncles SUs from correctly sending their data when SCR and CCC-based multipath approaches are used. This problem is completely annihilated with DEAR which achieves the best delay among all the three approaches.

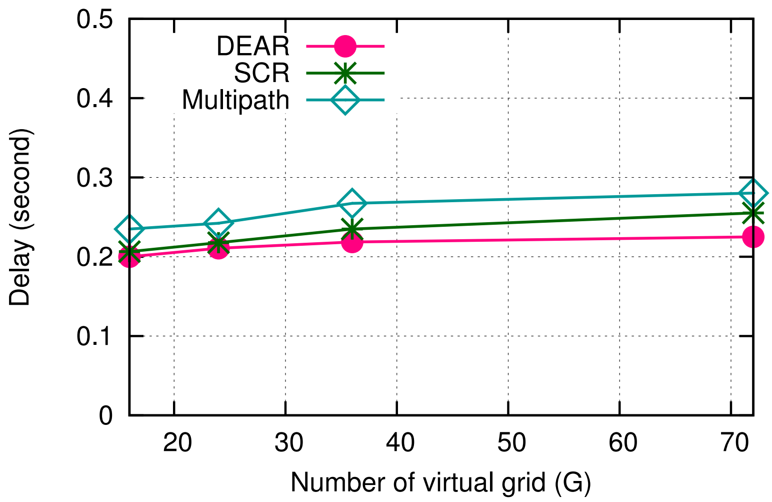

Figure 6.12: Time spent by the sink to receive the reports vs G.

6.7 Conclusion

In this chapter, we proposed a new distributed channel allocation mechanism for cognitive radio sensor networks to achieve an early abnormal event detection in electrical substation deployed in suburban environment. Our solution, called DEAR, achieves two channel assignment processes operating in tandem based on the graph coloring paradigms:

- A channel allocation algorithm allowing sensors, having detected an event, to aggregate their measured values at particular reporting nodes: Based on the detected event location, every node having detected a particular event estimates the list of other sensors that detected the same event. Then, using te graph coloring, each node locally derives the channel that will be used by every node.
- A channel assignment strategy for the data forwarding process: Once the reports are generated by the reporting nodes, sequentially, every node that is involved in the data forwarding to the sink constructs a graph. This graph is based on the nodes having reports to send at the same time. Thereafter, based on a distributed vertex coloring of graphs, the graph vertices are colored to obtain the channel allocated to every node during the Z_2 frames (Z_2 is the maximum number of frames that may be used to transmit a report).

We evaluated our proposed DEAR scheme through simulations. During the reporting phase, the simulation results showed that DEAR improves (minimizes) the failed data aggregation ratio for different values of Z_1. Moreover it demonstrated that DEAR achieves a better successful data reporting ratio compared to the non-constrained DEAR. In fact, the multipath beam data routing that we used during the reports' routing to the sink avoids the single path failure. It also limits the number of nodes involved in the constructed paths.

To conclude, the simulation results revealed that our approach succeeds in efficiently assigning channels during the data aggregation and the data reporting to the sink. DEAR represents a good candidate for distributed and fair spectrum sharing in CRSN-based earlier abnormal events' detection.

Chapter 7

Conclusion and Perspectives

Contents

The efforts to modernize traditional power grids have begun several years ago. In 2008, France has invested 508 million euros in the development of smart grids, the United Kingdom 497 million euros and Germany 363 million euros [140]. Despite these efforts, the United States that has one of the most mature smart grid infrastructure markets in the world, still until January 2017 has only half of its residential meter markets equipped with two-way communicating advanced metering infrastructure, leaving ample room for further growth [141]. A lot of research and industrial works are then still needed to make the smart grid technology into existence. In this thesis, we were interested in communication issues in smart grids. We focused on the deployment of cognitive radio sensor networks (CRSNs) for smart grid power access networks. The CRSNs represent an interesting technology to deal with the large traffic volumes in smart grids. It is an interesting and an intelligent technology for smart grid data gathering and transmission that does not necessitate real time processing.

Throughout this dissertation, we investigated the issues of communication aspects in smart grid power access networks. We focused on distributed and fair channel assignment in CRSN for smart grids. Our works consider eventual CRSNs deployment scenarios in different smart grid areas and diverse smart grid traffic characteristics. We targeted exclusively predictive channel assignment approaches for CRSNs in smart grids. Our solutions allowed a node to obtain its channel without using a common control channel (CCC) to exchange control messages before each individual spectrum access while considering neighboring nodes' need to transmit. In fact, even through it is widely used in literature in CRSNs, the use of a CCC presents multiple limitations that negatively impact the opportunistic spectrum access.

7.1 Contributions

All along this thesis, we proposed different probabilistic channel allocation approaches for CRSNs in smart grid to fit several smart grid CRSN deployment scenarios.

Initially, we were interested in channel assignment techniques in one-hop CRSN deployed to monitor two different systems in smart grid power access networks: smart homes (HANs) and neighborhood area networks (NANs). In smart homes, sensors have the same priority to transmit data. However, in a NANs, heterogeneous electrical elements are monitored. Thus, NAN sensors have different priorities to access the spectrum. Thence, given the differences between these two smart grid areas, we have proposed two channel allocation schemes: the Cooperative Spectrum Resource Assignment (CSRA) approach for CRSNs deployed in smart houses and Distributed Unselfish Spectrum Assignment approach (DUSA) for CRSNs deployed in NANs. In every system, the deployed smart grid sensors use a fairness metric to estimate neighboring nodes' priorities to access the spectrum. Then, based on Partially Observable Markov Decision Processes (POMDPs), every sensor predicts the channels that will be used by its neighbors. As a result, it obtains its associated channel. If a sensor founds that its neighbors are more prioritized to transmit data, then it postpones its data transmission. Otherwise, it gets a channel to send data. The main CSRA and DUSA's objective is to achieve a balanced spectrum sharing among smart grid sensors. Performance evaluation through simulations revealed that both CSRA and DUSA are able to fairly share the spectrum and to improve the radio resources' utilization compared to existing works.

In the second contribution, we tackled the short transmission range of smart grid NAN sensors. We first proposed a practical network architecture. We introduced the use of full functional nodes that we call forwarding nodes to extend smart grid sensors' coverage. Then, we proposed the Dual-Spectrum Assignment for NAN (D-SAN) based on two-Stage CRSNs. D-SAN is composed of two complementary channel assignment schemes: The first scheme is dedicated to the communication between smart grid monitoring sensors and forwarding nodes. The second one allocates channels for forwarding nodes to transmit data to a sink node. In both schemes, sensors use local estimates of their neighboring nodes' priorities to allocate channels for data transmissions and rely on POMDP to do so. Performance evaluation of D-SAN illustrated its efficiency in achieving fair spectrum sharing and its performances in term of network spectrum utilization.

The third contribution of this thesis focused on the multi-hop CRSN topology for smart grid NANs. We opted for a hierarchical CRSN self organization using clustering to monitor NANs. Thus, we first proposed a clustering algorithm to divide the network into multiple clusters based on sensors' priorities and channels' availability. Then, we developed the Predictive Hierarchical Spectrum Assignment (PHSA). Based on local estimates of neighboring clusters' priorities, every cluster head fairly assigns channels to its own and to its neighboring clusters for intra-cluster and inter-cluster communications. Thereafter, as an extension of PHSA, we introduced the Routing-based PHSA (R-PHSA) approach. R-PHSA takes into consideration the routing aspects during the inter-cluster channel assignment. PHSA and R-PHSA are based on POMDP formulations. Simulation results of both PHSA and R-PHSA showed their adaptability to the variations in the traffic priorities in addition their capability to outperform one of the main existing clustering approach, SCR, in terms of packet volume successfully received by the sink since both PHSA and R-PHSA don't rely on a CCC.

In the fourth contribution, we considered the randomly generated smart grid traffic. We focused on the distribution smart grid substation environment where abnormal events such as fire and equipment malfunctioning are more likely to happen. We introduced the Distributed Event-driven data Aggregation and constrained multipath Reporting (DEAR) approach. DEAR completely emancipates from the CCC limitations. It uses the graph coloring paradigm for the licensed spectrum allocation during the data aggregation and reporting phases and a constrained multipath "Beam" routing to prevent from packet loss and failures in the harsh environment in which the substations are deployed. Performance evaluation revealed that DEAR ensures a rapid data transmission and an efficient channel assignment in CRSNs.

In summary, the key contributions presented in this thesis have targeted fair channel allocations in CRSNs for smart grids. We considered different deployment scenarios of CRSNs in smart grids in addition to diverse smart grid traffic characteristics. Yet, different from most research works on channel allocation for smart grid cognitive radio sensor networks, we developed solutions where sensors don't use a CCC to harmonize their spectrum access trials. In fact, when using a CCC, control message exchange becomes conditioned on the CCC vacuity of licensed signals. Moreover, the CCC use may threaten the system's security since it is widely used by attackers. Finally, we avoided the CCC use to prevent the "single point of failure" eventual problems.

7.2 Perspectives

This dissertation has enabled us to study the advances in smart grid systems in addition to the integration of CRSNs as a key technology for smart grid monitoring besides leveraging new reflections for future works:

Underlay transmissions: All along this thesis, we considered only interweave transmissions. Sensors use only available frequency channels to transmit data. If an allocated channel is sensed used by licensed signals then the considered sensor postpones its transmission. We can extend the proposed solutions to consider an interweave spectrum access. If a given channel is sensed busy and the considered node has data waiting to be transmitted, then this one may simply adapt its transmission power and access the corresponding channel while making sure to not disturbing the licensed signal. This can improve the SG spectrum utilization.

Channel switching: In hierarchical CRSNs for NANs, channels are assigned for intra-cluster and inter-cluster communications while avoiding interferences among neighboring clusters. During the intra-cluster communication, at maximum one channel is assigned in every cluster. Moreover, during the inter-cluster data transmission, at maximum one channel is assigned to the cluster head to transmit data towards the sink direction. If during both communications a licensed signal arrives on the used channel, then the transmitting secondary user directly stops its transmission. In fact, the considered secondary user may have the opportunity to terminate its transmission on another available channel without interfering with neighboring clusters. Accordingly, we can use a channel switching process to allow smart grid sensors to look for new available channels not in use by secondary or primary users to continue their communication until the end of the frame.

Multi-event detection: Our last contribution, i.e., Distributed Event-driven data Aggregation and constrained multipath Reporting (DEAR), focused on the transmission of data related to only one detected event at a time. We can extend our work to consider the data transmission after the detection of multiple events at different locations of the substation environment. Thus, sensors should organize their transmissions to efficiently forward reports to the sink.

Mobile devices: During all this dissertation, sensors are assumed to be stationary. We can introduce mobile smart grid devices such as electric vehicles and drones that may use cognitive radio technology to transmit data. By adding such devices, in our approaches should be integrated the fact that every non mobile smart grid sensor has to consider the probability of mobile nodes' arrivals that may concur to the spectrum resource sharing.

List of Publications

International Conferences

- **Sabrine Aroua**, Inès El Korbi, Yacine Ghamri-Doudane and Leila Azouz Saidane, "Hierarchical Fair Spectrum Sharing in CRSNs for Smart Grid Monitoring". IEEE 87th Vehicular Technology Conference (VTC Spring), Porto, Portugal, 2018.

- **Sabrine Aroua**, Inès El Korbi, Yacine Ghamri-Doudane and Leila Azouz Saidane, "Event-driven Data Aggregation and Reporting for CRSN-based Substation Monitoring". IEEE 28th Annual International Symposium on Personal, Indoor, and Mobile Radio Communications (PIMRC), Montreal, QC, Canada, 2017.

- **Sabrine Aroua**, Inès El Korbi, Yacine Ghamri-Doudane and Leila Azouz Saidane, "A Distributed Cooperative Spectrum Resource Allocation in Smart Home Cognitive Wireless Sensor Networks". IEEE Symposium on Computers and Communications (ISCC), Heraklion, Greece, 2017.

- **Sabrine Aroua**, Inès El Korbi, Yacine Ghamri-Doudane and Leila Azouz Saidane, "A Distributed Unselfish Spectrum Assignment for Smart Microgrid Cognitive Wireless Sensor Networks". IEEE Wireless Communications and Networking Conference (WCNC), San Francisco, CA, USA, 2017.

National Conferences

- **Sabrine Aroua**, Inès El Korbi, Yacine Ghamri-Doudane and Leila Azouz Saidane, "Allocation non égoïste des canaux dans les réseaux à radio cognitive pour les smart grids", l'évaluation de performance et l'expérimentation des réseaux de communication (CORES) 2016, Bayonne, France.

- **Sabrine Aroua**, Inès El Korbi, Yacine Ghamri-Doudane and Leila Azouz Saidane, "Wireless Sensor Networks and Cognitive Radio technology adaptation for Smart Grid applications: A survey and open problems", International Conference on Performance Evaluation and Modeling in Wired and Wireless Networks (PEMWN) 2014, Sousse, Tunisia.

References

[1] Emmanuel U. Ogbodo, David Dorrell, and Adnan M. Abu-Mahfouz. Cognitive radio based sensor network in smart grid: Architectures, applications and communication technologies. *IEEE Access*, 5, 2017.

[2] Athar Ali Khan, Mubashir Husain Rehmani, and Martin Reisslein. Cognitive radio for smart grids: Survey of architectures, spectrum sensing mechanisms, and networking protocols. 18:860–898, 2016.

[3] Boban Panajotovic, Milan Jankovic, and Borislav Odadzic. Ict and smart grid. 2011.

[4] Adnan Anwar and Abdun Naser Mahmood. Cyber security of smart grid infrastructure. In *CRC Press*, 2014.

[5] U.S.-Canada Power System Outage Task Force. Blackout 2003: Final report on the august 14, 2003 blackout in the united states and canada: Causes and recommendations. 2004.

[6] M. Moretti, S. Njakou Djomo, H. Azadi, K. May, K. De Vos, S. Van Passel, and N. Witters. A systematic review of environmental and economic impacts of smart grids. *Renewable and Sustainable Energy Reviews*, 45:101–110, 2017.

[7] Energy efficiency in the power grid. *ABB Inc*, 2007.

[8] Bimal K. Bose. Global warming: Energy, environmental pollution, and the impact of power electronics. *IEEE Industrial Electronics Magazine*, 4:6–17, 2010.

[9] Jenkins Nick, Long Chao, and Wu Jianzhong. An overview of the smart grid in great britain. *Engineering*, 1:413–421, 2015.

[10] Mikael Hook and Xu Tang. Depletion of fossil fuels and anthropogenic climate change—a review. *Energy Policy*, 52:797–809, 2013.

[11] Fossil fuels. `http://www.eesi.org/topics/fossil-fuels/description`. Accessed: 2018-03-30.

[12] Bharat Raj Singh and Onkar Singh. Global trends of fossil fuel reserves and climate change in the 21st century. In *Fossil Fuel and the Environment*, pages 167–192, 2012.

[13] Eugene Y. Song, Gerald J. FitzPatrick, and Kang B. Lee. Smart sensors and standard-based interoperability in smart grids. *IEEE SENSORS JOURNAL*, 17:7723–7730, 2017.

[14] Qi Huang, Shi Jing, Wei Zhen, and Jianbo Yi. Cyber security of smart grid infrastructure. In *Technology and Engineering*.

[15] Bimal K. Bose. The role of advanced sensing in smart cities. *Sensors*, 13:393–425, 2013.

[16] Vehbi C. Gungor, Dilan Sahin, Taskin Kocak, Salih Ergut, Concettina Buccella, Carlo Cecati, and Gerhard P. Hancke. Smart grid technologies: Communication technologies and standards. *IEEE TRANSACTIONS ON INDUSTRIAL INFORMATICS*, 7:529–539, 2011.

[17] Iboun Sylla. Understanding regulations when designing a wireless product in the unlicensed frequency bands.

[18] Ian F. Akyildiz, Won-Yeol Lee, Mehmet C. Vuran, and Shantidev Mohanty. A survey on spectrum management in cognitive radio networks. 46, 2008.

[19] R.Challoo, A.Oladeinde, N.Yilmazer, S.Ozcelik, and L.Challoo. An overview and assessment of wireless technologies and co-existence of zigbee, bluetooth and wi-fi devices. 12:386–391, 2012.

[20] Shensheng Tang, Chenghua Tang, Rong Yu, Xiaojiang Chen, and Yi Xie. Analysis of spectrum utilization for ism band cognitive radio sensor networks. In *IEEE International Conference on Communication Software and Networks*, 2016.

[21] Sk. Shariful Alam, Lucio Marcenaro, and Carlo Regazzoni. Opportunistic spectrum sensing and transmissions. *Networking and Internet Architecture*, 2013.

[22] Ian F. Akyildiz, Brandon F. Lo, and Ravikumar Balakrishnan. Cooperative spectrum sensing in cognitive radio networks: A survey. *Physical Communication*, 4:40–62, 2011.

[23] Antonio De Domenico, Emilio Calvanese Strinati, and Maria-Gabriella Di Benedetto. A survey on mac strategies for cognitive radio networks. *IEEE Communications Surveys and Tutorials*, 14:21–44, 2010.

[24] Houda Daki, Asmaa El Hannani, Abdelhak Aqqal, Abdelfattah Haidine, and Aziz Dahbi. Big data management in smart grid: concepts, requirements and implementation. *Journal of Big Data*, 4, 2017.

[25] Hui Jiang, Kun Wang, Yihui Wang, Min Gao, and Yan Zhang. Energy big data: A survey. *IEEE Access*, 4:3844–3861, 2016.

[26] Azam Bagheri, Math H.J. Bollen, and Irene Y.H. Gu. Big data from smart grids. In *IEEE PES Innovative Smart Grid Technologies Conference Europe (ISGT-Europe)*, 2017.

[27] Seyed Morteza Mirhoseininejad, Mirhoseni Nezhadal, Reza Berangi, and FathyMahmood Fathy. Common control channel saturation detection and enhancement in cognitive radio networks. *International Journal of Distributed and Parallel Systems*, 4:26–39, 2012.

[28] Sabrine Aroua, Inès El Korbi, Yacine Ghamri-Doudane, and Leila Azouz Saidane. A distributed cooperative spectrum resource allocation in smart home cognitive wireless sensor networks. In *IEEE Symposium on Computers and Communications (ISCC)*, 2017.

[29] Sabrine Aroua, Inès El Korbi, Yacine Ghamri-Doudane, and Leila Azouz Saidane. A distributed unselfish spectrum assignment for smart microgrid cognitive wireless sensor networks. In *IEEE Wireless Communications and Networking Conference (WCNC)*, 2017.

[30] Sabrine Aroua, Inès El Korbi, Yacine Ghamri-Doudane, and Leila Azouz Saidane. Hierarchical fair spectrum sharing in crsns for smart grid monitoring. In *IEEE Vehicular Technology Conference (VTC Spring)*, 2018.

[31] Sabrine Aroua, Inès El Korbi, Yacine Ghamri-Doudane, and Leila Azouz Saidane. Event-driven data aggregation and reporting for crsn-based substation monitoring. In *IEEE Annual International Symposium on Personal, Indoor, and Mobile Radio Communications (PIMRC)*, 2017.

[32] Gao Jingcheng, Yang Xiao, Jing Liu, Wei Liang, and C.L. Philip Chen. A survey of communication/networking in smart grids. *Future Generation Computer Systems*, 28:391–404, 2012.

[33] John Fialka. Modernizing the grid: a tugboat 'trying to turn a big ocean liner'. In *E&E News reporter , https://www.eenews.net/stories/1060039806*, 2016.

[34] Jingfang Huang, Honggang Wang, and Yi Qian. Smart grid communications in challenging environments. In *IEEE Third International Conference on Smart Grid Communications (SmartGridComm)*, 2012.

[35] Ye Yan, Yi Qian, Hamid Sharif, and David Tipper. A survey on smart grid communication infrastructures: Motivations, requirements and challenges. *IEEE COMMUNICATIONS SURVEYS and TUTORIALS*, 15:5–20, 2012.

[36] Yan He, Nick Jenkins, and Jianzhong Wu. Smart metering for outage management of electric power distribution networks. *Energy Procedia*, 103:159–164, 2016.

[37] Bert Williams. Using wireless communication networks to enable outage management. 2016.

[38] Aswin Raj C, Aravind E, Ramya Sundaram B, and Shriram K.Vasudevanb. Smart meter based on real time pricing. *Energy Procedia*, 21:120–124, 2015.

[39] Jeannie Oliver and BenJamin Sovacool. The energy trilemma and the smart grid: Implications beyond the united states. *Asia and The Pacific Policy Studies*, 4:70–84, 2017.

[40] U.S. Department of Energy. National transmission grid. *Washington*, 2002.

[41] F.Richard Yu, Peng Zhang, Weidong Xiao, and Paul Choudhury. Communication systems for grid integration of renewable energy resources. *IEEE Network*, 25, 2011.

[42] Ruofei Ma, Hsiao-Hwa Chen, Yu-Ren Huang, and Weixiao Meng. Smart grid communication: Its challenges and opportunities. *IEEE TRANSACTIONS ON SMART GRID*, 4:36–46, 2013.

[43] Chun-Hao Lo and Nirwan Ansari. Decentralized controls and communications for autonomous distribution networks in smart grid. *IEEE TRANSACTIONS ON SMART GRID*, 4:66–77, 2013.

[44] Nipendra Kayastha, Dusit Niyato, Ekram Hossain, and Zhu Han. Smart grid sensor data collection, communication, and networking: a tutorial. *WIRELESS COMMUNICATIONS AND MOBILE COMPUTING*, 14:1055–1087, 2014.

[45] Kenneth C. Budka, Jayant G. Deshpande, L. Doumi Tewfik, Mark Madden, and Tim Mew. Communication network architecture and design principles for smart grids. *Bell Labs Technical Journal*, 15:205–227, 2010.

[46] Melike Erol-Kantarci and Hussein T. Mouftah. Wireless sensor networks for domestic energy management in smart grids. 2010.

[47] Weixiao Meng, Ruofei Ma, and Hsiao-Hwa Chen. Smart grid neighborhood area networks: A survey. *IEEE Network*, 28:24–32, 2014.

[48] Ho Quang-Dung, Yue Gao, and Tho Le-Ngoc. Challenges and research opportunities in wireless communication networks for smart grid. *IEEE Wireless Communications*, 20:89–95, 2013.

[49] Power generation and smart grid. *Alliance Commission on National Energy Efficiency Policy*, 2013.

[50] Rong Yu, Yan Zhang, Stein Gjessing, Chau Yuen, Shengli Xie, and Mohsen Guizani. Cognitive radio based hierarchical communications infrastructure for smart grid. *IEEE Network*, 25, 2011.

[51] Fang Wang, Yu Kang, Xiaobin Tan, and Kai Yu. A hybrid mac protocol for data transmission in smart grid. In *Chinese Control Conference (CCC)*, 2014.

[52] Hui Jiang, Kun Wang, Yihui Wang, Min Gao, and Yan Zhang. Impacts of large-scale intermittent renewable energy sources on electricity systems, and how these can be modeled.

[53] Florian Dorfler, Michael Chertkov, and Francesco Bullo. Synchronization in complex oscillator networks and smart grids. *Proceedings of the National Academy of Sciences*, 6:2005–2010, 2013.

[54] Pin-Yu Chen, Shin-Ming Cheng, and Kwang-Cheng Chen. Smart attacks in smart grid communication networks. *IEEE Communications Magazine*, 50, 2012.

[55] Xing He, Qian Ai, Robert Caiming Qiu, Wentao Huang, Longjian Piao, and Haichun Liu. A big data architecture design for smart grids based on random matrix theory. *IEEE TRANSACTIONS ON SMART GRID*, 8:674–686, 2017.

[56] D.Diamantoulakis Panagiotis, Vasileios M.Kapinas, and George K.Karagiannidis. A big data architecture design for smart grids based on random matrix theory. *IEEE TRANSACTIONS ON SMART GRID*, 8:674–686, 2017.

[57] M.Mayilvaganan and M.Sabitha. A cloud-based architecture for big-data analytics in smart grid: A proposal. In *IEEE International Conference on Computational Intelligence and Computing Research (ICCIC)*, 2013.

[58] Alberto Sendin, Javier Simon, Iker Urrutia, and Berganza Inigo. Plc deployment and architecture for smart grid applications in iberdrola. In *IEEE International Symposium on Power Line Communications and its Applications (ISPLC)*, 2014.

[59] Ales Krutina and Jan Bartovsky. Plc communication in smart grid. In *Proccedings International Scientific Conference on Electric Power Engineering (EPE)*, 2014.

[60] Mostafa Sayed and Naofal Al-Dhahir. Narrowband-plc/wireless diversity for smart grid communications. In *IEEE Global Communications Conference (GLOBECOM)*, 2014.

[61] Vehbi C. Gungor, Bin Lu, and Gerhard P. Hancke. Opportunities and challenges of wireless sensor networks in smart grid. *IEEE Transactions on Industrial Electronics*, 57:3557–3564, 2010.

[62] Melike Erol-Kantarci and Hussein T. Mouftah. Plc communication in smart grid. In *Saudi International Electronics, Communications and Photonics Conference (SIECPC)*, 2011.

[63] Cigdem Eris, Merve Saimler, Vehbi C. Gungor, Etimad Fadel, and Ian F. Akyildiz. Lifetime analysis of wireless sensor nodes in different smart grid environments. *Wireless Networks*, 20:2053–2062, 2014.

[64] Melike Yigit, Ozlem Durmaz Incel, and Vehbi C. Gungor. On the interdependency between multi-channel scheduling and tree-based routing for wsns in smart grid environments. *Computer Networks*, 14, 2012.

[65] Sebastian Kaebisch, Anton Schmitt, Martin Winter, and Jorg Heuer. Interconnections and communications of electric vehicles and smart grids. In *IEEE International Conference on Smart Grid Communications (SmartGridComm)*, 2010.

[66] Irfan Al-Anbagi, Melike Erol-Kantarci, and Hussein T. Mouftah. Priority- and delay-aware medium access for wireless sensor networks in the smart grid. 8:608–618, 2014.

[67] 802.15.4-2015 - ieee standard for low-rate wireless networks. 2016.

[68] Shahin Farahani. *Newnes Publications*, 2008.

[69] Anna N. Kim, Fredrik Hekland, Stig Petersen, and Paula Doyle. When hart goes wireless: Understanding and implementing the wirelesshart standard. *IEEE International Conference on Emerging Technologies and Factory Automation*, 2008.

[70] Yubing Jian. Coexistence of wifi and laa-lte in unlicensed spectrum. 2015.

[71] Moshe Timothy Masonta, Mjumo Mzyece, and Ntsibane Ntlatlapa. Spectrum decision in cognitive radio networks: A survey. *IEEE Communications Surveys and Tutorials*, 15:1088–1107, 2013.

[72] Claudia Cormio and Kaushik R. Chowdhury. A survey on mac protocols for cognitive radio networks. *Ad Hoc Networks*, 7:1315–1329, 2009.

[73] U. N. Ujam, Y. Gao, G. Goteng, and G. Onoh. Tv white space (tvws) field trial at short distant indoor locations using empirical method. In *nternational Conference on Electro-Technology for National Development (NIGERCON)*, 2017.

[74] Bo Ye, Maziar Nekovee, Anjum Pervez, and Mohammad Ghavami. Tv white space channel allocation with simulated annealing as meta algorithm. In *International ICST Conference on Cognitive Radio Oriented Wireless Networks and Communications (CROWNCOM)*, 2012.

[75] Hanna Bogucka, Marcin Parzy, Paulo Marques, Joseph W. Mwangoka, and Tim Forde. Secondary spectrum trading in tv white spaces. *IEEE Communications Magazine*, 50:121–129, 2012.

[76] Beibei Wang and K.J. Ray Liu. Advances in cognitive radio networks: A survey. *IEEE Journal of Selected Topics in Signal Processing*, 5:5–23, 2010.

[77] Gyumin Hwang, Kyubo Shin, Sanghyeok Park, and Hyoil Kim. Measurement and comparison of wi-fi and super wi-fi indoor propagation characteristics in a multi-floored building. *JOURNAL OF COMMUNICATIONS AND NETWORKS*, 18:476–483, 2016.

[78] Nima Noorshams, Mehdi Malboubi, and Ahmad Bahai. Centralized and decentralized cooperative spectrum sensing in cognitive radio networks: A novel approach. In *International Workshop on Signal Processing Advances in Wireless Communications (SPAWC)*, 2010.

[79] Shree Krishna Sharma, Tadilo Endeshaw Bogale, Symeon Chatzinotas, Bjorn Ottersten, Long Bao Le, and Xianbin Wang. Cognitive radio techniques under practical imperfections: A survey. *IEEE Communications Surveys and Tutorials*, 17:1858–1884, 2015.

[80] Andrea Goldsmith, Syed Ali Jafar, Ivana Maric, and Sudhir Srinivasa. Breaking spectrum gridlock with cognitive radios: An information theoretic perspective. *Proceedings of the IEEE*, 97:894–914, 2009.

[81] Brandon F. Lo. A survey of common control channel design in cognitive radio networks. *Physical Communication*, 4:26–39, 2011.

[82] Prasan Kumar Sahoo and Debasish Sahoo. Sequence-based channel hopping algorithms for dynamic spectrum sharing in cognitive radio networks. *IEEE Journal on Selected Areas in Communications*, 34:2814–2828, 2016.

[83] Chih-Min Chao, Hsiang-Yuan Fu, and Li-Ren Zhang. A fast rendezvous-guarantee channel hopping protocol for cognitive radio networks. *IEEE Transactions on Vehicular Technology*, 64:5804–5816, 2015.

[84] Yifan Zhang, Gexin Yu, Qun Li, Haodong Wang, Xiaojun Zhu, and Baosheng Wang. Channel-hopping-based communication rendezvous in cognitive radio networks. *IEEE/ACM Transactions on Networking*, 22:889–902, 2014.

[85] Shih-Lin Wu, Yu-Chee Tseng, Chih-Yu Lin, and Jang-Ping Sheu. A multi-channel mac protocol with power control for multi-hop mobile ad hoc networks. *The Computer Journal*, 45:101–110, 2002.

[86] Jenhui Chen and Yen-Da Chen. Amnp: ad hoc multichannel negotiation protocol for multihop mobile wireless networks. 2004.

[87] Peng-jung Wu and Chung-nan Lee. On-demand connection- oriented multi-channel mac protocol for ad-hoc network. 2006.

[88] Wassim El-Hajj, Haidar Safa, and Mohsen Guizani. Survey of security issues in cognitive radio networks. *China Communications*, 13:132–150, 2015.

[89] Chih-Min Chao, Hsiang-Yuan Fu, and Li-Ren Zhang. Common control channel security framework for cognitive radio networks. In *IEEE Vehicular Technology Conference (VTC Spring)*, 2009.

[90] J Huang, H Wang, Y Qian, and C Wang. Priority-based traffic scheduling and utility optimization for cognitive radio communication infrastructure-based smart grid. *IEEE Transactions on Smart Grid*, 4:78–86, 2013.

[91] Adnan Aijaz and Abdol-Hamid Aghvami. Prma-based cognitive machine-to-machine communications in smart grid networks. *IEEE TRANSACTIONS ON VEHICULAR TECHNOLOGY*, 64:3608–3623, 2015.

[92] Adnan Aijaz, Shuyu Ping, Mohammad Reza Akhavan, and Abdol-Hamid Aghvami. Crb-mac: A receiver-based mac protocol for cognitive radio equipped smart grid sensor networks. *IEEE SENSORS JOURNAL*, 14:4325–4333, 2014.

[93] Zhutian Yang, Shuyu Ping, Hongjian Sun, and A. Hamid Aghvami. Crb-rpl: A receiver-based routing protocol for communications in cognitive radio enabled smart grid. *IEEE TRANSACTIONS ON VEHICULAR TECHNOLOGY*, 66:5985–5994, 2016.

[94] Zhutian Yang, Shuyu Ping, Adnan Aijaz, and Abdol-Hamid Aghvami. A global optimization-based routing protocol for cognitive-radio-enabled smart grid ami networks. *IEEE SYSTEMS JOURNAL*, 99:1–9, 2016.

[95] Adnan Aijaz, Hongjia Su, and Abdol-Hamid Aghvami. Corpl: A routing protocol for cognitive radio enabled ami networks. *IEEE TRANSACTIONS ON SMART GRID*, 6:477–485, 2015.

[96] Honggang Wang, Yi Qian, and Hamid Sharif. Multimedia communication over cognitive radio networks for smart grid applications. *IEEE Wireless Communications*, 20:125–132, 2013.

[97] Ghalib A. Shah, Vehbi C. Gungor, and Ozgur B. Akan. A cross-layer design for qos support in cognitive radio sensor networks for smart grid applications. In *IEEE International Conference on Communications (ICC)*, 2012.

[98] Ghalib A. Shah, Vehbi C. Gungor, and Ozgur B. Akan. A cross-layer qos-aware communication framework in cognitive radio sensor networks for smart grid applications. *IEEE Transactions on Industrial Informatics*, 9:1477–1485, 2013.

[99] Narsingh Sahu and Vashudev Dehalwar. Intelligent machine to machine communication in home area network for smart grid. In *International Conference on Computing Communication & Networking Technologies (ICCCNT)*, 2012.

[100] Marco Levorato and Urbashi Mitra. Optimal allocation of heterogeneous smart grid traffic to heterogeneous networks. In *IEEE International Conference on Smart Grid Communications (SmartGridComm)*, 2011.

[101] Mubashir Husain Rehmani, Aline Carneiro Viana, Hicham Khalife, and Fdida Serge. Surf: A distributed channel selection strategy for data dissemination in multi-hop cognitive radio networks. *Computer Communications*, 36:1172–1185, 2013.

[102] Leslie Pack Kaelbling, Michael L.Littman, and Anthony R.Cassandra. Planning and acting in partially observable stochastic domains. *ARTIFICIAL INTELLIGENCE*, 101:99–134, 1998.

[103] Noorhayati Mohamed Noor, Norashidah Md Din, Ejaz Ahmed, and Awang Norsharim Awang Kadir. Omnet++ based cognitive radio simulation network. In *IEEE Control and System Graduate Research Colloquium (ICSGRC)*, 2016.

[104] Jose Marinho and Edmundo Monteiro. Omnet++ based cognitive radio simulation network. In *Conferencia sobre Redes de Computadores (CRC)*, 2011.

[105] Mubashir Husain Rehmani, Aline Carneiro Viana, Hicham Khalife, and Fdida Serge. Surf: A distributed channel selection strategy for data dissemination in multi-hop cognitive radio networks. *Computer Communications*, 36:1172–1185, 2013.

[106] Ejaz Ahmed, Abdullah Gani, Saeid Abolfazli, Liu Jie Yao, and Samee U. Khan. Channel assignment algorithms in cognitive radio networks: Taxonomy, open issues, and challenges. *IEEE Communications Surveys and Tutorials*, 18:795–823, 2014.

[107] Sana Rekik, Nouha Baccour, Mohamed Jmaiel, and Khalil Drira. Wireless sensor network based smart grid communications: Challenges, protocol optimizations, and validation platforms. 95:4025–4047, 2017.

[108] SHENGJIE XU, YI QIAN, and ROSE QINGYANG HU. On reliability of smart grid neighborhood area networks. *IEEE Access*, pages 2352–2365, 2015.

[109] Ines Hosni and Noureddine Hamdi. Cross layer optimization of end to end delay in wsn for smart grid communications. In *International Symposium on Signal, Image, Video and Communications (ISIVC)*, 2016.

[110] Irfan Al-Anbagi, Melike Erol-Kantarci, and Hussein T. Mouftah. An adaptive qos scheme for wsn-based smart grid monitoring. In *IEEE International Conference on Communications (ICC)*, 2013.

[111] Irfan Al-Anbagi, Melike Erol-Kantarci, and Hussein T. Mouftah. Qos-aware inter-cluster head scheduling in wsns for high data rate smart grid applications. In *IEEE Globecom*, 2013.

[112] Melike Erol-Kantarci and Hussein T. Mouftah. Suresense: Sustainable wireless rechargeable sensor networks for the smart grid. *IEEE Wireless Communications*, 19, 2012.

[113] Irfan Al-Anbagi, Melike Erol-Kantarci, and Hussein T. Mouftah. Time slot allocation in wsns for differentiated smart grid traffic. In *IEEE EPEC*, 2013.

[114] Kartik Vishal Deshpande and A. Rajesh. Investigation on imcp based clustering in lte-m communication for smart metering applications. *Engineering Science and Technology*, 20:944–955, 2017.

[115] Ameer Ahmed Abbasi and Mohamed Younis. A survey on clustering algorithms for wireless sensor networks. *Computer Communications*, 30:2826–2841, 2007.

[116] Rashad M. Eletreby, Hany M. Elsayed, and Mohamed M. Khairy. Cogleach: A spectrum aware clustering protocol for cognitive radio sensor networks. In *IEEE CROWNCOM*, pages 179–184, 2014.

[117] Ghalib A. Shah and Ozgur B. Akan. Spectrum-aware cluster-based routing for cognitive radio sensor networks. In *IEEE International Conference on Communications (ICC)*, 2013.

[118] Ghalib A. Shah and Ozgur B. Akan. A spectrum-aware clustering for efficient multimedia routing in cognitive radio sensor networks. *IEEE transactions on vehicular technology*, 64:3369–3380, 2014.

[119] Jingyi Dai and Shaowei Wang. Clustering-based spectrum sharing strategy for cognitive radio networks. *IEEE Journal on Selected Areas in Communications*, 35:228–237, 2017.

[120] Yasir saleem, KoK-lim alvin Yau, Hafizal moHamad, nordin ramli, mubasHir Husain reHmani, and Qiang ni. Clustering and reinforcement learning based routing for cognitive radio networks. *IEEE Wireless Communications*, 24:146–151, 2017.

[121] Mustafa Ozger, Etimad Fadel, and Ozgur B. Akan. Event-to-sink spectrum-aware clustering in mobile cognitive radio sensor networks. *IEEE Transactions on Mobile Computing*, 15:2221–2233, 2016.

[122] Tao Chen, Honggang Zhang, Gian Mario Maggio, and Imrich Chlamtac. Cogmesh: A cluster-based cognitive radio network. In *IEEE International Symposium on New Frontiers in Dynamic Spectrum Access Networks (DySPAN)*, 2007.

[123] Yang Xiao. Communication and networking in smart grids. In *CRC Press*, 2012.

[124] Liquan Chen, Zhezhuang Xu, Ting Liu, and Cailian Chen. A dynamic clustering and routing protocol for multi-hop data collection in wireless sensor networks. In *Chinese Control Conference (CCC)*, 2015.

[125] Yu-Ping Chen and Quincy Wu. Power consumption measurement and clock synchronization on low-power wireless sensor networks. In *International Conference on Advanced Communication Technology (ICACT)*, 2012.

[126] Majid Bahrepour, Nirvana Meratnia, Mannes Poel, Zahra Taghikhaki, and Paul J.M. Havinga. Distributed event detection in wireless sensor networks for disaster management. In *International Conference on Intelligent Networking and Collaborative Systems (INCOS)*, 2010.

[127] Edith C. H. Ngai, Yangfan Zhou, Michachel R. lyu, and Jiangchuan Liu. Reliable reporting of delay-sensitive events in wireless sensor-actuator networks. In *IEEE International Conference on Mobile Adhoc and Sensor Systems (MASS)*, 2006.

[128] Mustafa Ozger and Ozgur B. Akan. Event-driven spectrum-aware clustering in cognitive radio sensor networks. In *IEEE Infocom*, pages 2325–9418, 2013.

[129] Mustafa Ozger, Etimad Fadel, and Ozgur B. Akan. Event-to-sink spectrum-aware clustering in mobile cognitive radio sensor networks. In *IEEE Transactions on Mobile Computing*, pages 2221–2233, 2015.

[130] Irfan Al-Anbagi, Melike Erol-Kantarci, and Hussein T. Mouftah. Delay mitigation scheme for wsn-based smart grid substation monitoring. In *International Wireless Communications and Mobile Computing Conference (IWCMC)*, 2013.

[131] Mohammad Ekbatani Fard, H. Yaghmaee and Reza Monsefi. An adaptive cross-layer multichannel qos-mac protocol for cluster based wireless multimedia sensor networks. 2009.

[132] Divya Saini, Rajiv Misra, and Ram Narayan Yadav. Distributed event driven cluster based routing in cognitive radio sensor networks. pages 2325–9418, Dec 2016.

[133] Md. Abdur Tabassum, Madiha Razzaque, Md. Nazmus Sakib Miazi, Mohammad Mehedi Hassan, and Abdulhameed Atif Alelaiwi, Alamri. An energy aware event-driven routing protocol for cognitive radio sensor networks. *Wireless Networks*, 22:1523–1536, 2016.

[134] Feilong Tang, Can Tang, Yanqin Yang, Laurence T. Yang, Tong Zhou, Jie Li, and Minyi Guo. Delay-minimized routing in mobile cognitive networks for time-critical applications. 99, 2016.

[135] Amir Sepasi Zahmati, Xavier Fernando, and Ali Grami. Steady-state markov chain analysis for heterogeneous cognitive radio networks. 2010.

[136] A Lim, Y Zhu, Q Lou, and B Rodrigues. Heuristic methods for graph coloring problems. 2005.

[137] Bhagyashri Tushir, Sanjay K. Dhurandher, Isaac Woungang, Mohammad S. Obaidat, and Vinesh Teotia. Graph colouring technique for efficient channel allocation in cognitive radio networks. 2016.

[138] Severino F. Galán. Simple decentralized graph coloring. 66:163–185, 2017.

[139] Ram Narayan Yadav and Rajiv Misra. Multipath routing protocols in cognitive radio networks. 2014.

[140] France leads smart grids investments in europe. https://www.thinksmartgrids.fr/en/actualites/france-leads-smart-grids-investments-in-europe-2/. Accessed: 2018-03-23.

[141] United states smart grid: Market forecast (2017 - 2027). https://www.businesswire.com/news/home/20180130006397/en/United-States-Smart-Grid-Market-2017-Forecasts. Accessed: 2018-03-23.